Risk Assessment of Mildly Flammable Refrigerants

2012 Progress Report

April 2013

The Japan Society of Refrigerating and
Air Conditioning Engineers

Foreword

While great successes have been achieved in climate change mitigation, global emissions of greenhouse gases continue to rise. Greenhouse gas emissions from fossil fuels are the main issue, but emissions of fluorocarbon refrigerants from refrigeration and air conditioning appliances should not be ignored because of the large global warming potential (GWP) of fluorocarbons.

The progressively more severe impact of fluorocarbon refrigerants makes the need for urgent action abundantly clear. The basic measure to reduce the impact of refrigerants is the replacement of conventional hydrofluorocarbons (HFCs) with low-GWP refrigerants. Low-GWP refrigerants are not very stable in atmosphere and thus are sometimes flammable. According to Japan's High Pressure Gas Safety Act, the use of flammable refrigerants in refrigeration and air conditioning equipment is restricted in practice. For the safe use of flammable refrigerants and relaxation of the regulation, a risk assessment needs to be performed; only a scientific risk assessment can provide a sound basis for judgment and change in regulation.

The Ministry of Economy, Trade and Industry (METI) and the New Energy and Industrial Technology Development Organization (NEDO) have been subsidizing research to obtain basic information on mildly flammable refrigerants since 2011. In addition, a research committee was set up by the Japan Society of Refrigerating and Air Conditioning Engineers to assess the risks associated with mildly flammable refrigerants. The Japan Refrigerating and Air Conditioning Industry Association and the Japan Automobile Manufacturers Association are presently conducting very definitive risk assessments, and the results are being discussed by the research committee.

This 2012 progress report provides state-of-the-art information concerning the risk of mildly flammable refrigerants. I am sure that its information will be of much interest for the risk assessment. I thank all the members and observers of the committee who helped produce this progress report. I hope that you will find it a useful and stimulating summary of the ever-sustainable story at the heart of human progress.

Chairperson of the Committee
Professor at the University of Tokyo
Eiji HIHARA
April 2013

Table of Contents

1. Introduction

Eiji HIHARA
Graduate School of Frontier Sciences, The University of Tokyo

The use of chlorofluorocarbons (CFCs) and hydrochlorofluorocarbons (HCFCs) has been widely restricted. They have been replaced with hydrofluorocarbons (HFCs) in order to protect the ozone layer. However, leakage of the refrigerant into the air from active or end-of-life air-conditioners has been a serious environmental issue owing to its high global warming potential (GWP). It has therefore been widely recognized that the replacement of HFCs with low-GWP refrigerants is important as a reasonable solution to the problem. The numbers of room, package, and mobile air-conditioners shipped from Japan in 2011 were 8.20 million, 7.78 million, and 4.73 million, respectively. These are the major types of air-conditioning equipment produced in Japan. In the case of mobile air-conditioners, there is a high possibility of the conventional refrigerant being replaced with R1234yf. On the other hand, studies have been conducted over the last several years on the use of lower-GWP refrigerants in stationary air-conditioners.

To prevent global warming, regulations have been imposed in Japan and overseas regarding the use of high-GWP refrigerants such as the HFCs used in air-conditioning equipment.

1.1 Trends in the regulation of refrigerants

The EU protocol 2006/40/EC[1.1)] on mobile air-conditioning refrigerants prohibits the release of new cars using refrigerants with a GWP of over 150 from January 1, 2011. It also prohibits the release of any new car using such refrigerants from January 1, 2017. In 2009, the automobile industry decided to replace the conventional refrigerant R134a with the low-GWP refrigerant R1234yf. However, the EU

Table 1.1 Summary of the proposed regulation of HFCs

	Proposal by three North American countries	**Proposal by EU Commission**
Proposal date	24th meeting of the High Contracting Parties, November 2012	November 7, 2012
Evidential law	Montreal Protocol	Revised edition of Regulation (EC) No. 842/2006
Target refrigerants	21 types of HFCs (including R1234yf, ze)	HFCs (R1234yf, ze not included)
Baselines of HFC phase down	Average value between 2005 and 2008 Developed countries: HFCs and 85% of HCFCs Developing countries: HCFC	Average value between 2008 and 2011
Final values of HFC phase down	Developed countries: 15% of the 2033 baseline Developing countries: 15% of the 2043 baseline	21% of the 2030 baseline
Another regulation	Restriction on the co-product of HCFC22 and HFC23 to be imposed from 2016	Restriction on HFC23, etc.
Other restrictions		(1) Prohibition of refrigerant pre-charging in imported equipment (only field charging is permitted) (2) Refilling of refrigerants with GWPs of over 2500 in equipment with equivalent CO_2 emission of $5CO_2$ ton will be prohibited from January 1, 2020

Commission temporarily permitted the continued use of R134a in April 2012 owing to the supply shortage of R1234yf. The release of new model cars using refrigerants with a GWP of over 150 has been prohibited since January 1, 2013.

The regulation regarding the use of stationary air-conditioners is known as F-gas Regulation (EC) No. 842/2006[1.2)]. The present regulation focuses on reducing refrigerant leakage from air-conditioners and requires proper management, instructional courses for operators, the labeling of equipment containing F-gas, and reports by producers, importers, and exporters of F-gas.

In November 2012, the EU Commission proposed to enhance existing regulations[1.3)]. The new proposal aims to reduce the leakage of F-gas to two-thirds of the present level, and to prohibit the release of equipment using F-gas in a field where an environment-friendly refrigerant has been developed. To achieve this, a phase down schedule has been proposed, which assumes that the reduction in the annual amount of HFCs sold in the EU (the equivalent amount of CO_2 is obtained by multiplying the amount of each refrigerant by its GWP and summing them up) started in 2015, and has been reduced to one-fifth at the present time.

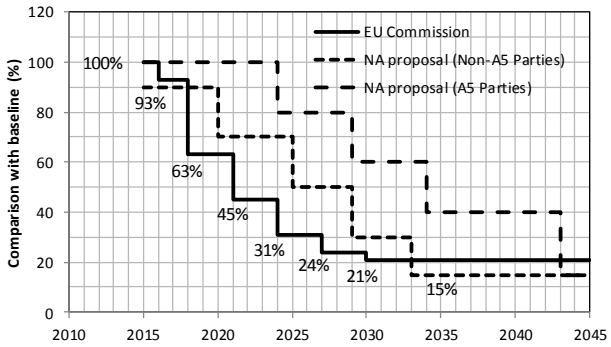

Fig. 1.1 Proposed HFC reduction stages.

On the other hand, three North American countries (US, Canada, and Mexico) submitted a proposal to revise the Montreal Protocol to restrict the production and sales of HFCs at the Conference of Parties, which aims to abolish practices that destroy the ozone layer. HFCs actually do not destroy the ozone layer; the global warming issue was caused by the replacement of prohibited CFCs and HCFCs, which destroy the ozone layer, with HFCs, which have high GWPs. The proposal suggests the restriction of the distribution of HFCs in the framework of the Montreal Protocol. Table 1.1 and Fig. 1.1 compare the proposals and schedules of the three North American countries with those of the EU Commission.

The EU Commission proposal prohibits pre-charging refrigerants at factories in order to effectively control the total volume. Moreover, in the near future, the recharge of refrigerants with GWPs above 2500 (the target refrigerant is R404A) will also be prohibited.

In Japan, the Global Environment Sub-Committee of the Central Environment Council and the Chemical and Biotechnology Sub-Committee of the Industrial Structure Council jointly set up a task force and compiled an outline[1.5)] for the regulation of HFCs.

The document released by the task force indicated that if no extra measures are taken, the emission of HFCs would double by 2020, and that the emission from the air-conditioning sector would account for 80% of the total emission. It noted the importance of taking appropriate measures in the air-conditioning sector. Approximately 60% of leakages in the air-conditioning sector occur during operation; the rest is from uncollected refrigerant of the end-of-life equipment. It is estimated that approximately 40% of all leakage during operation is from separate-type display cases. It is conventionally thought that the most important alleviatory measure is the recovery of refrigerants from end-of-life refrigerators and air-conditioners. This has, however, been found to be inadequate.

Against the above background, several policies were decided upon regarding the provision: the replacement of HFCs; proper management of equipment; recovery of refrigerants; reduction of HFC leakage into the air.

1.2 Trends in research on the safety of mildly flammable refrigerants

The development of environment-friendly refrigerants for room and package air-conditioners is imperative to the growth of air-conditioning technology. Low-GWP refrigerants R1234yf and R32 are promising candidates for conventional HFC refrigerants. However, these refrigerants are not very stable in air and are sometimes flammable. It is therefore essential to collect basic data about the flammability of low-GWP refrigerants and to research the safety of their practical use. The integration of basic information about their physical properties, cycle performance, life cycle climate performance (LCCP), flammability, and risk assessment will simplify selection and their practical use. These efforts are expected to contribute to the development of the global air-conditioning industry.

R1234yf and R32 are less flammable than propane and R152 and are therefore referred to as mildly flammable refrigerants. In ASHRAE Standard 34, the rank 2L was newly set up for mildly flammable refrigerants with burning heats lower than 19 MJ/kg and burning velocities lower than 10 cm/s. Together with ammonia, R1234yf and R32 are classified as 2L. The characteristics of the flammable refrigerants are given in Table 1.2, where LFL, UFL, BV, and MIE respectively denote lower flammability limit, upper flammability limit, burning velocity, and minimum ignition energy. Compared to propane, which is highly flammable, the other refrigerants have low BVs and high MIEs.

Table 1.2 Burning characteristics of flammable refrigerants[1.5)]

Refrigerant	GWP	LFL [vol%]	UFL [vol%]	BV [cm/s]	MIE [mJ]
R290 (Propane)	<3	1.8	9.5	38.7	0.246
R717 (Ammonia)	<1	15	28	7.2	21
R32	675	13.3	29.3	6.7	15
R1234yf	4	6.2	12.3	1.5	500

As illustrated in Fig. 1.2, all the following conditions must be satisfied by an ignitable refrigerant that leaks from an appliance near an ignition source:

(1) Refrigerant concentration must be within the range of the flammability.
(2) The energy of the ignition source must be higher than the MIE.
(3) The air velocity adjacent to the ignition source must be lower than the BV.

If the air velocity adjacent to the ignition source is higher than the BV, burning will not occur because fire cannot be propagated against airflow.

The setup of rank 2L on ASHRAE Standard 34 has changed the restriction on refrigerants regarding flammability and allows for the practical use of low-flammability refrigerants. In Japan, however, only “non-flammable” and “flammable” classifications are recognized in the High Pressure Gas Safety Act and the Ordinance on the Security of Safety at Refrigeration. With the objective of gathering essential data for the risk assessment of mildly flammable refrigerants, safety studies are being conducted by project teams from the Tokyo University of Science at Suwa, Kyusyu University, University of Tokyo, and National Institute of Advanced Industrial Science and Technology. They have been sponsored since 2011 by the project on the “Development on Highly Efficient and Non-Freon Air Conditioning Systems” of the New Energy and Industrial Technology Development Organization (NEDO).

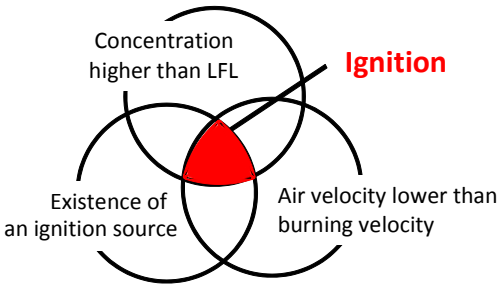

Fig. 1.2 Mechanism of ignition.

In addition, a research committee was set up by the Japan Society of Refrigerating and Air Conditioning Engineers to assess the risks associated with mildly flammable refrigerants. The Japan Refrigerating and

Air Conditioning Industry Association and the Japan Automobile Manufacturers Association are presently undertaking very definite risk assessments and the results are being discussed by the research committee. The 2012 activities of the committee for assessing the risks associated with mildly flammable refrigerants are compiled in this report. The committee members would be pleased if this report proves to be helpful to people working in associated fields.

References

1.1) Directive 2006/40/EC of the European Parliament, 17 May, 2006.

1.2) Regulation (EC) No. 842/2006 of the European Parliament, 17 May, 2006.

1.3) Proposal for a Regulation of the European Parliament and the Council on Fluorinated Greenhouse Gases, 7 November, 2012.

1.4) Summary Points: North American HFC Submission to the Montreal Protocol, EPA, US, 2012.

1.5) Kenji TAKIZAWA et al., “Flammability properties of 2L refrigerants”, The International Symposium on New Refrigerants and Environmental Technology 2012, (2012).

2. Legal issues with mildly flammable refrigerant

2-1. Explanation of High Pressure Gas Safety Law and legal issues with mildly flammable refrigerant

Akiyoshi TAKASHIMA and Kenji TSUJI
Japan Society of Refrigerating and Air Conditioning Engineers (JSRAE),
Safety committee

2.1.1 Introduction

The present Refrigeration Safety Regulations recognize four classifications: inactive gases, active gases, toxic gases, and fluorocarbons with the exception of inactive gas, and the former three gases are defined by listing of those names and are operated.

An outline of the regulatory system is provided in Fig. 2.1.1. We should clarify the usage of a mildly flammable refrigerant (ISO/DIS 817 A2L) as to whether it can be used as an A1 (inactive gas) or not to maintain the normal state of operation.

In particular, there is a high possibility that low GWP (Global Warming Potential) refrigerant gases will be needed in the future for a low-carbon society. Under the existing law, therefore, we must indicate the directionality of fluorocarbons with the exception of an inactive gas.

2.1.2 Daily issue for using the mildly flammable refrigerant (example)

To use a room air conditioner, package air conditioner, or turbo refrigerating machine (hereafter called refrigeration apparatus), the treatment of three fundamental elements, “operation,” “charging,” and “recovery,” must be considered in daily action and these elements are difficult to understand.

Regarding law and its response for each work, moreover, it is asked from all party, especially builders, producers and users.

(Operation and application law)

2.1.2.1 Although the law for a refrigeration apparatus has been adapted from Refrigeration Safety Regulations, it treats only “the act where a gas for refrigeration is compressed or liquefied to produce a high pressure gas.” Other acts are regulated by other rule such as the General High Pressure Gas Safety Regulations.

(Charging or recovery, and application law)

2.1.2.2 When the refrigerant gas of a refrigeration apparatus has leaked, charging is an act that produces a high pressure gas. The related law is based on the General High Pressure Gas Safety Regulations, and a notification report is required for every installation location. Charging with an inactive fluorocarbon or the act of recovery performed with a recovery subsystem is excluded[*1].

*1 The 2nd article 3rd clause No.6 of the High Pressure Gas Safety Law enforcement ordinance, and 2nd article of the High Pressure Gas Safety Law enforcement ordinance relation notification.

(Sale and application law)

2.1.2.3 The act of charging a refrigeration apparatus during an installation or repair service is not only an act of producing, but also one of selling the high-pressure gas (whether with or without consideration). Namely, it is necessary to follow the General High Pressure Gas Safety Regulations for sales business (or including a type change notification for the high-pressure gas regarding sales).

However, because an act that uses a small container (this is called a cylinder and the internal volume is less than 1 liter)[*2] is excluded from the High Pressure Gas Safety Law, it is also exempted from the notification report of producing and selling the high pressure gas. Moreover, when selling a class 1 refrigeration apparatus, the notification report of high pressure gas dealer of Refrigeration Safety Regulations is also needed separately.

*2 The 2nd article 3rd clause No.8 of the High Pressure Gas Safety Law enforcement ordinance, and 4th article of the High Pressure Gas Safety Law enforcement ordinance relation notification.

2.1.3 Legal treatment of R1234yf, R1234ze(E), R32, and others

2.1.3.1 Treatment by Refrigeration Safety Regulations

Although “flammable gases,” “toxic gases,” and “inactive gases” are defined by the second article of the Refrigeration Safety Regulations, and each refrigerant name is listed, the definition standard is not clear. Of course, there is no definition for “mildly flammable.” At present, R1234yf, R1234ze(E), and R32 are listed neither as the inactive gases nor as flammable

gases. In this case, the easing of various regulations is not applied to R1234yf, R1234ze(E) and R32.

2.1.3.2 Treatment by General High Pressure Gas Safety Regulations

"Flammable gases," "toxic gases," and "inactive gases" are defined by the second article of the General High Pressure Gas Safety Regulations, and the names of these gases are listed for each category.

Fluorocarbons (except for flammable gases) are described under "inactive gases." Gases (except for listed gases) with the following properties are described under "flammable gases."

1. The lower limit for an explosion is less than 10%
2. The difference between the higher limit and lower limit for an explosion is more than 20%

Figure 2.1.2 shows these types, along with where R1234yf, R1234ze(E), R32, and R717 would fall.

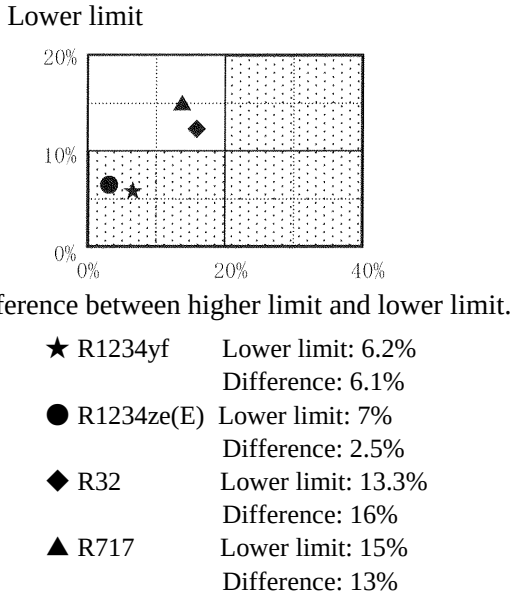

Fig. 2.1.2 Measurement results based on General High Pressure Gas Safety Regulations[2.1.1)]

In Fig. 2.1.2, the shaded and white parts indicate "flammable" and "not flammable," respectively.

2.1.3.3 ASHRAE (American Society of Heating, Refrigerating and Air-Conditioning Engineers) standard

In ASHRAE, although R1234yf, R1234ze(E), R32, and R717 were defined as "2L" by "ASHRAE standards 34" in 2010, their treatment is not clearly defined.

2.1.3.4 Recovery of R1234yf, R1234ze(E), and R32

Based on a related notification from the High Pressure Gas Safety Law enforcement ordinances, since the fluorocarbon (inactive gas) in the recovery equipment is being contracted out of law, R32 correspond to it. However, R1234yf and R1234ze(E) in the recovery equipment are handled based on the General High Pressure Gas Safety Regulations.

2.1.4 Issues with High Pressure Gas Safety Law regarding mildly flammable refrigerant

2.1.4.1 Revision of listing name principle

Although "flammable gases," "toxic gases," and "inactive gases" are defined by the second article of the Refrigeration Safety Regulations and each refrigerant name is listed, the definition standard is not indicated. It is doubtful that R413A which is classified as "A2" in "ASHRAE standard 34" is listed as an inactive gas.

Because the treatment of a new refrigerant gas (particularly a mildly flammable gas) or a mixed gas cannot presently be determined from the viewpoint of global warming prevention, it is tackled each time while asking to Commercial Affairs Circulation Preservation Group High Pressure Gas Preservation Section, Ministry of Economy, Trade and Industry. The "flammable" number concepts of the Refrigeration Safety Regulations should be stipulated for consistency with the General High Pressure Gas Safety Regulations.

2.1.4.2 Recovery and legislation of refrigerant gas that is not treated as inactive gas

Even when classified as flammable, gases should not be regulated uniformly. In particular, regarding a flammable gas close to an inactive gas (A2L of the mildly flammable gases), discussions are needed to ease the regulations. Moreover, it is necessary to inquire about the establishment of technical standards for the recovery subsystem.

<Draft proposal>

1. In principle, internal fittings are restricted to welding or brazing. However, if welding or brazing is not appropriate, it can be replaced by flange joints, which possess the strength required for safety (a threaded joint is inappropriate).
2. External connections are required for secure joinable coupling.

2.1.4.3 Easing requirements for specified equipment

Although the refrigerant which can be used by specified equipment is limited to only an inactive fluorocarbon by the

High Pressure Gas Safety Law enforcement ordinances relation notification[*3], it is also expected to discuss the range in application of the fluorocarbon that is not a flammable gas.

- Present state : fluorocarbon (inactive gas)
- Draft proposal: fluorocarbon that is not flammable gas

*3 Ministry of International Trade and Industry notification No. 139, 6th article, 2nd clause No. 2, March 24, 1997.

2.1.5 Issues with the mildly flammable refrigerants from foreign countries

From the safety administration perspective, it is desirable to clarify several issues from a professional standpoint.

1. If R32 is listed as an inactive gas, assiduity for foreign countries is required because they might feel as heterogeneous about the listing.
2. We should clarify what is eased or changed by changing from A2 to A2L.
3. In legislation, an explanation of the movement of many foreign countries is needed.

References

2.1.1) Japan Fluorocarbon Manufacturers Association (JFMA), Table of environment and safety data of specific freon (CFC/HCFC) and fluorocarbon, http://www.jfma.org/database/table.html, 2012.

2.1.2) Journal of The High Pressure Gas Safety Institute of Japan, Vol. 47, 11, 2010 (published by The High Pressure Gas Safety Institute of Japan).

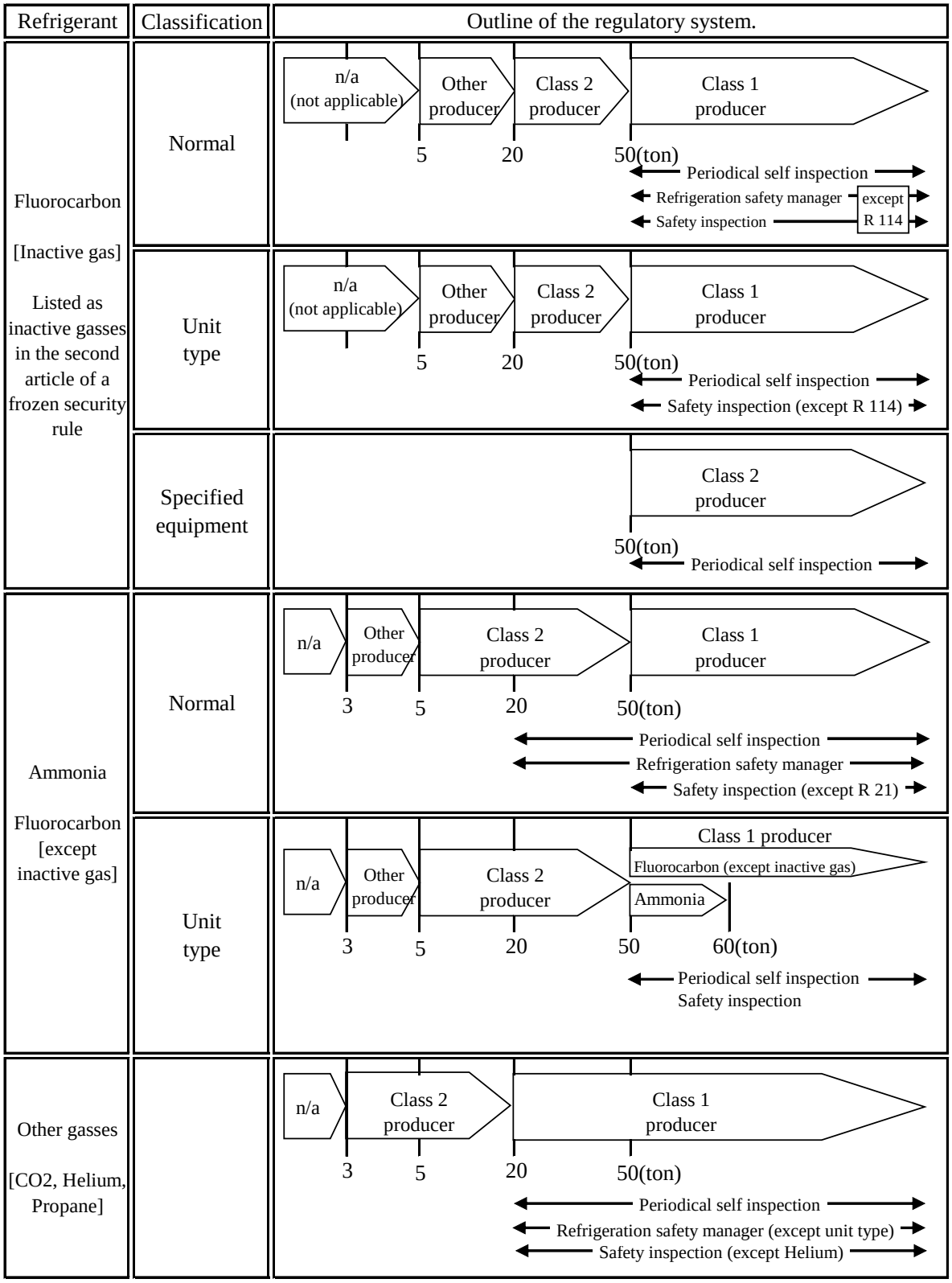

Fig. 2.1.1 Outline of regulation system in Refrigeration Safety Regulations [2.1.2)]

2-2. Current international trends regarding refrigerant

Satoru FUJIMOTO
JRAIA, WG for Risk Assessment of A2L Refrigerant

The refrigerant trends seen around the world are briefly outlined here. Only officially announced material and commentaries on the current trends regarding refrigerants are cited because matters that are still fluid cannot be stated as being definite. It should be duly noted that the information presented here is only a partial account of the information available concerning refrigerants and is by no means comprehensive.

2.2.1 Trends in Japan

The Japanese government is revising the Law Concerning the Recovery and Destruction of Fluorocarbons in 2013 to prevent leakage at the time of fluorocarbon use and to raise the current recovery ratio from roughly 30% to 60%. The law is scheduled to go into effect in 2014. In revising the law, a revision draft was announced, and comments were solicited from the public. Currently, the following four main points serve as the main pillars for the law revision.

1) Promotion of refrigerant conversion
   To encourage the conversion to low-GWP/non-fluorocarbon equipment, the country establishes GWP-based numerical values that are considered safe for each product classification and requires that manufacturers and importers achieve these by a specified fiscal year. The targets are not only for commercial-use refrigeration and air conditioning equipment; residential-use air conditioners are also included.
2) Promotion of recovery and recycling of refrigerants to substantially phase down fluorocarbons
   Concerning the recovery and recycling of refrigerants, the government introduces regulations for refrigerant manufacturers and importers on GWP aggregate amounts for HFCs and establishes a policy to promote the recycling and destruction of recovered refrigerants. Additionally, the law creates a certification system for refrigerant recycling contractors to ensure product quality for the recycled refrigerant.
3) Prevention of leakage at time of use
   The government requires periodic inspections for new users of specified commercial-use equipment. The target is refrigeration and air conditioning equipment with large refrigerant charges or emissions. It is anticipated that the inspection method and frequency will be relaxed for equipment using a low-GWP refrigerant or remote monitoring (such as Daikin's "Air Conditioning Network Service System"). Furthermore, there is a movement to restrict the people allowed to perform refrigerant charging to prevent repeated refrigerant charging without servicing when refrigerant leakage is known to exist.
4) Expansion of scope for management control of recovery process
   The government constructs a mechanism that can confirm from the user (the actual person disposing of the equipment or the person placing a maintenance order) whether or not the recovered refrigerant has been recycled or destroyed.

In addition, the Japan Society of Refrigerating and Air Conditioning Engineers (JSRAE), the Japan Refrigeration and Air-conditioning Industry Association (JRAIA), Japan Automobile Manufactures Association (JAMA) and the New Energy and Industrial Technology Development Organization (NEDO) are working in cooperation on the scientific clarification of the risks involved with using mildly flammable refrigerants because their use is inevitable for converting to low-GWP refrigerants. The achievement of the primary goal for the joint project has been set for the spring of 2014. A progress report is issued annually in April.

2.2.2 Trends in Europe

Revision of the current F-gas regulations that were

issued in 2007 is moving ahead, with the goal of completion in 2013. The overall concept of that basic policy was clarified at the end of 2012. The contents of this revision have been already introduced in first chapter.

2.2.3 Trends in United States

In the United States, the Department of Energy (DOE) regulates the energy efficiency and consumption amount of air conditioners and water heaters, and the Environmental Protection Agency (EPA) regulates refrigerants that destroy the ozone layer. Although the United States has taken positive steps internationally such as introducing F-gas phase-down plans (85% by 2033) to the Montreal Protocol Conference as proposals for the three North American countries, it has not developed a clear policy concerning global warming measures for refrigerants within the United States. The current activities of the EPA primarily involve refrigerant conversion to HFCs to protect the ozone level. However, industrial and scientific societies have started earnest activities and have defined mildly flammable refrigerants in Standard 34 for the American Society of Heating, Refrigerating and Air Conditioning Engineers (ASHRAE). Currently, these usage standards are being investigated in Standard 15. The Air-Conditioning, Heating, and Refrigeration Institute (AHRI) is also starting to evaluate new refrigerants.

This document primarily describes the AHRI refrigerant evaluation program “Low-GWP Alternative Refrigerant Evaluation Program (AREP).” The “Low-GWP AREP” began in the spring of 2011. Alternative refrigerant candidates are being solicited, and the test results by standardized methods have been announced. However, the policy is to entrust market evaluation without prioritizing refrigerant candidates. In this program, 21 entities participate as evaluators, and six chemical companies participate as refrigerant suppliers.

Low-GWP refrigerant candidates were announced at the end of October (see Table 2 below). Refrigerant performance is now being evaluated using compressor calorimeter testing, system drop-in testing, and soft-optimized system testing. The basic policy of AHRI is that air conditioner energy consumption causes approximately 90% of the greenhouse gas emissions, whereas less than 10% is the direct result of refrigerant emissions. Accordingly, in evaluating alternative refrigerants, not only is GWP important, but energy efficiency is also extremely important, and the need to evaluate alternative refrigerants based on their Life Cycle Climate Performance (LCCP) and Total Equivalent Warming Impact (TEWI) is being emphasized.

Table 2.2.2 Refrigerant candidate list (AHRI)

Alternative Refrigerants for Testing and Evaluation[1]

Baseline Refrigerants	Alternative Refrigerant Candidates Classifications according to ASHRAE Standard 34			Others[2]
	A1	A2L	A3	
R-134a	AC5X, ARM-41a, D4Y, N-13a, N-13b, Opteon™XP10	AC5, R-1234yf, R-1234ze(E), ARM-42a	R-290+R-600a (40%+60%), R-600a	
R-404A	ARM-32a, N-40a, N-40b, DR-33	ARM-31a, ARM-30a, D2Y-65, L-40, R-32, R-32+R-134a (50%+50%), DR-7	R-290	R-744
R-410A		R-32, ARM-70a, D2Y-60, DR-5, HPR1A L-41a, L-41b, R-32+R-134a (95%+5%), R-32+R-152a (95%+5%)		R-744
R-22/R-407C	ARM-32a, LTR4X, N-20	D52Y, L-20, LTR6A	R-290	R-1270, R-717

Furthermore, an evaluation for the risks of A2L (mildly flammable) refrigerants has been executed, and it has been confirmed that the ignition risk is low in the case of using R32 in residential-use heat-pump-type unitary air conditioners.

2.2.4 Trends in developing countries

In relation to the special characteristics of developing countries, the United Nations Environment Program (UNEP) has taken the lead, and each country is proceeding with their own reduction plan. Although R410A should be selected as the alternative refrigerant for R22 if past procedures are followed, because R410A is not recommended by the UNEP, it seems that many developing countries want to skip this in favor of the next-generation refrigerant.

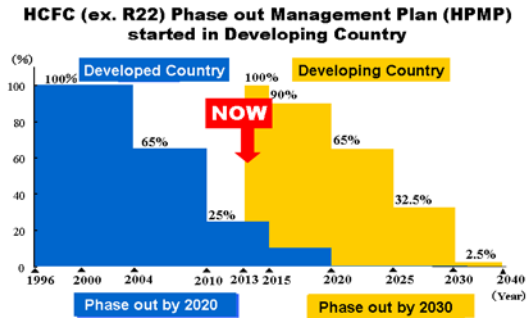

Fig. 2.2.1 Phase out schedule for HCFCs (Montreal Protocol)

1) China

The total amount for refrigeration and air conditioning production is RMB 510 billion (approximately 82 billion U.S. dollars, source: CRAA), and because this is an extremely important country that uses a large amount of refrigerant, funding in the huge amount of 265 million dollars (including the foaming and solvent fields) was obtained from the United Nations Multilateral Fund for measures to protect the ozone layer.

The Chinese government, working with the China Household Electrical Appliances Association (CHEAA), drafted a refrigerant conversion plan for residential-use air conditioners, and conversion is planned mainly from R22 to R290 (propane). A plan is in place to utilize a large number of production lines for this conversion to the new refrigerant type. An advisory committee has been organized, and basic research has been performed on compressors, the maximum amount of charge, and safety design, as well as on connections and a leak detection methodology. This research also includes an evaluation of the combustion risk for a refrigerant leak that exceeds the current limit for the indoor amount of charge (300g) . Furthermore, the domestic standards in GB4706.32-2012 were created in April 2012 in reference to the international standards in IEC 60335-2-40. UN report mentioned that the preparation of the usage standards will be completed in the middle of 2013. To promote these, there will be funding only in the first period (2013–2015) of approximately 75 million dollars from the UN, along with economic and technological assistance from Germany.

An advisory committee for commercial-use air conditioners was established, centering on the China Refrigeration and Air-Conditioning Industry Association (CRAA), and conversion is proceeding from R22 to R32 and R410A. A survey has already been started on the safety standards and product specifications for mildly flammable refrigerants, and research has been performed on the safety of equipment using R32 and its production. The survey is now largely complete, and a proposal was made to the government agency in change (FECO). Based on the results, the preparation of safety standards and product standards is scheduled for completion by 2015. For freezing and refrigeration, the development of an ammonia/CO_2 cascade method as a substitution for R22 is underway. A prototype has already been completed and testing facilities, etc., have been established. To promote refrigerant conversion in the fields of commercial-use refrigeration and air conditioning, support in the amount of approximately 61 million dollars is being provided for the first period (2013–2015) from the UN.

2) India

Concerning refrigerants for the air conditioning field, an announcement was made about a conversion plan that prohibits increasing R22 production line facilities from 2013 and importing air conditioners that use R22 from 2015. Concerning the refrigerant used in the after-sales service sectors, a proposal has been made to use the existing infrastructure to limit increases in consumption amounts. There is also a plan to promote the conversion of R141b in the foaming field.

3) Indonesia

The Indonesian government has set out a policy to phase out R22 in refrigeration and air conditioning equipment by 2015. For this reason, the following regulatory measures are planned. For example, the import and local production of refrigeration and air conditioning equipment that uses R22 will be prohibited from 2015.

Although this plan is to be achieved initially by using R410A, a changeover to R32 is scheduled for the second period (from 2015), involving system preparation related to the mild flammability of this refrigerant. Concerning the refrigerant conversion

for Indonesia, the Japanese Ministry of Economy, Trade and Industry (METI) and two private companies are scheduled to cooperate. Support in the amount of 12.7 million dollars is to be provided from the UN for the conversion expense in the first period (2013–2015), with the fields of freezing and refrigeration to account for more than two-thirds.

4) Thailand

Because the conversion plan to R410A in Thailand supported by the World Bank was rejected by the Multilateral Fund 64th Executive Committee Meeting (July, 2011), the conversion to R32 was proposed and accepted at the 68th Executive Committee Meeting as an alternative low-GWP refrigerant with higher efficiency than R410A. To realize this conversion, it is necessary to improve the testing equipment, refrigerant charging equipment, charge pumps, and gas leak detectors, and it simultaneously becomes necessary to ensure the safety of manufacturing and storage facilities. To facilitate this conversion, the UN and Japan are providing support in the amount of 25.5 million dollars.

References

2.2.1) "Direction for Measures such as Future of Fluorocarbons" Central Environment Council/Industrial Structure Council (Dec. 2012)

2.2.2) "Research project on risk assessment of mildly flammable refrigerants in JSRAE" Hihara *et al.*, JRAIA 2012 Kobe (Nov. 2012)

2.2.3) "Proposal for a regulation on F-gas" EU Commission (Nov. 7, 2012)

2.2.4) "F-Gas Regulation in Europe" EPEE, JRAIA 2012 Kobe (Nov. 2012)

2.2.5) "Overview of AHRI Low Global Warming Potential Alternative Refrigerants Evaluation Program" Amrane. JRAIA 2012 Kobe (Nov. 2012)

2.2.6) JARN Interview of AHRI Amrane (Dec. 25, 2012)

2.2.7) UNEP Multilateral Fund 64th Executive Committee Meeting (Jul. 2011)

2.2.8) UNEP Multilateral Fund 66th Executive Committee Meeting (Apr. 2012)

2.2.9) UNEP Multilateral Fund 68th Executive Committee Meeting (Dec. 2012)

2.2.10) "HPMP Implementation Progress and Risk Assessment of R32 in China" Zhan *et al.*, JRAIA 2012 Kobe (Nov. 2012)

3. Research on safety of mildly flammable refrigerants

3-1. Progress of the University of Tokyo

Eiji HIHARA*, Tatsuhito HATTORI*, Makoto ITO*

* Graduate School of Frontier Sciences, The University of Tokyo

3.1.1 Introduction

According to the Kyoto Protocol, greenhouse gas emissions, including HFCs, should be suppressed. Therefore, low-global warming potential (GWP) refrigerants (R32, R1234yf, etc.) are expected to be the next generation of refrigerants. However, these low-GWP refrigerants are often flammable. Table 3.1.1 lists the physical and flammability properties of the typical refrigerants[3.1.1), 3.1.2)]. Here, LFL expresses the lower flammability limit, UFL expresses the upper flammability limit, BV expresses the burning velocity, and MIE expresses the minimum ignition energy.

Table 3.1.1 Physical and flammability properties of lower-GWP refrigerants[3.1.1), 3.1.2)].

Refrigerant	GWP	LFL [vol%]	UFL [vol%]	BV [cm/s]	MIE [mJ]
R290 (Propane)	< 3	1.8	9.5	38.7	0.246
R32	675	13.3	29.3	6.7	15
R1234yf	4	6.2	12.3	1.5	500

Then, to acquire sufficient information to assess the risks in the usage of these refrigerants, we performed studies in the following areas.

1. Simulation of leakage of mildly flammable refrigerants
2. Thermal decomposition products of lower-GWP refrigerants
3. Self-ignition combustion by the compression of mixed gases consisting of mildly flammable refrigerant, lubricant oil, and air

3.1.2 Study on simulation of leakage of mildly flammable refrigerants

3.1.2.1 Introduction

When refrigerants leak into a space, they tend to accumulate at the floor if they are heavier than air[3.1.3)]. As shown in Fig. 4.1.1, if the refrigerant concentration is higher than the LFL, if there is an ignition source, and if the air velocity is lower than the burning velocity, the refrigerant may ignite. When leakage occurs from a room air conditioner (RAC), there is always a region where the refrigerant concentration is higher than the LFL because the refrigerant concentration is 100% near the outlet from the air conditioner. Thus, appropriate safety standards must be prepared for using RACs containing flammable refrigerants because of the risk of explosion.

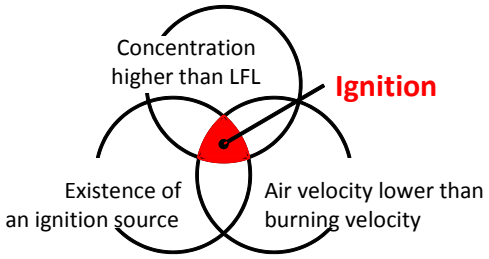

Fig. 3.1.1 Mechanism of ignition

It is important to understand the refrigerant diffusion phenomena when preparing the safety standards. It is also necessary to clarify the effects of parameters on the diffusion phenomena of refrigerants heavier than air. Numerical analysis is an effective tool because it is very difficult to measure the diffusion of a refrigerant in a large space. In this study, diffusion phenomena were numerically analyzed when a refrigerant leaked into a large space such as a living room and office. For an RAC, the calculation results were verified using a refrigerant leakage experiment.

3.1.2.2 Calculation method

The commercial CFD program STAR-CD[3.1.4)] was used to simulate the refrigerant diffusion phenomena. The advection–diffusion problem of a mixture in a three-dimensional space is governed by the continuity, Navier–Stokes, energy conservation, and convective diffusion equations.

Both the air and the refrigerant were assumed to be ideal gases, and the density was calculated using the equation of state of an ideal gas. PISO or SIMPLE was used for the pressure–velocity coupling scheme, and UD and MARS were employed for the discretization scheme. A standard k-ε turbulence model was used. For the boundary conditions, a constant flow condition was applied at the inlet boundary, and a constant pressure condition corresponding to the atmospheric pressure or free outflow condition was applied at the outlet boundary. The law of the wall was assumed at the wall boundary. Table 3.1.2 lists the leakage scenarios for the RAC and Table 3.1.3 lists the leakage scenarios for variable refrigerant flow (VRF) air conditioning systems.

3.1.2.3 Analytical model

(1) Leaks from wall-mounted indoor unit

The size of the space the refrigerant leaks into from a wall-mounted indoor unit was assumed to be 2.8 m × 2.5 m × 2.4 m. The indoor unit was located 1.8 m above the floor at the center of one of the walls. The size of the indoor unit was 0.6 m × 0.24 m × 0.3 m, and the indoor unit had an air outlet with a size of 0.6 m × 0.06 m. The refrigerant leaked from this air outlet. The measuring points for the concentration were located 0.6 m from the opposite side of the wall and 0.01, 0.2, 0.4, 0.6, 1.0, and 1.5 m above the floor. In total, 195,516 non-equidistant mesh points were used to discretize the governing equations. Figure 3.1.2 shows the geometry of the calculation field of the wall-mounted indoor unit.

Table 3.1.2 Leakage scenarios for RAC

No.	Position of leakage	Refrigerant	Amount [g]	Flow rate [g/min]
1	Wall-mounted indoor unit	R32	1000	250
2	ditto	R1234yf	1400	350
3	ditto	R32	1000	125
4	ditto	R1234yf	1400	175
5	ditto	R32	1000	1000
6	ditto	R1234yf	1400	1400
7	ditto	R290	500	125
8	ditto	R290	200	50
9	Floor-mounted indoor unit	R32	1000	250
10	ditto	R1234yf	1400	350
11	Outdoor unit	R32	1000	250
12	ditto	R1234yf	1400	350
13	ditto	R32	1000	250
14	ditto	R1234yf	1400	350
15	ditto	R32	1000	250
16	ditto	R1234yf	1400	350

Table 3.1.3 Leakage scenarios for VRF

No.	Refrigerant	Amount [kg]	Flow rate [kg/h]	Forced air [m^3/h]	Air vent
1	R32	26.3	10	0	none
2	R1234yf	29.4	10	0	none
3	R32	26.3	10	0	exists
4	R1234yf	29.4	10	0	exists
5	R32	26.3	10	169	exists
6	R1234yf	29.4	10	169	exists
7	R32	26.3	10	0→169	exists
8	R1234yf	29.4	10	0→169	exists
9	R32	26.3	10→0	0	exists
10	R1234yf	29.4	10→0	0	exists

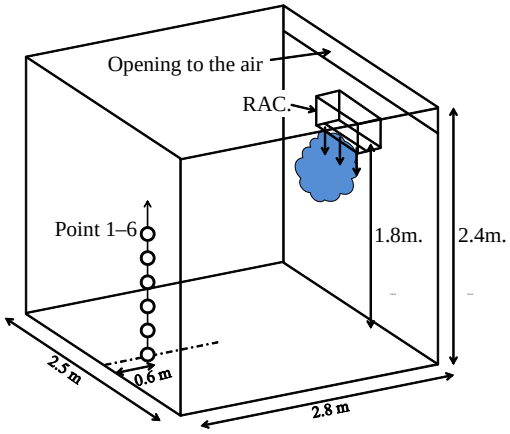

Fig. 3.1.2 Indoor space, including wall-mounted indoor unit

(2) Leaks from floor-mounted indoor unit

The size of the space where the refrigerant leaked from the floor-mounted indoor unit was equal to that where the refrigerant leaked from the wall-mounted indoor unit. The indoor unit was located on the floor at the center of one of the walls. The size of the indoor unit was 0.7 m × 0.21 m × 0.6 m, and the indoor unit had an air outlet with a size of 0.46 m × 0.045 m. The refrigerant leaked from this air outlet. The measuring points for the concentration were located 0.6 m from the opposite side of the wall and 0.01, 0.05, 0.1, 0.2, 0.4, and 0.6 m above the floor. In total, 235,144 non-equidistant mesh points were used to discretize the governing equations. Figure 3.1.3 shows the geometry of the calculation field, including the floor-mounted indoor unit.

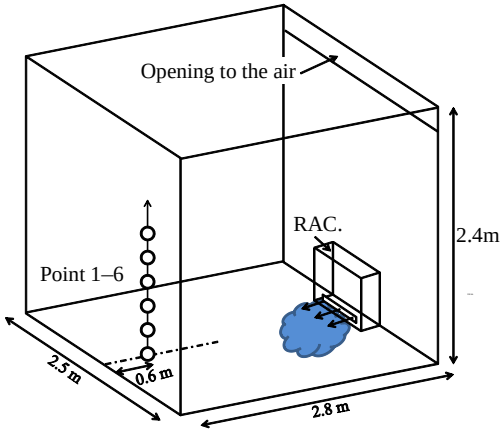

Fig. 3.1.3 Indoor space, including floor-mounted indoor unit

(3) Leaks from outdoor unit

The refrigerant leaked from an outdoor unit placed on a balcony with a size of 5.0 m × 1.2 m × 1.1 m. The outdoor unit was located on the floor at the left side of the balcony. The size of the outdoor unit was 0.77 m × 0.29 m × 0.68 m, and the outdoor unit had a fan that was 0.4 m in diameter. For No. 13 and No. 14, a drain with a diameter of 0.05 m was located on the floor at the right side of the balcony. For No. 15 and No. 16, the drain and a 0.03 m × 1.2 m undercut were located on the floor at the right side of the balcony. The refrigerant leaked from the fan. In addition, a wind of 0.5 m/s was assumed to be blowing around the balcony. The measuring points for the concentration were located at the center of the balcony and 0.01, 0.05, 0.1, 0.2, 0.4, and 0.6 m above the floor. In total, 348,492 non-equidistant mesh points were used to discretize the governing equations. Figure 3.1.4 shows the geometry of the calculation field.

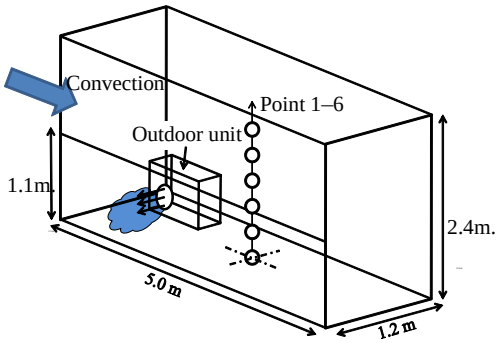

Fig. 3.1.4 Outdoor space, including outdoor unit

(4) Leaks from variable refrigerant flow

The refrigerant leaked from a VRF placed in an office with a size of 6.5 m × 6.5 m × 2.7 m. The indoor unit of VRF was located on the ceiling at the center of the office. It had an air outlet that was 0.45 m × 0.0645 m in size and a suction that was 0.37 m in diameter. The refrigerant leaked from the air outlet and suction. The office also had 0.2 m × 0.2 m air supply and exhaust grills, and the gap under the door was 1.5 m × 0.01 m. The measuring points for the concentration were located 1.0 m from the wall and 0.01, 0.2, 0.4, 0.6, 1.0, and 1.5 m above the

floor. In total, 195,516 non-equidistant mesh points were used to discretize the governing equations. Figure 3.1.5 shows the geometry of the calculation field, including the VRF.

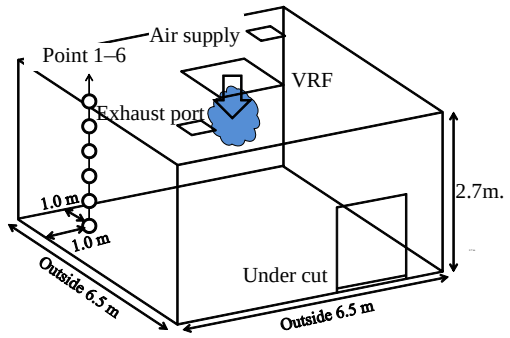

Fig. 3.1.5 Office, including VRF

3.1.2.4 Results and discussion

Table 3.1.4 lists the calculation results for the RAC and Table 3.1.5 lists the calculation results for the VRF. Σ(V·t) expresses products of the flammable gas volume and presence time. This value is involved in the risk and is called the flammable volume time (FVT) below. In addition, V_{FL} represents the flammable gas volume, whereas V_{BVFL} is the flammable gas volume with air velocity lower than the burning velocity.

(1) Leaks from wall-mounted indoor unit

Figure 3.1.6 shows the concentration distributions of R32 at the end of leakage for No. 1 in Table 3.1.2. The green surfaces in these figures indicate isosurfaces of the concentration at the LFL (13.3 vol%), which suggest the presence of flammable gas. According to Fig. 3.1.6, a combustible gas region only exists just below the air outlet of the indoor unit, even if all of the refrigerant is discharged.

According to Table 3.1.4, the FVT is very small, even if a mildly flammable refrigerant leaks from the wall- mounted indoor unit. In addition, from No. 1 to No. 6, the FVT values that consider the burning velocity are equal 0. This indicates that ignition does not occur because of the convection caused by the refrigerant leakage, even if an ignition source exists. Therefore, no combustion occurs if no ignition source exists inside the indoor unit. For No. 7, although the calculated value is higher than the maximum allowable fill ration of propane, it represents a great hazard because the FVT value is very high compared to the others. For No. 8, the MIE of propane is lower than R32 and R1234yf and the quenching distance of propane is very narrow. Therefore, it is a hazard because a flame transmits easily.

Table 3.1.4 Results of calculation for RAC

No.	Presence time [min]	$\Sigma(V_{FL}\cdot t)$ [m^3·min]	$\Sigma(V_{BVFL}\cdot t)$ [m^3·min]
1	4.01	1.18×10^{-2}	0
2	4.01	1.23×10^{-2}	0
3	8.01	9.79×10^{-3}	0
4	8.01	1.07×10^{-2}	0
5	1.03	3.73×10^{-2}	0
6	1.05	4.34×10^{-2}	0
7	1473	7689	7688
8	4.73	0.258	0.161
9	111	136.83	136.81
10	309	507.82	507.50
11	45	43.01	42.50
12	93	62.54	61.53
13	15	8.93	8.43
14	15	5.81	4.61
15	4.33	9.70×10^{-1}	1.01×10^{-1}
16	4.33	1.03	1.67×10^{-2}

Table 3.1.5 Results of calculation for VRF

No.	Presence time [min]	$\Sigma(V_{FL}\cdot t)$ [m^3·min]	$\Sigma(V_{BVFL}\cdot t)$ [m^3·min]
1	157.85	1.622	0.021
2	176.47	2.152	0
3	157.82	0.831	0.011
4	176.42	0.661	0
5	157.82	0.702	0.014
6	176.41	0.583	0
7	157.82	0.725	0.011
8	176.41	0.592	0
9	8.36	3.14×10^{-2}	0

10 10.25 2.14×10^{-2} 0

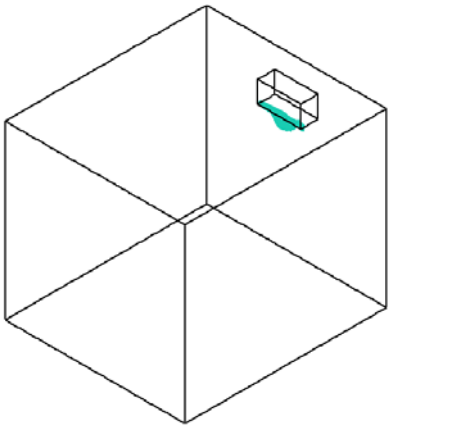

Fig. 3.1.6 Concentration profiles of R32 at end of leakage (No. 1 in Table 3.1.2)

(2) Leaks from floor-mounted indoor unit

The green surfaces in Figure3.1.7 indicate isosurface of the concentration at the LFL (13.3 vol%) at the end of the leakage. Figure 3.1.7 shows that the combustible gas region spreads over the floor. Thus, the flammable gas volume exists for a long time, more than 100 min for No. 9 and more than 300 min for No. 10. Therefore, the FVT value is larger than that for the wall-mounted indoor unit.

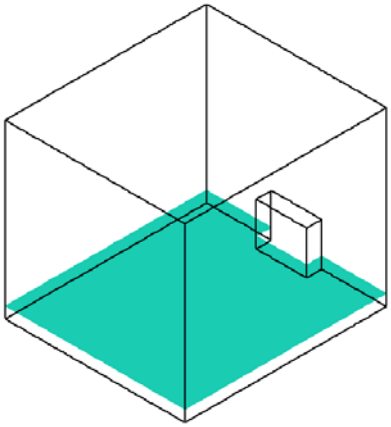

Fig. 3.1.7 Concentration profiles of R32 at end of leakage (No. 9 in Table 3.1.2)

According to Table 3.1.4, both of the FVT is very similar. It is indicated that the air velocity is lower than the burning velocity in the combustion region. Therefore, if an ignition source exists in the combustion region, there is a risk of combustion throughout much of the combustion region. In addition, because the LFL of R1234yf is lower than that of R32, the presence time of R1234yf is longer than that of R32. Thus, the risk with R1234yf is higher than that with R32.

Therefore, safety regulations are required when flammable refrigerants are used in air conditioners, because the risk of leakage from a floor-mounted indoor unit is higher than with a wall-mounted indoor unit.

(3) Leaks from outdoor unit

The green surfaces in Figure3.1.8 indicate isosurface of the concentration at the LFL at the end of the leakage for No. 11 in Table 3.1.2. According to Fig. 3.1.8, the combustible gas region spread on the floor at the end of the leakage because the outdoor unit was set on the floor.

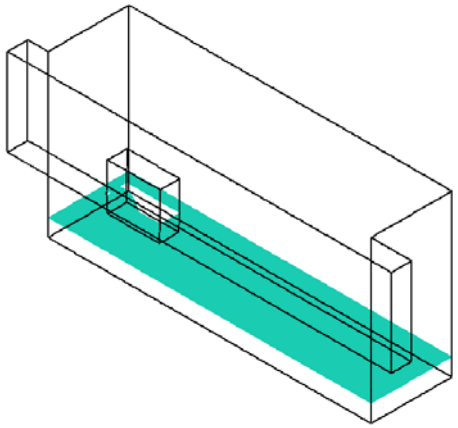

Fig. 3.1.8 Concentration profiles of R32 at end of leakage (No. 11 in Table 3.1.2)

According to Table 3.1.4, the flammable gas volume existed for a long time, for the same reason as that explained for the floor-mounted indoor unit. In addition, considering the drain and under cut, the presence time is shorter and the FVT is smaller.

(4) Leaks from variable refrigerant flow

The green surfaces in Figure3.1.9 indicate isosurface of the concentration at the LFL at the end of the leakage for No. 3 in Table 3.1.3. According to Fig. 3.1.9, a combustible gas region only exists just

below the air outlet and the suction of the VRF, even if the entire quantity of refrigerant is discharged.

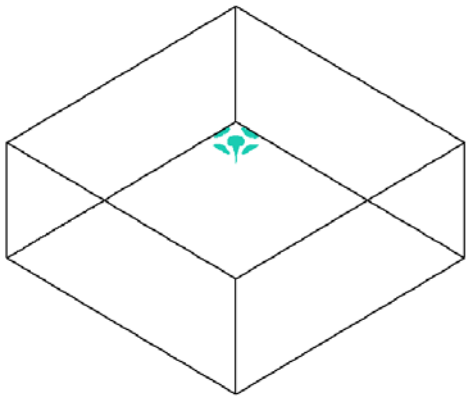

Fig. 3.1.9 Concentration profiles of R32 at end of leakage (No. 3 in Table 3.1.3)

According to Table 3.1.5, the existence of an air vent as an air supply source affects the FVT and presence time. In addition, the released period of VRF is more than 150 min because of the large leaked amount. Therefore, although the flammable gas volume is small, the FVT ($\Sigma(V_{FL}\cdot t)$) is longer than that for leakage from a wall-mounted RAC. On the other hand, the FVT decreases significantly when considering the air velocity. For R1234yf, the risk of ignition is very low because the burning velocity is low. For R32, safety regulations, pertaining, for example, to a refrigerant leakage sensor, alarm, and ventilation, are required when flammable refrigerants are used in air conditioners.

3.1.2.5 Refrigerant leakage experiment

(1) Experiment method and conditions

The refrigerant concentration was measured in an experiment room of the same size as that used for the numerical RAC calculation. Figure 3.1.10 shows a diagram of the experiment system. When the refrigerant is discharged from a gas cylinder, it is cooled by evaporative latent heat. Then, the temperature of the refrigerant was raised to a prescribed value using a thermostatic bath. The flow rate was controlled using a mass flow controller. Refrigerant was leaked into the experiment room, and the refrigerant concentration was measured using a concentration sensor. The experiment was carried out under the same conditions as No. 1, No. 3, and No. 9 in Table 3.1.2.

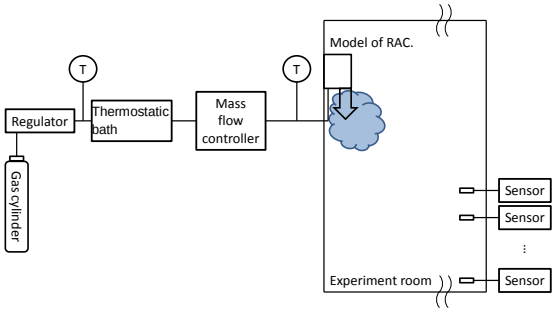

Fig. 3.1.10 Diagram of experiment system

(2) Results and discussion

Figures 3.1.11 show a comparison of the experimental and calculation results for each experimental condition.

For the leakage from the wall-mounted indoor unit, both sets of results suggest that lower positions lead to higher refrigerant concentrations, whereas the time of arrival of the refrigerant also showed a positive inclination in the calculation results. However, the refrigerant concentration at a low position resulted in a lower concentration than the calculation results at the end of the leakage, indicating that the experiment with the wall-mounted indoor unit yielded safer results than those found in the calculation.

For the experiment on the leakage from a floor-mounted indoor unit, the refrigerant concentration on the floor was more or less equal to the calculation results. However, the time before the concentration on the floor became less than the LFL was shorter than that in the calculation results. Such a result could have been affected by the difficulty of creating a completely windless environment within the experiment room. For example, the exhaust duct of the experiment room was connected to the exterior of the room, which raised an issue with

convection because of the pressure difference between the experiment room and the exterior. With this in mind, it might be suggested that suppressing the convection would yield a safer result. This creates a favorable situation when making risk assessments. Thus, the simulation of the diffusion phase proved to be valuable for this research.

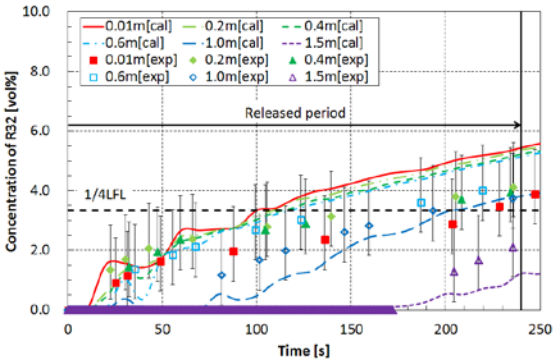

(a) Wall-mounted, R32, 1000 g, 250 g/min

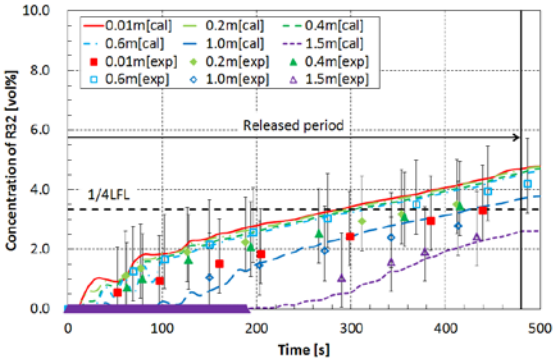

(b) Wall-mounted, R32, 1000 g, 125 g/min

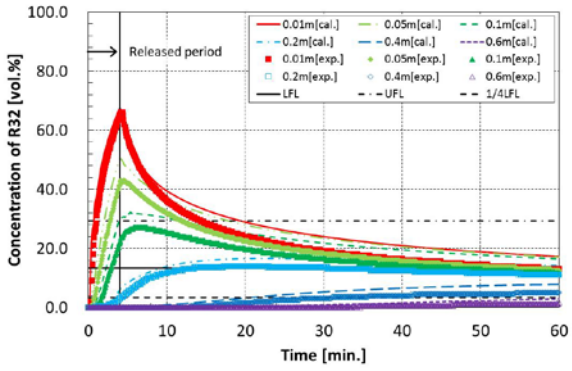

(c) Floor-mounted, R32, 1000 g, 250 g/min

Fig. 3.1.11 Comparison of experimental and calculation results

Moreover, the fact that the concentration on the floor, which is thought to be the least affected by convection, did not result in the LFL by the leakage from the wall-mounted indoor unit concurred with the calculation results. In the experiment on the leakage from a floor-mounted indoor unit, the fact that the concentration on the floor exceeded the UFL at the end of the leakage from the floor-mounted indoor unit also concurred with the calculation results. Therefore, the experiment confirmed that the concentration on the floor does not reach the LFL with the leakage from the wall-mounted indoor unit and exceeds the UFL for the leakage from the floor-mounted indoor unit.

3.1.2.6 Conclusions

In this study, the following information was obtained by the simulation and experiments involving refrigerant leaking into a space.

1) With leakage from a wall-mounted indoor unit, combustion does not occur if no ignition source exists inside the indoor unit.
2) In relation to the leakage from a floor-mounted indoor unit, safety regulations are required when flammable refrigerants are used in air conditioners.
3) For the leakage from an outdoor unit, considering the drain and under cut, the presence time is shorter and the FVT is smaller.
4) For the leakage from a floor-mounted indoor unit and outdoor unit, the risk with R1234yf is higher than that with R32.
5) For the leakage from VRF, considering the burning velocity, FVT is much smaller.
6) The experiment confirmed that the concentration on the floor does not reach LFL with leakage from a wall-mounted indoor unit and exceeds the UFL with leakage from a floor-mounted indoor unit.

3.1.3 Thermal decomposition products of lower GWP refrigerants

3.1.3.1 Introduction

To analyze the risks when using lower-GWP refrigerants, it is necessary to clarify their decomposabilities and products. However, the high reactivities of products like hydrogen fluoride (HF) make this quantification difficult. Moreover, Takizawa et al.[3.1.5)] proposed that the reactivity of a molecule with more fluorine atoms than hydrogen atoms, like R1234yf, is affected by humidity. Thus, its flammability limits and product composition are changed.

This study was carried out to quantify HF, the main toxic product, and to analyze other products in the thermal decomposition of refrigerants.

3.1.3.2 Experimental apparatus and methods

(1) Experimental apparatus

There are two causes of HF generation from refrigerants: thermal decomposition by heating and combustion. In this research, only an experimental apparatus for thermal decomposition was fabricated.

This experimental apparatus consisted of four parts: gas mixing, heating, measuring, and detoxification parts.

The gas mixing part was used to mix refrigerant and air at a specified concentration and humidity. The concentration was controlled by mass flow controllers, and the humidity was controlled by a dehumidifier and humidifier.

The heating part was used to heat a gas sample and make it react in a straight pipe. This consisted of a mullite ($3Al_2O_3 \cdot 2SiO_2$) pipe (inner diameter: 11 mm) and 550-mm-long electric furnace around the pipe. Three thermocouples were set on the outside wall and three were set on the inside wall of the pipe. To prevent these thermocouples from corroding, the inside ones were mounted in a mullite protection tube (the outer diameter was 6 mm). The gas sample flowed in the gap between the two tubes. This was 2.5 mm wide, with a cross-section of 2.67 cm^2.

The measuring part consisted of gas cells for FT-IR. To broaden the concentration measurement range, two cells with different path lengths were used.

The detoxification part consisted of an absorbance tube, which exhausted into a fume hood.

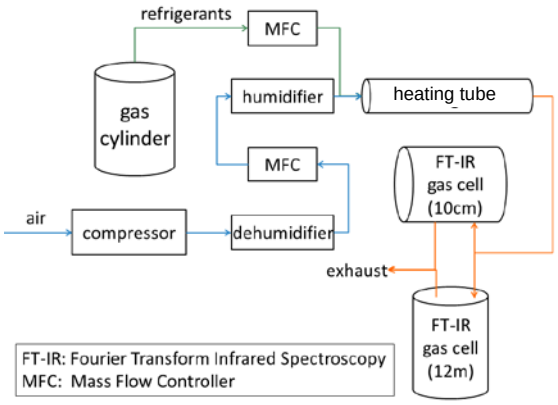

Fig. 3.1.12 Schematic diagram of experimental apparatus

(2) Target materials

The target materials were mixtures of refrigerants (R32, R1234yf) and air, and traditional refrigerants like R134a are under consideration.

(3) Measuring instruments

An FT/IR-4200 (by JASCO) and gas cell (temperature-controlled, 10-cm path length, by Harrick) were applied to measure the concentrations of the refrigerants and products.

To avoid instrument corrosion caused by HF, FT-IR was applied, using a detector that was not exposed to the sample gas.

(4) Measuring method

Examples of the spectra of R32 and R1234yf are shown in Figs. 3.1.13 and 3.1.14, respectively, where “Abs.” (absorbance) on the vertical axis is defined as

$$\text{Abs.} = \log_{10}\left(B_e^{\,R}/B_e^{\,S}\right) \qquad (3.1.1)$$

$B_e^{\,S}$: Signal strength when sample fills gas cell

B_e^R: Signal strength when sample is removed

and it is proportional to the concentration, pressure, and path length.

To quantify the refrigerant, a calibration curve showing the absorbance at each wavenumber was used. The following were considered when selecting the wavenumbers in Table 3.1.6: not close to strong peaks of other materials like H_2O and CO_2, linearity, and moderate concentration under LFL.

For hydrogen fluoride, 3877 cm^{-1}, which is used in quantitative analysis[3.1.6)] as the influence on absorbance caused by hydrogen bonds, was changed by the temperature and concentration. In addition, a calibration curve was drawn for nitrogen diluted gas (118, 301, 770 ppm) and used.

The relative calibration errors for R32 and R1234yf are shown in Figs. 3.1.15 and 3.1.16, respectively. That for R32 has a range of ±4%, whereas that for R1234yf has a range of ±10%, except at lower concentrations.

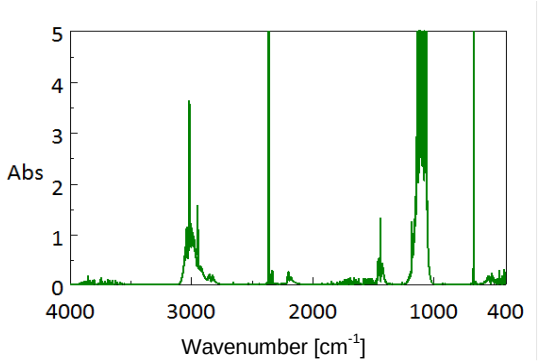

Fig. 3.1.13 Spectrum of R32 (12% in air)

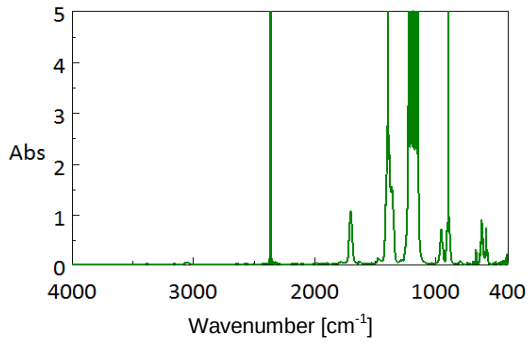

Fig.3.1.14 Spectrum of R1234yf (5% in air)

Table 3.1.6 Wavenumbers used for quantification

Material	Wavenumber [cm^{-1}]	Corresponding bond
R32	2947	$-CH_2-$
R1234yf	1356	C=C
HF	3877	HF

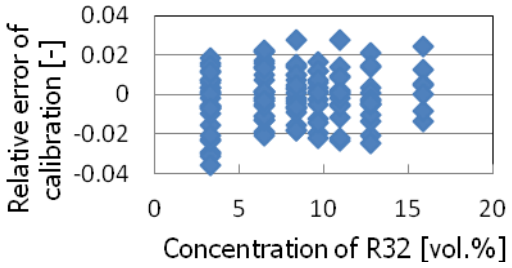

Fig. 3.1.15 Relative error of calibration (R32)

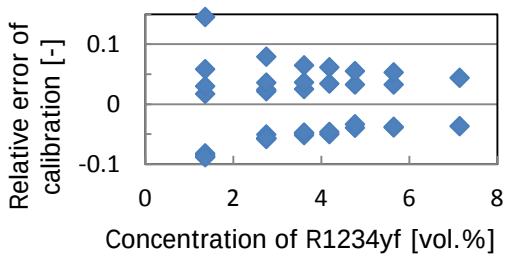

Fig. 3.1.16 Relative error of calibration (R1234yf)

(5) Experimental conditions

The following parameters were used as the experimental conditions.

1) Temperature of heater: 450–700°C
2) Concentration of refrigerant: four points under its LFL
3) Total flow rate: 100–200 ml/min
4) Humidity: 0–60% RH

3.1.3.3 Results

(1) Decomposition of refrigerants

First, the remain rates of the refrigerants versus the heater temperature without humidification are shown in Figs. 3.1.17 and 3.1.18. The parameter is the refrigerant concentration (vol. %), and the flow rate shown is the total for the refrigerant and air. For

both refrigerants, there was little decomposition when the heater temperature was 500°C or lower, but when it was 550°C or higher, the remain rate decreased.

Next, the remain rates of R1234yf versus humidity when it was humidified are shown in Figs. 3.1.19 and 3.1.20. Takizawa et al.[3.1.2)] proposed that the reactivity of R1234yf is affected by humidity, but in this result, the reactivity was not affected.

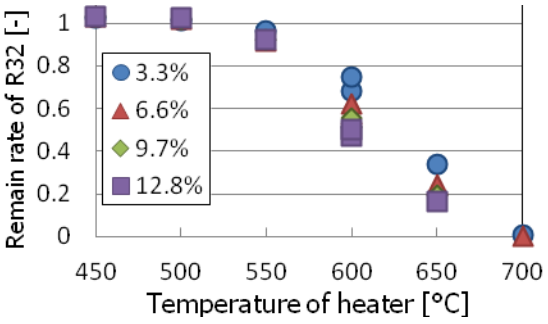

Fig. 3.1.17 Remain rate of R32 and heater temperature (dry, total 100 ml/min with air)

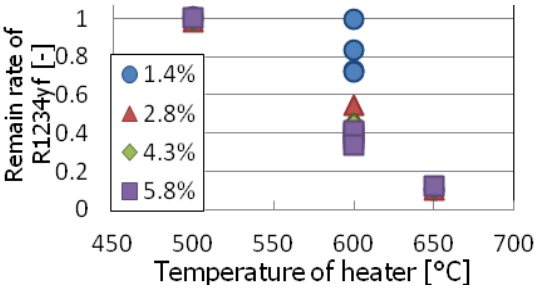

Fig. 3.1.18 Remain rate of R1234yf and heater temperature (dry, total 100 ml/min with air)

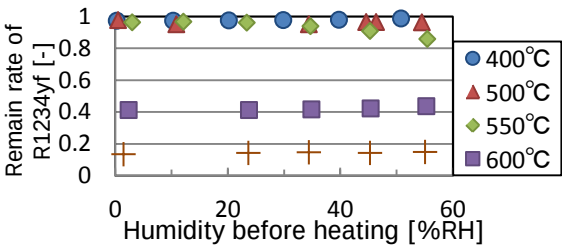

Fig. 3.1.19 Remain rate of R1234yf and humidity (total 100 ml/min, 2.8 vol% in air)

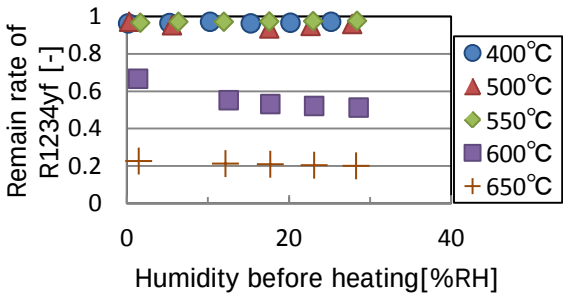

Fig. 3.1.20 Remain rate of R1234yf and humidity (total 200 ml/min, 2.8 vol% in air).

(2) Decomposition products

The amount of generated HF in the experiment of Fig. 3.1.17 is shown in Fig. 3.1.21. As the temperature and/or concentration increased, the generation of HF also increased. However, despite an estimation that the HF concentration would be proportional to that of R32, the effect of the concentration was much less, and the HF quantity itself was $^{1}/_{10}$–$^{1}/_{30}$ of the value estimated from the decomposition of R32.

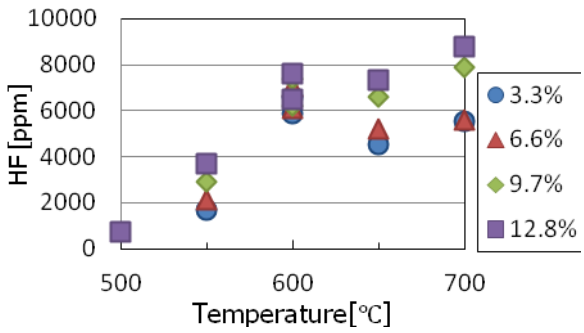

Fig. 3.1.21 Hydrogen fluoride and heater temperature (R32, dry, total 100 ml/min with air)

In experiments with R1234yf, the amount of HF generation was too small to detect. It is estimated that this did not mean that the amount of HF was too small, but rather that R1234yf or its decomposition products trapped the HF on the wall of the heating pipe. However, the mechanism for this trapping is not clear.

3.1.3.4 Discussion

The chemical reaction in the thermal decomposition can be estimated as listed below[3.1.5]. That for R32 is

$$CH_2F_2 + O_2 \rightarrow 2HF + CO_2,$$

And that for R1234yf is

In the absence of H_2O,

$$CF_3CF=CH_2 + 5/2O_2 \rightarrow 2CO_2 + COF_2 + 2HF$$

In the presence of H_2O,

$$CF_3CF=CH_2 + 5/2O_2 + x(H_2O) \rightarrow (2+x)CO_2 + (1-x)COF_2 + 2(1+x)HF$$

However, in the experiments performed in this research, not only was the amount of HF generated lower than the estimated value, but the COF_2 peak at around 1930 cm^{-1} [3.1.5] was also not detected under the condition that the R1234yf was sufficient to run out of humidity (H_2O) in the air.

The reason for the absence of R1234yf was estimated to be because the wall and HF reacted like

$$AlO_3 + 3HF \rightarrow AlF_3 + {}^3/_2H_2O + {}^3/_4O_2$$

and provided H_2O, which reacted with COF_2.

It is not clear why no HF was detected in the experiment with R1234yf. However, after this experiment, under the conditions that only air flowed and the heater was set at 600°C, HF was detected after one or two hours. Thus, the HF trapping on the wall was assisted more by R1234yf than R32.

In almost all of the applied conditions, which were the risk assessment targets, these products reacted with a hot surface. Thus, clarifying the effect of materials of hot surfaces is important.

3.1.3.5 Conclusion

In the experiment in the mullite pipe, the decomposition reaction rate of R32 increased at temperatures higher than 500–550°C, whereas that of R1234yf increased at temperatures higher than 500–600°C. However, no effect from the humidity was detected in the interaction with the wall. Clarifying the effect of the wall materials will require further investigation.

3.1.4 Self-ignition combustion by compression of mixed gas of mildly flammable refrigerant, lubricant oil, and air

3.1.4.1 Introduction

As an event that can be expected during the pump down of flammable refrigerants (refrigerant collection) in refrigeration equipment, the lubricant oil and refrigerant may reach the self-ignition combustion point during the temperature rise caused by the adiabatic compression of a mixed gas consisting of a mildly flammable refrigerant, lubricant oil, and air. It is possible that this will increase the pressure and damage the equipment. In connection with such events, the accidental destruction of outdoor air conditioning units have been reported[3.1.8), 3.1.9)]. Here, we conducted an experiment that compressed a mixed gas consisting of a mildly flammable refrigerant (R32, R1234yf), lubricant oil, and air in a model engine, and report the existence or condition of self-ignition combustion.

3.1.4.2 Experimental device and method

Figure 3.1.22 below shows a schematic of the equipment used in the experiment. This was mainly composed of a refrigerant supply system, air supply system, lubricant oil supply system, and compressor (model engine) driven by a motor.

(1) Compressor

We used a model engine (4-cycle R115-4C, stroke volume was 25.42 cc, compression ratio was 6.7, and it was made by ENYA) for the compressor, and drove it using a motor (servo-motor HF-JP703(B), made by Mitsubishi Electric) directly connected to the crank shaft of the engine. We also controlled the rotational speed using a personal computer.

(2) Air supply system

A compressor (oil-less air compressor 39L/ACP-160SL, made by EARTH MAN) raises the air pressure to 0.7 MPa, after which it passes

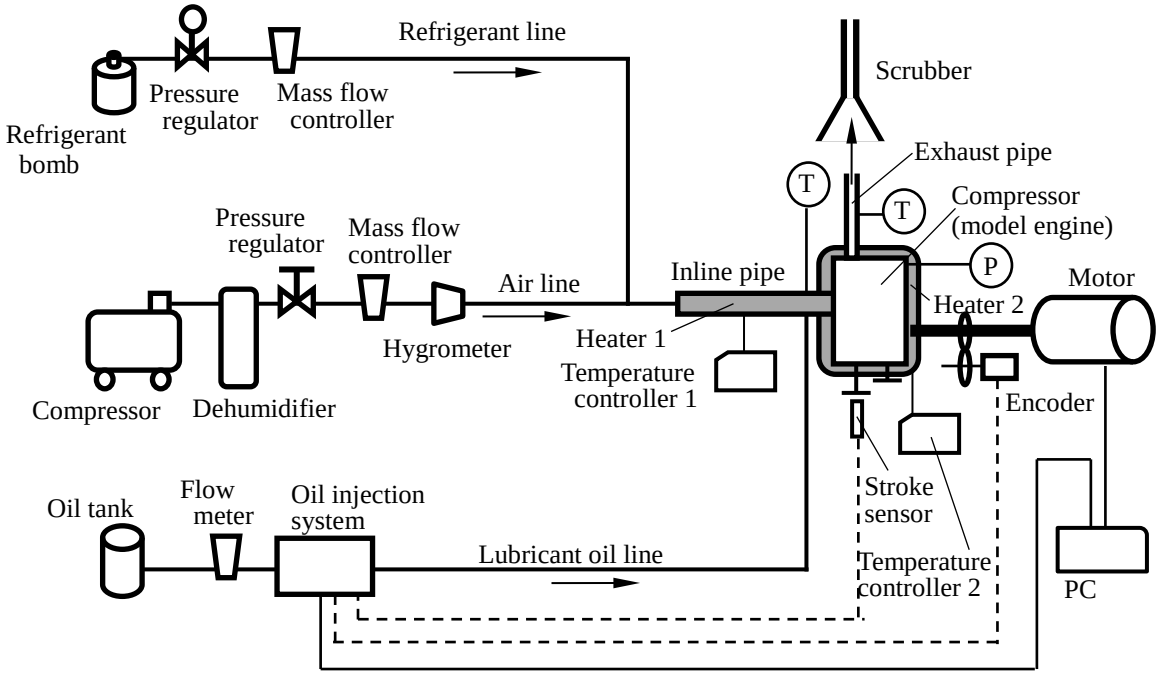

Fig. 3.1.22 Experimental apparatus

through a dehumidifier (air dryer GK3103, made by CKD) and is reduced to 0.4 MPa by a pressure regulator. Then, the flow rate is controlled by a mass flow controller (Model8500, made by Kofloc). The air goes through a hygrometer and humidity transmitter EE33-MFTE3022HA03D05, made by TEKHNE) and enters an inline pipe.

(3) Lubricant oil supply system

The lubricant oil exits the oil tank and passes through a flow meter (micro-flow meter MODEL213-311/295, made by TOYO CONTROL). Then, it is raised to a pressure of 150–180 MPa by the oil injection system (common rail electric control fuel injection system, made by FC DESIGN), and is injected in the form of a spray. It is injected from the upstream side (about 6 cm) of the engine intake in the direction of the intake. We determined the timing of the injection from the encoder and the stroke sensor.

(4) Refrigerant supply system

The refrigerant moves from the refrigerant bomb to the pressure regulator in the form of a gas and reaches a pressure of 0.3 MPa. Then, it is mixed with the air, where the flow rate is controlled by the mass flow controller (FCST1500FC, made by Fujikin), and enters the inline pipe.

The inlet temperature of the mixed gas at the inline pipe of the compressor (model engine) is raised by heater 1 around the inline pipe (the diameter inside is 10 mm and it is made of stainless steel), and its temperature is controlled by temperature controller 1. Heater 2 heats the outside of the compressor, with temperature controller 2 controlling its temperature to ensure that it is the same as the inlet temperature of the mixed gas at the inline pipe.

The gas temperatures at the inlet and outlet of the compressor are measured using sheathed thermocouples, and the pressure in the compressor is measured using a pressure gauge (6045A31, made by KISTLER). These values, along with the flow rates of the air, refrigerant, and lubricant oil, are recorded on a computer using a data logger (data logger system NR-2000, made by KEYENCE).

Table 3.1.7 lists the refrigerant and lubricant oil that we used. We determined the lubricant oil's flow rate on the basis of the theoretical air/fuel ratio.

This ratio was calculated from the air flow rate determined by the rotational speed and stroke volume of the engine. Table 3.1.8 lists the results of the CHO component analysis of the oil (by SVC Tokyo). The theoretical air/fuel ratio of the PAG (VG46) is 9.5. We used the rotational speed, inlet temperature of the mixed gas at the inline pipe, flow rate of the lubricant oil, and flow rate of the refrigerant as experimental parameters.

Table 3.1.7 Refrigerant and lubricant oil

Item	Test substance
Refrigerant	R1234yf, R32
Lubricant oil	PAG (VG46)

Table 3.1.8 CHO component analysis of oil

PAG (VG46)	mass%
C	61.7
H	10.5
O	26.2

We investigated the self-ignition combustion of a mixed gas consisting of air and lubricant oil in experiment 1, and its conditions are listed in Table 3.1.9. We mainly used the theoretical air/fuel ratio for the flow rate of the lubricant oil. When the rotational speed was 500 rpm and the amount of lubricant oil that was the same as the theoretical air/fuel ratio was expressed as 100, we changed the flow rate of the lubricant oil from 60 to 120 and checked the influence of the density of this amount of lubricant oil.

Table 3.1.9 Conditions of experiment 1

Air-oil mixed gas	
Rotational speed [rpm]	500–1500
Air flow rate [l/min]	6.3–18.8
Inlet air temperature [°C]	25–300
Oil flow rate [l/min]	$(5.1–25.7) \times 10^{-4}$

In experiment 2, we investigated the self-ignition combustion of a mixed gas of air, lubricant oil, and the refrigerant R1234yf, and its conditions are listed in Table 3.1.10. The total flow rate was the sum of the air and refrigerant flow rates, and we did not consider the amount of lubricant oil. The refrigerant flow rates listed in Table 2.11 varied from 20% to 90% of the total flow rate.

Table 3.1.10 Conditions of experiment 2

Air-R1234yf-oil mixed gas	
Rotational speed [rpm]	500–1000
Total flow rate [l/min]	6.3–12.5
Inlet mixture gas temperature [°C]	260
R1234yf flow rate [l/min]	2.5–12.5

We also investigated a mixed gas consisting of air, lubricant oil, and the refrigerant R32 in experiment 3, and its conditions are listed in Table 3.1.11. The flow rate of R32 varied from 30% to 90% of the total flow rate. We set the flow rate of the lubricant oil in experiments 2 and 3 as the theoretical air/fuel ratio.

Table 3.1.11 Conditions of experiment 3

Air-R32-oil mixing gas	
Rotational speed [rpm]	500–1250
Total flow rate [l/min]	6.3–15.6
Inlet mixture gas temperature [°C]	260
R32 flow rate [l/min]	5–14.1

All of the experiments were conducted under each condition for the flow rate, inlet temperature of the mixed gas, rotational speed, and lubricant oil injection shown above, and we recorded the data.

3.1.4.3 Results

We changed the inlet temperature of the mixed gas at the inline pipe and checked the condition of the inlet temperature when self-ignition combustion of the lubricant oil occurred in experiment 1. In experiments 2 and 3, under the inlet temperature condition known from experiment 1, we investigated the self-ignition combustions of mixed gases containing R1234yf or R32, and looked for the existence of self-ignition compared with

experiment 1. We determined that self-ignition existed based on the pressure in the cylinder, the temperature of the exhaust gas (as measured by a thermocouple at the exhaust port), an exhaust gas' analysis (using a combustion exhaust gas analyzer, testo340, made by Testo), and observation of the exhaust gas.

(1) Results of experiment 1

Figure 3.1.23 shows the representative pressure change in the cylinder when we changed the temperature of the mixed gas at the inline pipe. The rotational speed was 500 rpm, and the flow rate of the lubricant oil was the same as the theoretical air/fuel ratio in this experiment. The horizontal axis in this figure shows the rotary angle, where the highest position of the piston (top dead center) is the standard. When the inlet temperature was 30°C, the pressure started rising at 220° and reached the highest pressure of 1 MPa at 360°. Afterward, the pressure decreased. The pressure rose and dropped smoothly. The exhaust valve began to open at around 470°, and the pressure reached atmospheric pressure.

When the inlet temperature rose to around 227°C, the rotational sound of the engine came to give off abnormal noise and the pressure waveform started to change at 300°. The highest pressure was 1.35 MPa. In this case, the temperature of the exhaust gas rose slightly higher than the inlet temperature, and the color of the gas tended to be white. When the inlet temperature rose to 291°C, the rotational sound became abnormal, and the pressure rose suddenly to 1.3 MPa at angles greater than 330°. Then, the pressure fell to 1.05 MPa, rose again, and decreased. In this case, the temperature of the exhaust gas rose 20–50°C higher than the inlet temperature, and the color of the exhaust gas was white. These changes had plasticity. As for the analysis of the exhaust gas, in the case where the inlet temperature of the mixed gas was 150°C, the O_2 density was 21%, CO was 500 ppm, and NO was 3 ppm. On the other hand, in the case of 250°C, the O_2 density was 12%, CO was 2200 ppm, and NO was 300 ppm. It is significant that the O_2 density decreased and the CO and NO densities increased when the inlet temperature increased to 250°C from 150°C. From these results, it is theorized that combustion was generated at 250°C.

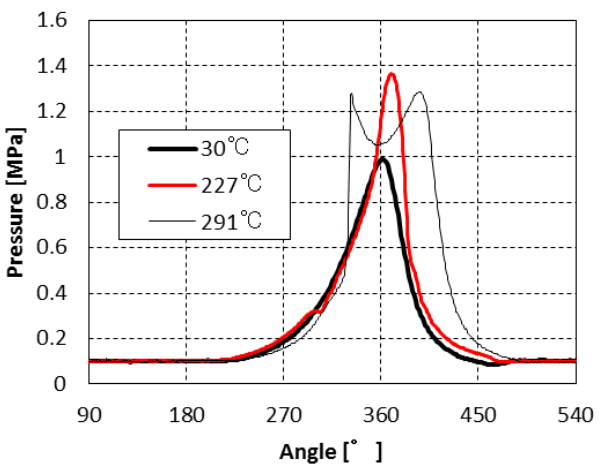

Fig. 3.1.23 Pressure changes for 500 ppm

(2) Results of experiment 2

Based on the results of experiment 1, we set the temperature of the mixed gas (R1234yf, air, and lubricant oil injection) at the inline pipe at 260°C, where self-ignition combustion would occur, and performed an experiment under the conditions listed in Table 3.1.10. The results are as follows.

Figure 3.1.24 shows the results with and without R1234yf. When it was included, we set the mass flow rates of the refrigerant and air the same, and the amount of lubricant oil was the same as the theoretical air/fuel ratio. As the figure shows, when the refrigerant R1234yf was present, the pressure waveform resembled the one without self-ignition, and the highest pressure was low (about 0.7 MPa). Judging from the pressure waveform, highest pressure, rotational sound, exhaust gas, exhaust gas temperature, and so on, it was concluded that self-ignition did not occur. Then we performed experiments by changing the rotational speed (from 500 to 1000 rpm) and the volume rate of the refrigerant flow against the total flow rate (from 17

to 90%). Under these experimental conditions, self-ignition did not occur by the incorporation of R1234yf.

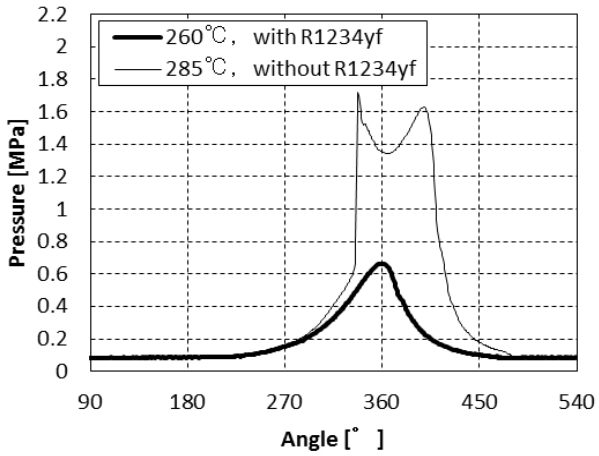

Fig. 3.1.24 Pressure change of mixed gas with refrigerant R1234yf

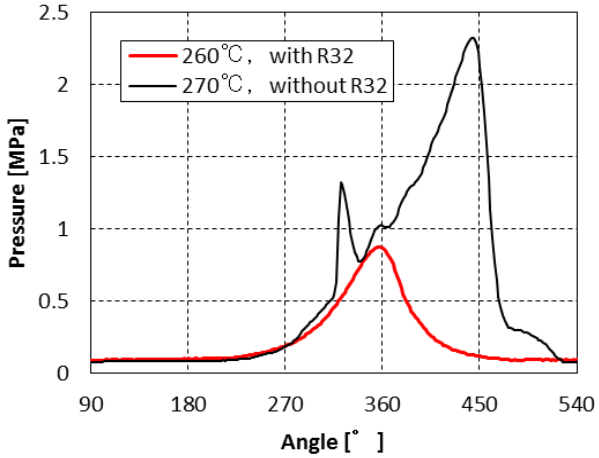

Fig. 3.1.25 Pressure change of mixed gas with refrigerant R32

(3) Results of experiment 3

Figure 3.1.25 shows the changes in pressure with and without the incorporation of refrigerant R32. The experiment conditions were a rotational rate of 1250 rpm and a refrigerant flow rate of 40% against the total flow rate. As the pressure waveform in this figure shows, without the refrigerant, 2 pressure peaks can be seen, where the second rises to 2.3 MPa at about 450°, compared with the pressure waveform without refrigerant in Fig. 3.1.24. The second peak has a different angle and pressure. Based on the pressure waveform with R32 shown in this figure, we cannot find a change that may show self-ignition, although the highest pressure is 0.8 MPa. However, increasing the rotational rate caused an increase in the highest pressure, and white smoke appeared, which could be regarded as the existence of self-ignition.

3.1.4.4 Conclusion

We studied the existence of self-ignition and the condition where self-ignition occurs by using PAG (UG46) as a lubricant oil for refrigerant R1234yf and compressing a mixed gas of air and lubricant oil by changing the gas temperature. In addition, on the basis of the above results, we performed compression experiments with mixed gases containing refrigerant R1234yf or R32. In the case of a mixed gas containing R1234yf, it could not be determined that self-ignition occurred. However, with a mixed gas containing R32, we found an increase in pressure and white smoke could be seen when self-ignition occurred. Therefore, we need to perform further study by increasing the range of the experiment conditions.

Acknowledgment

During the experiments and numerical simulation, we received great contributions from our colleagues. We are grateful to Associate Professor Chaobin Dang, Dr. Shizuo Saito, and Ms. Yurika Funasaka of the University of Tokyo.

References

3.1.1) Kenji TAKIZAWA et al., “Flammability properties of 2L refrigerants”, The International Symposium on New Refrigerants and Environmental Technology 2012, (2012).

3.1.2) Japan Fluorocarbon Manufacturers Association, “List of CFCs, HCFCs and fluorocarbons’ environmental and safety data,”

http://www.jfma.org/atabase/table.html (2012) (in Japanese)

3.1.3) O. Kataoka, et al. “Flammability evaluation of HFC-32 and HFC-32/134a under practical operating conditions”, International Refrigeration Conference, Purdue, July 1996.

3.1.4) User’s Manual for STAR-CD.

3.1.5) Takizawa et al. 49th combustion symposium, pp146-147, Yokohama (2011).

3.1.6) O.J. Nielsen et al. Chemical Physics Letters Vol. 439, Issues 1–3, pp. 18–22 (2007).

3.1.7) D.M. Manuta “Quantitative infrared analysis of hydrogen fluoride” American Chemical Society National Meeting, San Francisco, California, April 13-1 7, 1997.

3.1.8) NIST Chemistry WebBook

3.1.9) Tokyo Metropolitan Government: ”The Report of Products Safety Measures Meeting in Tokyo” (2012) (in Japanese)

3.1.10) Tokyo Metropolitan Association of Refrigerating and Air Conditioning Equipment: “TRK the Technical Report” (in Japanese)

3-2. Research and Development of Low-GWP Refrigerants Suitable for Heat Pump Systems

Shigeru KOYAMA*, Yukihiro HIGASHI**, Akio MIYARA***, Ryo AKASAKA****

* Faculty of Engineering Sciences, Kyushu University

** Faculty of Science and Engineering, Iwaki Meisei University

** Faculty of Science and Engineering, Saga University

**** Faculty of Engineering, Kyushu Sangyo University

3.2.1 Introduction

The present research group has been conducting research on the following subjects related to the development of low-GWP refrigerants suitable for vapor compression heat pump systems: (1) to clarify the chemical characteristics, thermophysical properties, and heat transfer characteristics of HFO-1234ze(Z), and to theoretically and experimentally evaluate the cycle performance of HFO-1234ze(Z), and (2) to search for low-GWP refrigerant candidates suitable for use in air-conditioning systems, and to evaluate their cycle performances theoretically and experimentally. In this paper, the results of the following investigations are presented: (1) flammability test of HFO-1234ze(Z), (2) toxicity test of HFO-1234ze(Z), (3) thermophysical properties and heat transfer characteristics of HFO-1234ze(Z), and (4) evaluation of the cycle performance of low-GWP refrigerants.

3.2.2 Flammability test of HFO-1234ze(Z)

To evaluate the combustion safety of HFO-1234ze(Z), we measured the flammability range, minimum ignition energy, and flash point.

(1) Measurement of flammability range

Gas explosion test equipment with an internal volume of 1000 cc was used to measure the flammability range. The mixture of air and HFO-1234ze(Z), the composition of which had been adjusted to a predetermined concentration at 25 °C and 0.1013 MPa, was introduced into the test equipment and ignited by the metal wire blow-out method. The combustion state of the mixed gas was judged on the basis of the following conditions:

- Case of combustion: the pressure increase should be 100 kPa or more.
- Case of no combustion: the pressure increase should be less than 100 kPa.

(2) Measurement of minimum ignition energy

Cylinder-type burning test equipment with an internal volume of 270 cc was used to measure the minimum ignition energy. The mixture of air and HFO-1234ze(Z), the composition of which had been adjusted to a predetermined concentration at 25 °C and 0.1013 MPa, was introduced into the test equipment and ignited by a spark generator, with the electrical energy of the spark increased gradually up to a maximum energy of 800 mJ. The combustion state of the mixed gas was judged on the basis of the following conditions:

- Case of combustion: the pressure increase should be 100 kPa or more and the temperature increase should be 5 K or more.
- Case of no combustion: the pressure increase should be less than 100 kPa and the temperature increase should be less than 5 K.

Cylinder-type burning test equipment with an internal volume of 270 cc was used to measure the minimum ignition energy. The mixture of air and HFO-1234ze(Z), the composition of which had been adjusted to a predetermined concentration at 25 °C and 0.1013 MPa, was introduced into the test equipment and ignited by a spark generator, with the electrical energy of the sparks increased

gradually up to a maximum energy of 800 mJ. The combustion state of the mixed gas was judged on the basis of the following conditions:

- Case of combustion: the pressure increase should be 100 kPa or more and the temperature increase should be 5 K or more.
- Case of no combustion: the pressure increase should be less than 100 kPa and the temperature increase should be less than 5 K.

(3) Measurement of flash point

Based on JIS K2265, the flash point of HFO-1234ze(Z) was measured using a tag closed cup tester.

According to the present flammability test of the air/HFO-1234ze(Z) mixture, the flammability range was confirmed to be 7.5–16.4 vol%. During the measurement of the minimum ignition energy, it was observed that the air/HFO-1234ze(Z) mixtures (8.0, 10.0, 12.0, 14.0, 16.0 vol%) were nonflammable for an applied energy of 800 mJ. Moreover, there was no flash point.

3.2.3 Toxicity test of HO-1234ze(Z)

To evaluate the toxicity, the bacterial reverse mutation test and the acute inhalation toxicity check using rats were carried out based on OECD guideline for testing of chemicals 471. From the results, it was confirmed that HFO-1234ze(Z) had no mutagenic activity against bacteria (Escherichia coli and Salmonella typhi). The LC50 (4h) was higher than 21695 ppm, which means that HFO-1234ze(Z) was negative in the acute inhalation toxicity check.

3.2.4 Thermodynamic properties and heat transfer characteristics of HFO-1234ze(Z)

3.2.4.1 Thermodynamic properties of HFO-1234ze(Z)

The P-ρ-T property of HFO-1234ze(Z) was measured by the constant-volume method. A certain mass of HFO-1234ze(Z) was charged in a cell placed in a thermostatic bath, and the pressure and density of the HFO-1234ze(Z) in the cell were measured at various temperatures.

Figure 3.2.1 shows the P-ρ-T property of HFO-1234ze(Z) measured by this method. From these measurement results and the observation of the meniscus behavior, the critical parameters were determined as follows:

$$T_c = 423.27\ \mathrm{K},\ P_c = 3533\ \mathrm{kPa},\ \rho_c = 470\ \mathrm{kg/m^3}$$

Using these parameters, an equation of state formulated by the Helmholtz free energy is proposed. Figure 3.2.2 shows the P-h diagram obtained from the proposed equation.

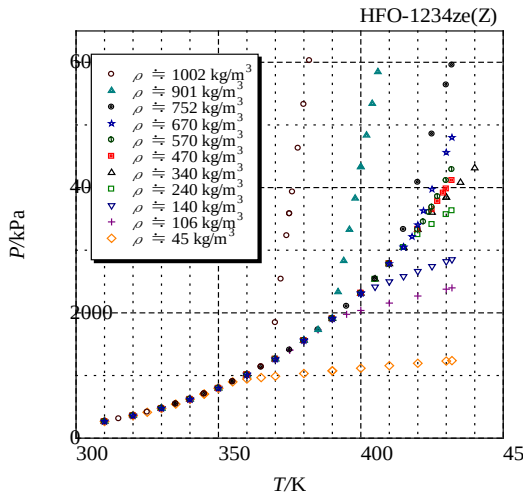

Figure 3.2.1 Experimental *P*-ρ-*T* data for HFC-1234ze(Z).

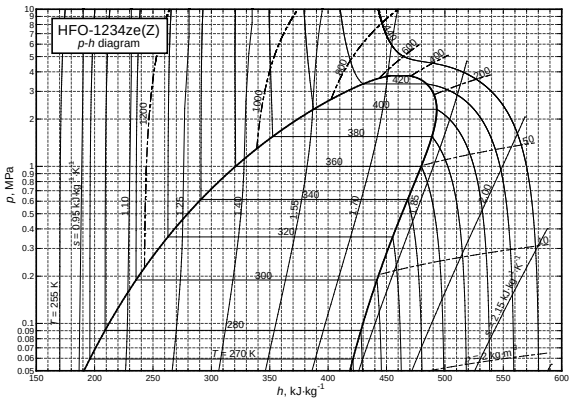

Figure 3.2.2 *P-h* diagram of HFO-1234ze(Z).

3.2.4.2 Transportation properties of HFO-1234ze(Z)

The thermal conductivity of HFO-1234ze(Z) was measured by the transient hot-wire method, using two Pt wires (φ15 mm) of different lengths. Figure 3.2.3 shows the measurement results of the thermal conductivity of the saturated liquids. The figure shows the experimentally determined thermal conductivities for HFO-1234ze(Z), HFO-1234ze(E), HFO-1234yf, HFC-32, and HFO-1234ze(Z)/HFC-32 (50/50 mass%). The lines represent the thermal conductivities calculated by Refprop Ver. 9.0 for HFO-1234ze(E), HFO-1234yf, and HFC-32. The high degree of overlap between the measured and calculated values for HFC-32, HFO-1234ze(E), and HFO-1234yf validates the measurement method. As shown in Fig. 3.2.3, the thermal conductivity of HFO-1234ze(Z) was higher than that of HFO-1234yf but lower than that of HFC-32.

The viscosity of HFO-1234ze(Z) was measured by a capillary viscometer using two capillary tubes of different lengths. Figure 3.2.4 shows the measured viscosities of the saturated liquids for HFO-1234ze(Z), HFO-1234ze(E), and HFC-32, and also the viscosity of HFC-32 calculated by Refprop Ver.9. The overlap of the measured and calculated values validates the measurement method. As shown in Fig. 4, the viscosity of HFC-1234ze(Z) was the highest of the three tested refrigerants.

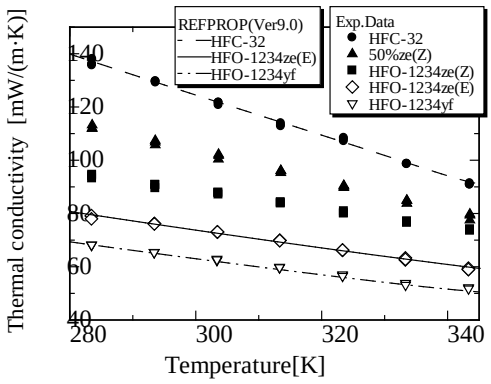

Figure 3.2.3 Thermal conductivity of saturated liquids.

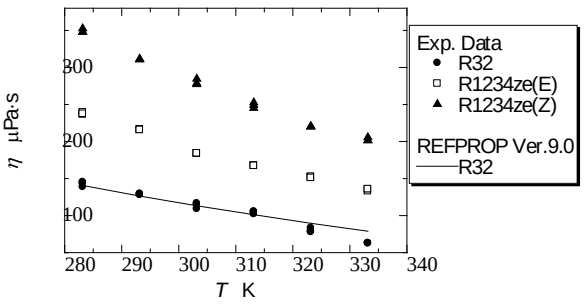

Figure 3.2.4 Viscosity of saturated liquids.

3.2.4.3 Heat transfer characteristics of HFO-1234ze(Z)

The evaporation and condensation heat transfer characteristics of HFO-1234ze(Z) flowing in a horizontal microfin tube were investigated using a vapor compression cycle. The tube used for the test was a copper helical microfin tube of outer diameter 6.08 mm, maximum inner diameter 5.49 mm, equivalent diameter 5.34 mm, and fin height 0.255 mm. It had a lead angle of 20.1°, 48 fins, and a 2.24 area enlargement ratio relative to an equivalent smooth tube. The test section of length 2216 mm was subdivided into four equal subsections. The average heat transfer coefficient (HTC) over the 414 mm active heating/cooling length and the pressure drop at 554 mm intervals, which coincided with the boundaries of the subsections, were measured.

Figures 3.2.5 and 3.2.6 show the pressure gradient and HTC during the evaporation and condensation of HFO-1234ze(Z). In a future work, the experimental results and predicted values will be compared with those of other refrigerants.

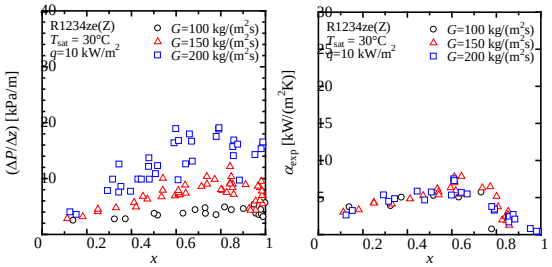

(a) Pressure gradient (b) HTC

Figure 3.2.5 Evaporation characteristics of HFO-1234ze(Z).

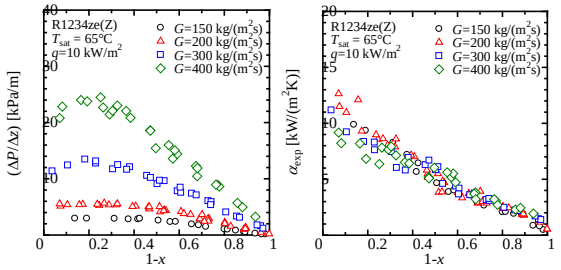

(a) Pressure gradient (b) HTC

Figure 3.2.6 Condensation characteristics of HFO-1234ze(Z).

3.2.5 Thermodynamic analysis of the heat pump cycle using low-GWP refrigerants

3.2.5.1 Potentials of low-GWP refrigerants for various heat pumps

To determine the optimum temperature range of the heat source, thermodynamic analyses and drop-in experiments were conducted for high-temperature applications of HFO-1234ze(E) and HFO-1234ze(Z). Table 3.2.1 lists the calculation conditions of the thermodynamic analyses for HFC-410A, HFO-1234ze(E), and HFO-1234ze(Z). The degrees of subcooling at the condenser outlet and superheating at the evaporator outlet were fixed at 10 and 3 K, respectively. The difference between the condensation and evaporation temperatures was fixed at 35 K. Under these conditions, the coefficient of performance (COP) and volumetric capacity were evaluated at a condensation temperature of 30–150 °C. Figure 3.2.7 shows the results of the thermodynamic analyses for HFC-410A, HFO-1234ze(E), and HFO-1234ze(Z). Each refrigerant had a maximum COP at a certain condensation temperature for which the volumetric capacity was relatively high. From the results, it was found that the optimum condensation temperature ranges for HFC-410A, HFO-1234ze(E), and HFO-1234ze(Z) were 30–50 °C, 60–90 °C, and 100–130 °C, respectively.

Based on the results of the thermodynamic analyses, drop-in experiments were conducted for HFO-1234ze(E), HFO-1234ze(Z), and a HFO-1234ze(E)/HFC-32 mixture (95/5 mass%).

Table 3.2.1 Conditions of thermodynamic analyses for high-temperature applications

Cond. Temp.-Eva. Temp.	[K]	35
Degree of subcooling	[K]	10
Degree of superheating	[K]	3
Range of Cond. Temp.	[°C]	>30

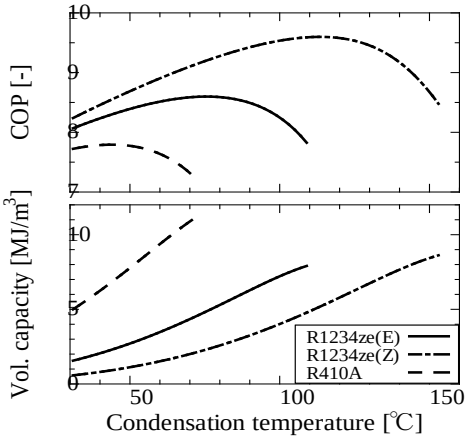

Figure 3.2.7 Results of thermodynamic analyses for condensation temperatures of 30–150 °C.

The test loop mainly consisted of a hermetic compressor, a solenoid expansion valve, and two double-tube-type heat exchangers with counter flow configurations. Table 3.2.2 lists the heat-source and heat-sink temperatures (i.e., the water temperatures in the condenser and evaporator), the degree of superheating at the evaporator outlet, and the heat transfer rate in the condenser (i.e., the heating capacity). Figure 3.2.8 shows the experimental results of the COP and heating capacity Q_h. For a heat-sink temperature distribution of 50–75 °C through the condenser, the COP and heating capacity of HFO-1234ze(E) were higher than those

Table 3.2.2 Conditions of drop-in experiment for high-temperature applications

Water Temp.	Cond.	[°C]	50→75
	Eva.		45→39
Degree of superheating		[K]	3
Heat transfer rate		[kW]	1.2～2.4

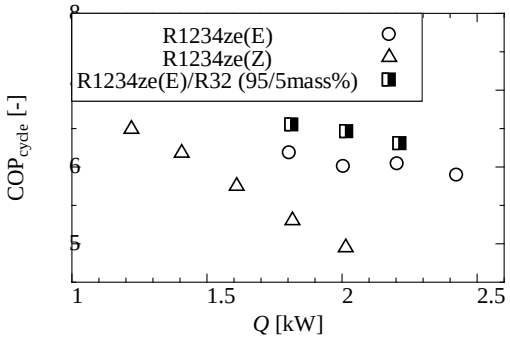

Figure 3.2.8 Results of drop-in experiment on COP and Q_h.

of HFO-1234ze(Z). The addition of HFC-32 (5 mass%) to HFO-1234ze(E) improved the COP and volumetric capacity of both. On the other hand, the COP of HFO-1234ze(Z) reduced significantly with increasing heating capacity. This suggests that HFO-1234ze(Z) was suitable for condensation temperatures higher than the test range.

3.2.5.2 Survey of low GWP refrigerant blends for commercial air-conditioners

As the first step of the survey, the drop-in test was conducted on binary mixtures of HFO-1234ze(E) and HFC-32 from April 2011 to March 2012. The investigations confirmed that a mixture composed of close to 50 mass% of each component was a promising candidate to replace R410A, which is the most widely used refrigerant in commercial air-conditioners. However, for a mass fraction of HFO-1234ze(E) below 50 mass%, the GWP of the mixture was greater than 340. To reduce the GWP to below 300, the addition of CO_2 as a third component to the binary mixture of HFO-1234ze(E) and HFC-32 was attempted.

As the next step, the thermodynamic analysis of of air-conditioners on the heating condition was conducted from April 2012 to March 2013. Table 3.2.3 lists the condition of the analysis. The GWP, temperature glide (i.e., the temperature variation during the phase change) in the evaporator, volumetric capacity, and COP ratio relative to HFC-410A were calculated under this condition. Based on the criteria listed in Table 3.2.4, two compositions were selected. The ternary blend A (HFO-1234ze(E)/HFC-32/CO_2, 53/43/4 mass%) was used to achieve a GWP just below 300. The ternary blend B (HFO-1234ze(E)/HFC-32/CO_2, 62/29/9 mass%) was used to achieve a GWP just below 200. Figure 3.2.9 illustrates the calculation results for the ternary blends. The lines represent the contour of the GWP, temperature glide, and the

Table 3.2.4 Conditions of thermodynamic analyses of air-conditioners

Condensation temperature	[°C]	30
Degree of subcooling	[K]	0
Evaporation temperature	[˚C]	-3
Degree of superheating	[K]	3
Efficiency of compressor	[-]	0.85

Table 3.2.5 Criteria for determining mass fraction of refrigerant candidates in ternary blends

Condition	A	B
GWP	<300	<200
Temperature glide	<10 K	<15 K
Volumetric capacity ratio	>0.8	
COP ratio	>1.0	

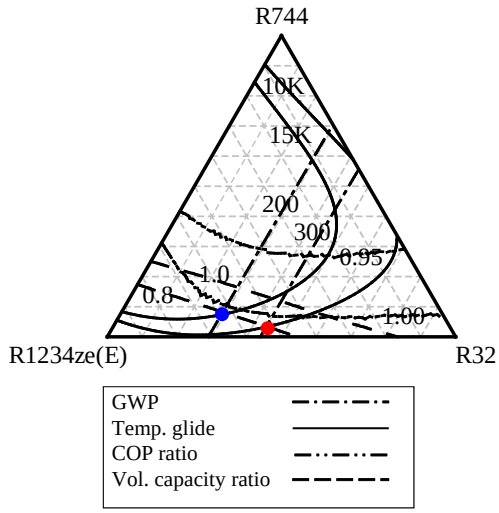

Figure 3.2.9 Results of thermodynamic analyses of ternary blends.

COP and volumetric capacity ratios relative to HFC-410. The red symbol indicates the selected ternary blend A with a GWP below 300, and the blue symbol indicates the ternary blend B with a GWP below 200.

3.2.6 Conclusions

The progress of the NEDO research project from April 2012 to March 2013 has been reported in this article. Through this work, fundamental information about the new low-GWP refrigerant HFO-1234ze(Z) has been provided. Its compatibility with various materials and its flammability and toxicity have been clarified. Additionally, data on its thermodynamic and transportation properties have been provided. The thermodynamic property, heat transfer characteristics, and cycle performance of the selected ternary blends HFO-1234ze(E)/ HFC-32/CO_2 will be investigated in a future work.

The present study was sponsored by the project on the “Development on Highly Efficient and Non-Freon Air Conditioning Systems” of the New Energy and Industrial Technology Development Organization (NEDO), Japan.

3-3. Physical Hazard Evaluation of A2L-Class Refrigerants using Several Types of Conceivable Accident Scenarios

Tomohiko IMAMURA and Osami SUGAWA
Department of Mechanical Systems Engineering, Tokyo University of Science, Suwa

Summary

The purpose of this study was to evaluate the physical hazards of A2L-class refrigerants based on several types of conceivable accident scenarios: (1) A case where an air conditioner containing an A2L-class refrigerant is used simultaneously with a fossil-fuel heating system in a general living space, (2) a case where a serviceman uses a portable piezo lighter to smoke in a space where an A2L-class refrigerant has leaked and is still present, (3) a case where an A2L-class refrigerant has leaked from a pinhole in a pipe or hoses, and (4) a case where an A2L-class refrigerants has leaked inside a device used for service and maintenance.

3.3.1 Introduction

Recently, alternative refrigerants with zero ODP and low-GWP values have been required to prevent global environment. Refrigerants such as R1234yf, R1234ze(E), and R32, which satisfy above requirements, have been designated as A2L-class refrigerants. However, because A2L-class refrigerants have low flammability, which the present refrigerants employed in air conditioners do not have, investigations and evaluations on the combustion properties of A2L-class refrigerants are indispensable. Takizawa[3.3.1),3.3.2)] reported the fundamental combustion properties of A2L-class refrigerants, including their flammable range, minimum ignition energy, burning velocity, and so on. Based on these fundamental results, physical hazard evaluations in cases involving conceivable accident scenarios are necessary as risk assessments before A2L-class refrigerants can be utilized for air conditioners.

The purpose of this study was to experimentally clarify the physical hazards of A2L class refrigerants based on conceivable accident scenarios. We focused on four types of accident scenarios.

3.3.2 Assumed accident scenarios

3.3.2.1 Scenario #1

Conceivable accident scenario #1 is a case where an air conditioner containing an A2L-class refrigerant is simultaneously used with a fossil-fuel heating system in a general living space. In this scenario, we examined the ignition and flame propagation properties, along with the generation behavior of the combustion products (HF: hydrogen fluoride).

3.3.2.2 Scenario #2

Conceivable accident scenario #2 is a case where a serviceman uses a portable piezo lighter to smoke in a space where an A2L-class refrigerants has leaked and is still present. In this scenario, the possibility of ignition and flame propagation was simply predicted, and then verification experiments were carried out based on the above prediction.

3.3.2.3 Scenario #3

Conceivable accident scenario #3 is a case where an A2L-class refrigerant leaks from a pinhole in a pipe or hose such as is used to connect a car air-conditioner and a collection device. In this scenario, we examined the location of the flammable zone and whether a jet flame was formed instantaneously if an ignition source existed.

3.3.2.4 Scenario #4

Conceivable accident scenario #4 is a case where an A2L-class refrigerant leaks inside a piece of equipment used for service and maintenance such as a collection device. In this scenario, the staying and ignition behaviors of A2L-refrigerants in a model collection device were examined.

3.3.3 Progress on Scenario #1

3.3.3.1 Outline

In Scenario #1, two types of sub-scenarios were assumed.

(a) sub-scenario A: in a case where an A2L refrigerant leaked from an air conditioner into a model living room where the fossil-fuel heating system was operating

(b) sub-scenario B: in a case where the fossil-fuel heating system was operated after the A2L refrigerant leaked and stayed in the model living room

3.3.3.2 Experiment

Test refrigerants

R1234yf and R32 were used as the test A2L refrigerants, and R410A (a representative refrigerant now in use) was used for comparison. The size of the refrigerant leak was set 800 g based on the amount installed in a typical room air conditioner on the market[3.3.3)]. The leakage rates were set 10 g/min and 60 g/min as target values.

Experimental setup

A schematic diagram of the experimental setup is shown in Figure 3.3.1.

A room air conditioner on the market for an area of 6 tatami mats (about 11 m^2) was installed in a wall, with the center of the ventilation outlet 700 mm below the ceiling and at a horizontal distance of 1400 mm away from the corner of the experiment room. An outdoor unit was not used because we focused only on the influence of air circulation on the ignition behavior and HF generation. A φ6.35mm hole was made in the front panel of the air conditioner, and a refrigerant supplying tube was inserted in this hole, which allowed the refrigerant to leak through the ventilation outlet.

The refrigerant and HF concentrations were measured using two Fourier transform infrared spectrometers (FT-IR). In sub-scenario A, the refrigerant and HF concentrations were measured

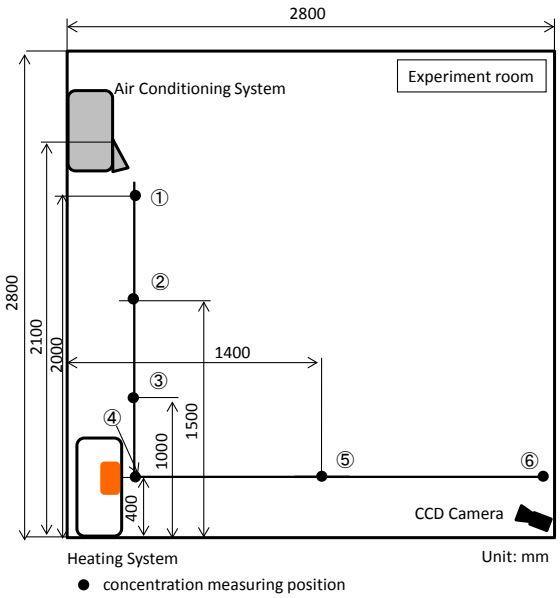

Fig.3.3.1 Schematic diagram of experimental setup for Scenario #1.

only at position 4, as shown in Figure 3.3.1, which was in front of the heating system outlet. In sub-scenario B, refrigerant concentrations at positions 1-6 before operating the heating system were measured. After operating the heating system, only the refrigerant and HF concentrations at position 4 were measured.

In sub-scenario A, a radiative oil stove (power: 2.4 kW, designed to heat 13 m^2) and an oil fan heater (power: 3.2 kW, designed to heat 16 m^2) were employed. In sub-scenario B, a heating device consisting of a copper sheet placed on a ceramic heater (FPS1, Yarcar Ceramic Co., Ltd.) was employed as the heating source. This was an AC 130 V heating source that used about 1 kW of power and had a surface temperature of about 700 °C.

3.3.3.3 Results and discussions

Sub-scenario A

In all of the present experimental cases, no flame propagation to the leaked and still-present A2L refrigerant in the experimental room was observed, and the situation of the experimental room was not changed before and after the experiment.

Figure 3.3.2 shows the time history of the refrigerant and HF concentrations at position 4 in the case where the oil fan heater was employed and R32

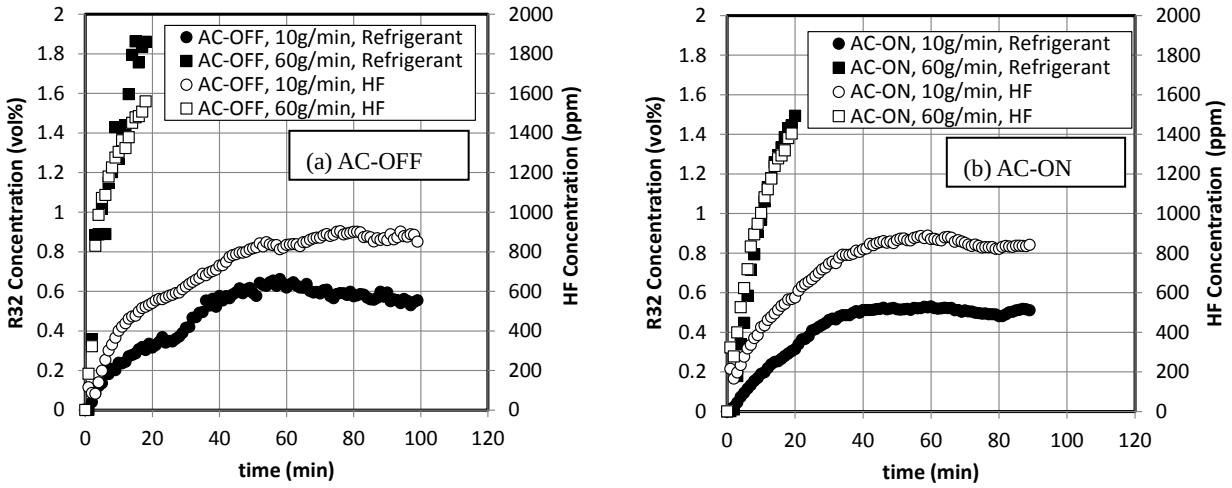

Fig.3.3.2 Time history of refrigerant concentration and HF concentration at front of heating system.
Heating system: fan heater, Refrigerant: R32, Capacity of the experiment room: 22 m^3
(a) Air conditioning system non-operated (b) Air conditioning system operated

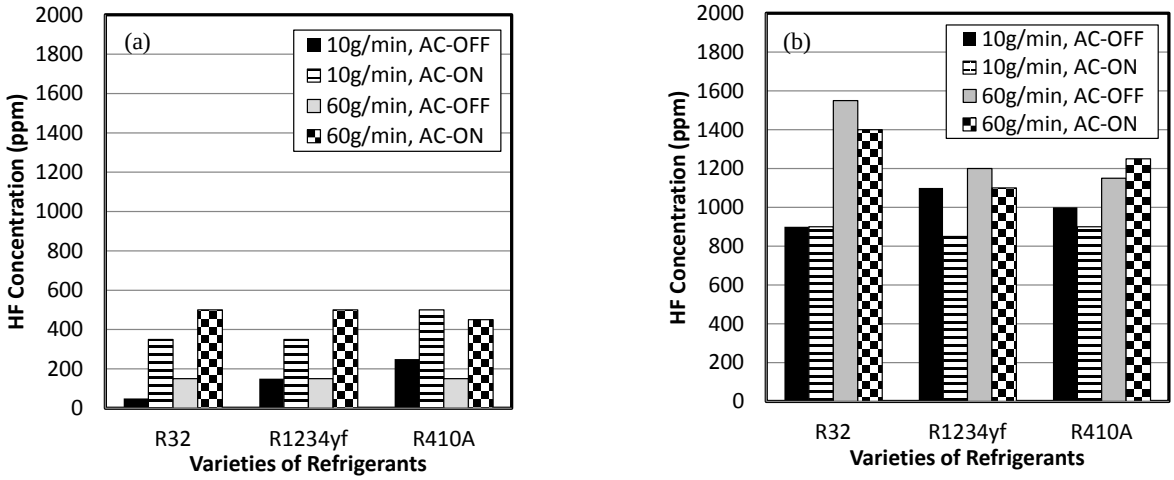

Fig.3.3.3 Comparison of HF concentration with leakage rate and operation of air conditioning system.
(a) using a radiation stove (b) using a fan heater

was employed as the test refrigerant. The time history of the refrigerant concentration was similar to that of the HF concentration regardless of the operation of the air conditioner. The maximum concentration of refrigerant was about 2 vol%, which was much lower than the LFL of R32. Namely, even if all of the R32 installed in the room air conditioner on the market was leaked into the general living space (about 8 m^2), the R32 concentration did not exceed the LFL. Thus, no flame propagation occurred in the room. These behaviors were also confirmed in the case of R1234yf.

Figure 3.3.3 shows the HF concentration for each refrigerant. HF was produced at about 50-1500 ppm, which is much greater than the permissible value designated by the Japan Society for Occupation and Health. The amount of HF produced in the case with the oil fan heater was much greater than that with the radiative stove. This was because the refrigerant that was sucked into the fan heater burned completely, whereas in the case with the radiative oil fan heater, a portion of the refrigerant in contact with the heated body might have only been decomposed instead of burned.

In the case with the radiative oil stove (Figure 3.3.3(a)), the HF concentration with the operation of the air conditioner was apparently greater than that

without the operation of the air conditioner regardless of the variety of refrigerant. However, this trend was not always the same in the case with the oil fan heater (Figure 3.3.3(b)). This can be considered to be because the flow in the experimental room became complex as a result of the interaction between circular flow from the fan heater and it from the air conditioner. In addition, although the HF generation of R32 was slightly greater than those of R1234yf and R410A, the HF generation ability of the A2L refrigerants was as great as that of R410A.

Sub-scenario B

The refrigerant concentration in the experimental room was at most 2 vol%, which is much lower than the LFL of R32. Flame propagation to unburned refrigerant did not occur, and HF was hardly produced (less than 50 ppm, which is the guaranteed limit of the data).

3.3.3.4 Conclusions for Scenario #1

(1) Even if all of the A2L refrigerant installed in a room air conditioner on the market leaked and remained in the model general living space (about 8 m^2), no flame propagation across the whole room was observed because the refrigerant concentration in the room did not exceed the LFL.
(2) If the refrigerant contacted the heated body of a radiative stove and/or the open flame of the fan heater, an HF concentration of more than 3 ppm, which is the permissible concentration, was generated regardless of the variety of refrigerant including R410A.
(3) In the case with the radiative stove, the HF concentration increased with the operation of the air conditioner and an increase in the leak rate. However, in the case with the fan heater, this trend was not always confirmed.
(4) The HF concentration in the case with the fan heater was apparently greater than that in the case with a radiative stove.

3.3.4 Progress on Scenario #2

3.3.4.1 Outline

In this scenario, we focused on a lighter used for smoking as the ignition source. We focused only on a piezo lighter as the ignition source. In addition, the possibility of ignition from the heat of the cigarette tip was ignored because this type of ignition rarely occurs even for methane gas, which is famous for being a flammable gas[3.3.4)].

3.3.4.2 Refrigerant composition for evaluation

The refrigerants used in the evaluation were R1234yf, R1234ze(E), and R32. The ignition possibility of a piezo lighter igniting an A2L refrigerant that leaked and remained in the ambient atmosphere was estimated simply to determine the generally composition of the refrigerant for the experiment.

The concentration of the lighter gas at the outlet of the lighter must be within the flammable range. We assumed that the fuel gas of the lighter was *n*-butane, and that an *n*-butane/A2L refrigerant/air mixture was formed at the outlet of the lighter. We assumed that the *n*-butane/A2L refrigerant mixture could be treated as a single fuel gas.

Le Chatelier's law has been employed to estimate the flammable range of a gas mixture. Although the flammable range of this mixture could not be estimated strictly using Le Chatelier's law because of the difference in the LH_c values of Burgess-Wheeler's law for the different refrigerants[3.3.5)], the flammable range of *n*-butane/A2L refrigerant mixture was estimated using Le Chatelier's law as follows to determine the general composition. As a result, the concentration of the *n*-butane/A2L mixture when the amount of the A2L refrigerant was less than the LFL was within the flammable range estimated by Le Chatelier's law. These trends were confirmed for all of the refrigerants.

The ignition energy of *n*-butane with the same equivalent ratio as the above composition mixture was within the range of 0.25-2.40 mJ, that is as large

as (or less than) the energy of a piezo electric spark[3.3.6]. Therefore, the *n*-butane/A2L mixture had some ignition potential. In addition, the ignition energies of A2L refrigerants are at least greater than about 30 mJ, which is much higher than that of *n*-butane. Thus, the ignition energy of the n-butane/A2L mixture would be much greater than that of *n*-butane. Therefore, the actual ignition potential was very low. The ignition potential of the above composition was the worst conceivable case.

3.3.4.3 Experiments

Figure 3.3.4 shows schematic diagrams of the experimental setup. A push device for a piezo lighter was set at a height of 300 mm from the bottom of a cubic acrylic pool. This push device consisted of a pneumatic cylinder (CKD, SSD-X) and a jig. Air for operation was supplied remotely using a solenoid valve at a pressure of 0.15 MPa. A piezo lighter on the market was used for the experiment.

R1234yf, R1234ze(E), and R32 were employed in the evaluation. The A2L refrigerant was leaked in a downward direction from a height of 500 mm above the bottom of the pool. The leakage rate was set at 10 g/min as the target value for all of the refrigerants. The refrigerant concentrations at 6 vertical positions were measured using FT-IR before pushing the button of the piezo lighter. The measurement positions had heights of 0, 100, 300, 500, 750, and 1000 mm from the bottom of the acrylic pool.

The operation to push the button of the piezo lighter was maintained for 10 s per cycle. This

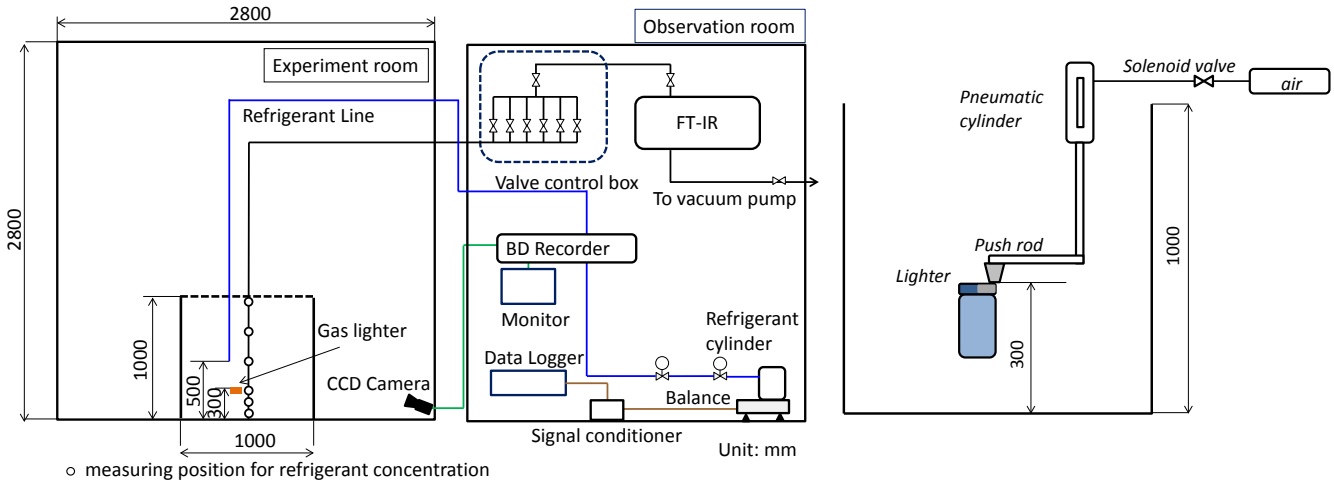

(a) configuration of experimental apparatus

(b) configuration of remote ignition system of a piezo gas lighter

Fig.3.3.4 Schematic diagram of experimental apparatus for Scenario #2. Unit: mm

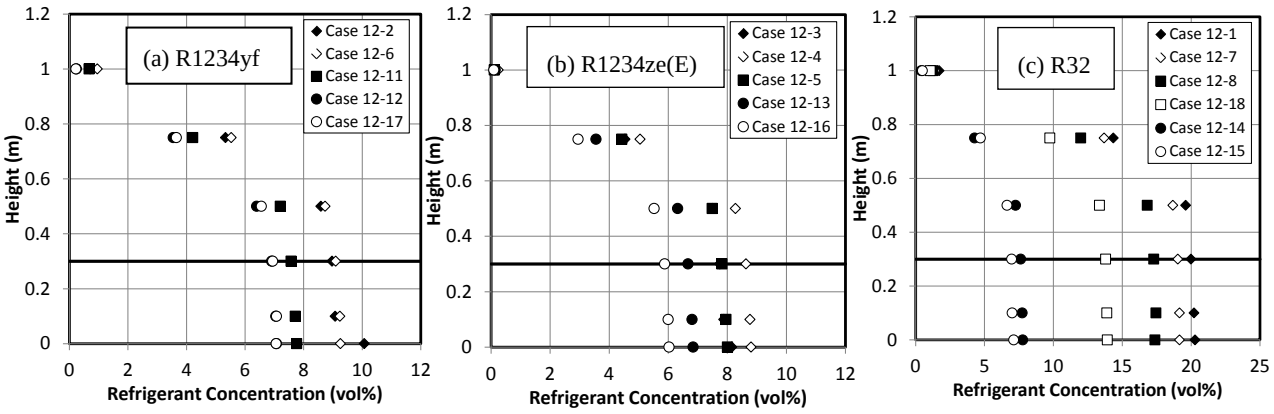

Fig.3.3.5 Vertical distribution of refrigerant concentration in a 1m-cube acrylic pool.

operation was repeated for 5 or 9 cycles at intervals of 5 s per cycle. The situation at the outlet of the piezo lighter was observed using digital video camera (SANYO Xacti, 30 fps).

3.3.4.4 Results and discussions

Concentration distribution of refrigerant

Figure 3.3.5 shows the vertical distribution of the refrigerant concentration. The solid line at a height of 0.3 m indicates the outlet of the piezo lighter. In the region under a height of 0.5 m, the concentration distribution was almost uniform regardless of the height. The refrigerant concentration at a height of 0.3 m was within the range of 0.76-2.18 of the equivalent ratio, which is the ignitable range by a spark from a piezo lighter.

Results of pushing the button

Figure 3.3.6 shows photographs of the outlet of the piezo lighter when the button was pushed. Ignition was observed for an instant at the outlet, as shown by the white luminescence in Figure 3.3.6, but flame propagation from the outlet of the piezo lighter to the surrounding *n*-butane/A2L refrigerant mixture was not confirmed for any of the A2L refrigerants employed in the present experiment when the A2L refrigerant at the LFL was mixed with *n*-butane and air. The flame at the outlet was quenched in less than 1/30 s. One of the reasons was that the ignition energy of the *n*-butane/A2L refrigerants was much greater than that of *n*-butane alone. Another reason was considered to be the low burning velocity. The discharging velocity of the lighter gas (*n*-butane) at the outlet was estimated to be about 2 m/s, assuming the flame length was 3 cm and the diameter of the outlet was 1 mm. The burning velocity of the A2L refrigerants was less than 10 cm/s.

3.3.4.5 Conclusions for Scenario #2

Even if a piezo lighter was used in an area where an A2L refrigerant leaked and remained in the ambient air, no flame propagation was observed for two major reasons: the ignition energy of the n-butane/A2L refrigerants was much greater than the electric spark of the piezo lighter, and the fuel velocity was much faster than the burning velocity of A2L refrigerants.

3.3.5 Progress on Scenario #3

3.3.5.1 Outline

This scenario focused on the ignition hazard when an A2L refrigerant leaked from a pinhole in a pipe

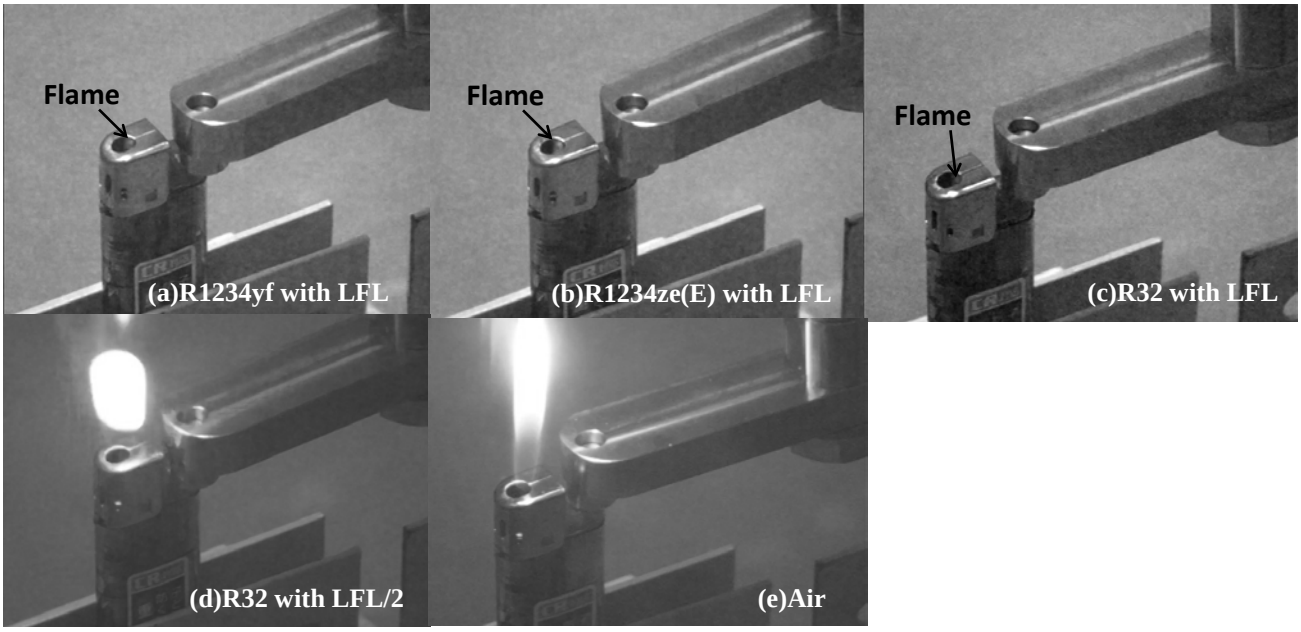

Fig.3.3.6 Photographs of outlet of electric piezo lighter in mixture.

and/or hose. For example, a case was considered where the refrigerant leaked from a pinhole or a break formed in the hose connecting the refrigerant collection device and car air conditioning unit during servicing and maintenance in the factory.

3.3.5.2 Experiment

The pinhole was modeled using a cap type coupling (1/4”, Swagelok SS-400-C) with a hole in the center. Two patterns were used for the pinhole shape: a circular hole and rectangular slit. The pinhole diameter was 0.2, 1.0, 3.0, or 4.0 mm, and the dimensions of the slit were 1.0 mm × 4.0 mm. Two patterns were used for the direction of the rectangular slit: the longer side was oriented either vertically or horizontally.

Two different leak pressure cases were considered: one was the vapor pressure in the cylinder and the other was a reduced pressure. The maximum leakage rate was about 700 g/min. R32, R1234yf, and R1234ze(E) were used as the representative A2L refrigerants.

The jet concentrations of the leaked refrigerants were measured using an ultrasonic gas analyzer (US-II-T-S, Daiichi Nekken Co., Ltd). The measured area had a horizontal width of 500 mm and a vertical height of ± 50 mm from the pinhole.

A single spark, continuous spark, and open flame were employed as the ignition source. A single spark was generated using a high-voltage system (MEL1140B, Genesis Co.,Ltd.). A continuous spark was generated using a Neon transformer (CR-N16, Kodera Electronics Co., Ltd.). The open flame length was 3 cm.

3.3.5.3 Results and discussions

Even if R1234yf was leaked from a 4 mm pinhole, the flammable zone was only 10 cm from the pinhole in downstream region. Of course, the flammable zone decreased with a decrease in the pinhole diameter.

In the ignition test, no ignition and flame propagation were observed when a single spark was employed as the ignition source. In the case of a continuous spark as the ignition source, pale luminescence from the ignition of the A2L refrigerant was confirmed only near the spark, but no flame propagated to the entire refrigerant jet. In the case of an open flame, the open flame was blown out by the refrigerant jet, and the no ignition and flame propagation were confirmed. These behaviors were caused by the difference between the burning velocity and refrigerant flow velocity.

3.3.5.4 Conclusions for Scenario #3

The ignition hazard when an A2L refrigerant leaked from a pinhole in a pipe and/or hose was examined experimentally. A flammable zone was formed locally, and no jet flame was formed in any of the cases in the present experiments.

3.3.6 Progress on Scenario #4

3.3.6.1 Outline

In this scenario, the ignition hazard in a case where an A2L refrigerant leaked into a device used for servicing and maintenance was examined experimentally. For example, a case was considered where an A2L refrigerant leaked into a collection device and was ignited by a spark from an electric relay in the collection device.

3.3.6.2 Experiment

A 1000 mm × 1000 mm × 1000 mm acrylic pool was employed as a model collection device. This model collection device contained an oncoming slit to diffuse and leak the refrigerant. We measured the refrigerant concentrations in this collection device using several slit widths: 1, 5, 10, and 20 mm. The amount of leaked refrigerant was approximately 380 g at a leakage rate of 380 g/min. An ignition test was conducted after the refrigerant concentration measurement was finished. An electric spark with an energy of 16 J at 6 Hz was used as the ignition source. This ignition source was located at a height of 500 mm from the bottom of the acrylic pool. Only R1234yf was tested.

3.3.6.3 Results and discussions

In the case without an oncoming slit, the concentration of R1234yf hardly changed with time. Namely, a flammable concentration of R1234yf remained in the model collection device. In the case with a 20 mm wide slit, the R1234yf in the model collection device was diffused from the slit. The concentration of R1234yf at 500 mm became less than the LFL 3 min after the leakage began.

In the ignition test, no ignition and flame propagation were observed, even though a spark was generated after 30 sec after the leakage began. This was because the R1234yf remaining in the model collection device moved as a result of the pressure difference originating from the oncoming slit, which dispersed the energy of the spark to the refrigerant.

3.3.6.4 Conclusions for Scenario #4

The R1234yf in the model collection device diffused through the oncoming slit, and if the collection device had a 20 mm-wide oncoming slit, no ignition and flame propagation were observed.

3.3.7 Conclusions

We conducted physical hazard evaluations for A2L refrigerants based on conceivable accident scenarios, and obtained valuable and useful data.

Acknowledgements

The authors would like to sincerely thank all of members of the research committee for the risk evaluation of low flammability refrigerants. Some of the experiments for the scenario #3 and #4 were conducted at the Japan Automobile Research Institute (JARI). The authors sincerely thank Mr. Hiroyuki Mitsuishi and Dr. Yosuke Tamura of JARI. The authors also thank to Mr. Tatsuya Miyashita, who is a graduate student at the Tokyo University of Science, along with Mr. Takanori Morimoto, Dr. Kyoko Kamiya, and Mr. Yuta Yamazaki of Japan Specialist in Law Engineering Corp. for their kind help with the experiments and analyses.

References

3.3.1) Takizawa, K., et al.: J. Fluorine Chemistry, 129, pp.713-719, 2008.

3.3.2) Takizawa, K. et al: J. Hazardous Materials, 172, pp.1329-1338, 2009.

3.3.3) Website on National Institute on Technology and Evaluation (NITE): http://www.prtr.nite.go.jp/prtr/pdf/estimation21/syosai/19ozon.pdf (2013.2.22 accessed), in Japanese.

3.3.4) Holleyhead, R.: Science and Justice, 36, pp.257-266, 1996.

3.3.5) JSSE: Practice Safety Engineering, Series 1, pp.61-64, 2012, in Japanese.

3.3.6) Matsui, H.: Newsletter of TIIS, No.247, p.6, 2012, in Japanese.

3-4. Progress Report by Research Institute for Innovation in Sustainable Chemistry, AIST

Kenji TAKIZAWA and Masanori TAMURA
Research Institute for Innovation in Sustainable Chemistry,
National Institute of Advanced Industrial Science and Technology

3.4.1 Ignition and Quenching of Refrigerants

Generally speaking, the following factors are considered the three elements necessary for combustion: flammable material, oxidizer, and ignition source. For the first two factors, we may refer to flammability limits (LFL and UFL). For the last one, we may refer to minimum ignition energy (MIE, E_{min}). The flammability limits are widely used, and a test method to measure flammability limits that is applicable to 2L refrigerants has been established. For E_{min}, however, no appropriate test methods seem to be applicable to 2L refrigerants. As shown in Fig. 3.4.1.1, the published values of E_{min} for 2L refrigerants vary widely from <10 mJ to >10 J, which makes fire risk assessment based on E_{min} almost impossible. The difficulty in determining a reliable E_{min} lies in the fact that E_{min} is very dependent on the electrode geometry and ignition spark density and duration; these do not appear in the first-order theoretical expressions of E_{min}.

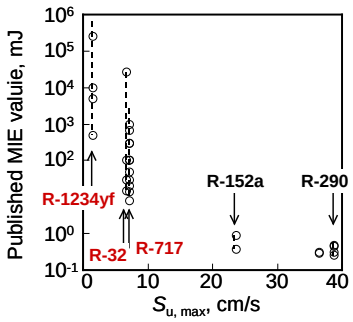

Fig. 3.4.1.1 Wide variations in published E_{min} values for flammable refrigerants.

On the other hand, several theoretical equations correlate E_{min} with the burning velocity (S_u) and quenching distance (d_q). Compared to measuring E_{min}, measuring d_q is much easier and provides reliable data on 2L refrigerants. Therefore, we first comprehensively measured d_q of various flammable refrigerants and then attempted to estimate E_{min} from the experimental S_u and d_q values.

3.4.1.1 Quenching distance (d_q)

We measured d_q of the 10 flammable compounds listed in Fig. 3.4.1.1. Because the purpose of this study was risk assessment of low GWP 2L refrigerants, our target compounds were mainly 2L refrigerants and 2/2L boundary compounds. The experimental setup and procedure were similar to those specified by ASTM-E582. We judged whether self-sustained propagation of a flame kernel generated by an ignition spark could be achieved between the parallel flat plates. By changing the gap between the plates by a micrometer screw gauge, we obtained d_q. We tested parallel plates with three diameter sizes: 5, 25, and 50 mm. Fig. 3.4.1.2 shows the results for R-290 and R-32. For R-290, a converged d_q value could be obtained by using parallel plates with diameters of 25 mm or more. However, the 25 mm diameter plates were not large enough to obtain the converged d_q value for R-32. Hereafter, we show the results obtained by the 50 mm plates.

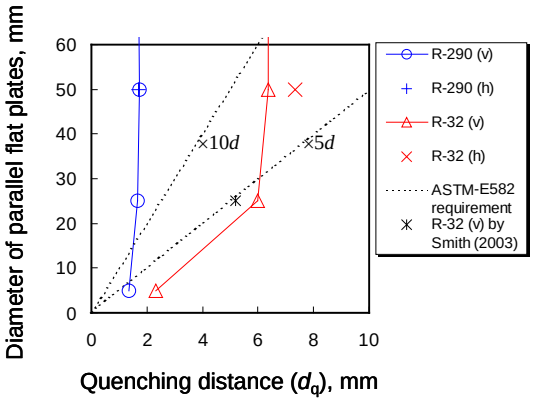

Fig. 3.4.1.2 Relationship between size of the parallel plates and measured d_q value.

Considering wide applications of the test method, we measured d_q by using both a DC high-voltage spark generator (spark duration of typically 3 ms) and an AC neon transformer (spark duration of 0.1 s) to understand the effect of the ignition source on d_q. Because the flame propagation of 2L refrigerants is affected by buoyancy, we measured d_q in terms of both the vertical (v) and horizontal (h) positions of the parallel plates. Fig. 3.4.1.3 shows the propagation of the R-1234yf flame between parallel plates in 1-g and μ-g. In 1-g (Fig. 3.4.1.3(a)), the flame between the plates in the vertical position escaped from the gap with assistance from the buoyancy, which made d_q significantly small. Therefore, we also measured d_q in the μ-g environment, as shown in Fig. 3.4.1.3(b). Only by obtaining this value could the experimental and theoretical values for all of the 2L refrigerants be compared without consideration of the buoyancy effect.

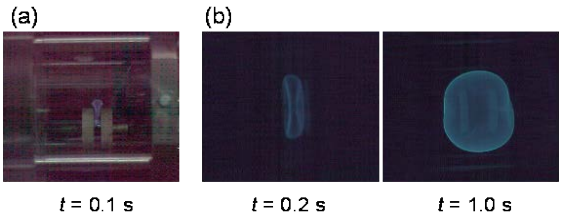

Fig. 3.4.1.3 Flame propagation of 10 vol% R-1234yf/air mixture between parallel plates in the vertical position: (a) in 1-g; (b) in μ-g.

Fig. 3.4.1.4 shows the measured d_q in the vertical (v) and horizontal (h) positions of the parallel plates and using two types of ignition sources in 1-g and μ-g. Overall, the AC spark in the vertical position gave the smallest d_q followed by the DC spark in the vertical position, AC spark in the horizontal position, and DC spark in the horizontal position. In the horizontal position of the parallel plates, the relative difference in d_q between DC ignition and AC ignition was within 8.5% for all of the compounds. For the DC ignition, the relative difference in d_q between the vertical and horizontal positions of the plates was within 10% for all of the compounds except R-32 and R-1234yf. For R-32 and R-1234yf, d_q in the vertical position was 14% and 27% smaller, respectively, than d_q in the horizontal position. In this study, we employed d_q obtained by DC ignition in the horizontal position of the parallel plates; for R-1234yf, d_q in a μ-g environment was used as the quenching distance.

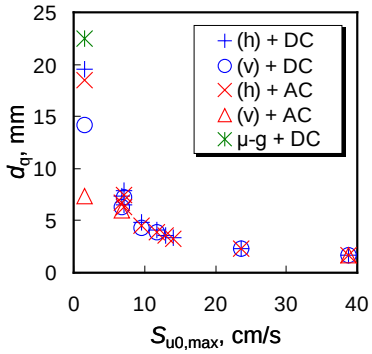

Fig. 3.4.1.4 Quenching distances as a function of $S_{u0,max}$; $S_{u0,max}$ on the horizontal axis corresponds to the compound with the specified $S_{u0,max}$ (see Table 3.4.1.1).

Table 3.4.1.1 Quenching distances of 10 compounds

Name	Formula	$S_{u0,max}$, cm/s	ρ_0, kg/m^3	d_q [a], mm
R-290	C_3H_8	38.7	1.21	1.705
R-152a	CH_3CHF_2	23.6	1.32	2.33
1243zf	CH_2=$CHCF_3$	14.1	1.40	3.33
HFC-143	CH_2FCHF_2	13.1	1.45	3.58
R-152a/134a (50/50 vol%)	CH_3CHF_2 /CH_2FCF_3	11.7	1.45	4.08
HFC-254fb	$CF_3CH_2CH_2F$	9.5	1.49	4.83
R-717	NH_3	7.2	1.08	7.85
R-143a	CH_3CF_3	7.1	1.46	6.51
R-32	CH_2F_2	6.7	1.38	7.35
R-1234yf	CH_2=$CFCF_3$	1.5	1.53	22.5[b]

a) Values were based on DC spark in the horizontal position of the parallel plates.

b) Measured in μ-g.

We examined the relationship between d_q and S_u.

Theoretically, d_q is expressed by

$$d_q = a\left(\lambda_{av}/c_p\rho_0 S_u\right), \qquad (3.4.1)$$

where a is a proportionality coefficient, λ_{av} is the averaged thermal conductivity, c_p is the isobaric heat capacity, and ρ_0 is the unburned gas density. Eq. (3.4.1) indicates that d_q is related to the reciprocal of S_u.

Fig. 3.4.1.5 shows the raw data of d_q plotted against $1/S_{u0,max}$. The broken and solid curves represent the results of linear and exponential fitting, respectively. Agreement between the experiment and linear fitting was not sufficient in the high $S_{u,max}$ region. On the other hand, agreement between the experiment and exponential fitting was good for all of the compounds except R-717. This fitting function is given by

$$d_q = 32.94\, S_{u0,max}^{-0.830}. \qquad (3.4.2)$$

The relative deviation between the results calculated by Eq. (3.4.2) and the experimental results was 18.0% at maximum and 7.0% on average.

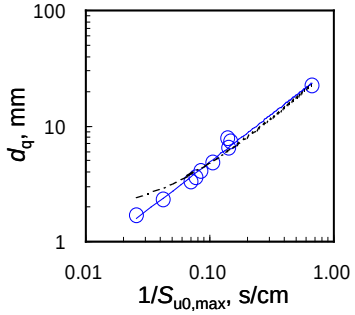

Fig. 3.4.1.5 Experimental d_q vs. $1/S_{u0,max}$. Broken curve: linear fitting. Solid curve: exponential fitting.

Based on Eq. (3.4.1), ρ_0 is more sensitive to the variation in compounds than c_p and λ_{av}. Therefore, we plotted d_q against $1/\rho_0 S_{u0,max}$. Fig. 3.4.1.6 shows the results with their fitting curves. The exponential fitting curve can represent the results for all of these compounds. The fitting curve is given by

$$d_q = 47.61\left(\rho_0 S_{u0,max}\right)^{-0.871}. \qquad (3.4.3)$$

The relative deviation between the results calculated by Eq. (3.4.3) and the experimental results was 6.7% at maximum and 3.6% on average. Note that the present experiment covered the most and least flammable refrigerants, unsaturated compounds, a flammable/nonflammable blend, and nonfluorinated compounds. Therefore, Eq. (3.4.3) is considered to be valid for all of the flammable refrigerants. If $S_{u0,max}$ of a new refrigerant is unknown, it can be estimated by using the experimental d_q and Eq. (3.4.3). In particular, if d_q is larger than 5 mm, the compound will be classified as 2L.

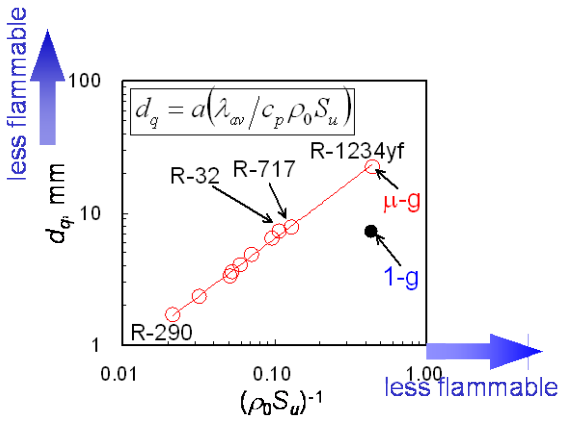

Fig. 3.4.1.6 d_q vs. $1/\rho_0 S_{u0,max}$. Solid curve: exponential fitting.

3.4.1.2 Minimum Ignition Energy (E_{min})

E_{min} is defined as the amount of energy needed to raise a spherical volume of gas mixture of d_q up to the flame temperature: i.e.,

$$E_{min} = (\pi/6) d_q^{\,3} \rho_b\, c_p\, (T_b - T_0). \qquad (3.4.4)$$

This can also be expressed as

$$E_{min} = \pi d^2 \frac{\lambda_{av}(T_b - T_0)}{S_u}. \qquad (3.4.5)$$

Assuming that $T_b - T_0 = 1900$ K, E_{min} is obtained from the experimental d_q. The results are listed in the third column of Table 3.4.1.2. The estimated value of R-290 was more than three times the experimental value of 0.246 mJ.

We calibrated the calculated E_{min} so that E_{min} of R-32 could become 15 mJ; these values are listed in the fourth column of Table 3.4.1.2 and represented by curves in Fig. 3.4.1.7. The

agreement between the calibrated and experimental E_{min} can be greatly improved. Thus, to discuss the E_{min} quantitatively, at least one reliable value of E_{min} for 2L refrigerants is necessary for calibration.

Note that the above calculation of E_{min} was based on the experimental d_q. According to Eq. (3.4.3), the experimental d_q is related to the experimental $S_{u0,max}$, but the exponent of $(1/S_{u0,max})$ is not unity but rather 0.871. This indicates that the experimental E_{min} in Eqs. (3.4.4) and (3.4.5) is dependent on $(1/S_{u0,max})^{2.61}$ and $(1/S_{u0,max})^{2.74}$, not $(1/S_{u0,max})^{3}$. This finding agrees qualitatively with the experimental relationship between E_{min} and d_q reported by Lewis and Von Elbe (1987, p. 355). Thus, the experimental E_{min} may be more mildly dependent on $S_{u0,max}$ than the theoretical prediction.

As noted above, the experimental E_{min} is greatly dependent on the electrode geometry. Unfortunately, most of the reported values for 2L refrigerants were measured with the electrode gap narrower than d_q. Therefore, these values were significantly affected by heat loss to the electrodes. For example, Smith et al. (J. Testing and Evaluation, 31, 178-182 (2003)) reported E_{min} and d_q for four flammable refrigerants using electrodes with 25-mm diameter parallel plates as follows: 0.30 mJ and 1.7 mm for R-290, 0.89 mJ and 3.2 mm for R-152a, 18,421 mJ and 4.3 mm for R-143a, and 26,300 mJ and 5.2 mm for R-32. Compared to our results in Table 3.4.1.1, they ignited R-143a and R-32 with a spark gap that was 2 mm narrower than our d_q. As shown in Fig. 3.4.1.2, the 25-mm parallel plates were not large enough to obtain the converged value of d_q for R-32. In other words, if an extremely high spark energy is discharged between electrodes with 25-mm parallel plates, ignition of R-32 can occur with gaps narrower than d_q. For R-290 and R-152a, Smith et al. measured E_{min} with the electrode gap wider than our d_q, and their results agreed sufficiently well with our data listed in Table 3.4.1.2. Thus, when considering the ignition energy in the laboratory and practical situations, we should verify whether the spark was generated with the electrode gap wider than the quenching distance. The flame heat loss to the electrodes increases the ignition energy considerably. This is considered to be one of the main reasons why ignition from high-voltage sparks barely occurs for magnetic contactors, relays, and sockets for 2L refrigerants with a large d_q.

Table 3.4.1.2 Calculated minimum ignition energies

Name	$S_{u0,max}$, cm/s	calc. E_{min}, mJ [a)]	calib. E_{min}, mJ [b)]	exp. E_{min}, mJ
R-290	38.7	0.79	0.20	0.246 [c)]
R-152a	23.6	2.0	0.51	
R-717	7.2	82	21	
R-143a	7.1	48	12	
R-32	6.7	59	(15)	15 [d)]
R-1234yf	1.5	2000	520	<500 [d)]

a) Calculated by Eq. (3.4.4).

b) Calibration was performed so that E_{min} of R-32 may become 15 mJ.

c) From Lewis and Von Elbe (1987). d) This work.

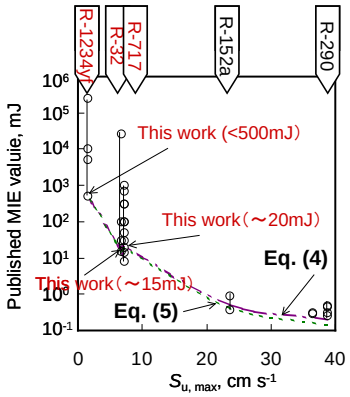

Fig. 3.4.1.7 Comparison between calibrated and experimental values of E_{min}.

3.4.1.3 Extinction Diameter of Opening (d^*)

When electric equipment with openings, such as a circuit breaker and magnetic contactor, operate in a flammable gas atmosphere, the electric spark generated by these pieces of equipment can be an ignition source. Even though ignition occurs at the electrode gaps inside the enclosure, combustion will

not be transmitted to the flammable gas atmosphere outside the enclosure unless the diameter of the opening of the enclosure exceeds the critical value d^*. In this report, we call d^* the "extinction diameter." Fig. 3.4.1.8 shows a schematic drawing of the apparatus for extinction diameter measurement. Experiments were carried out in the same vessel as that used for the quenching distance measurement. A thin square PTFE plate with an circular opening was set at distance h from the ignition point. The square plate had a side of 70 mm and thickness of 1 mm. We observed whether the flame sphere could go through the opening.

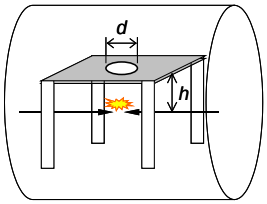

Fig. 3.4.1.8 Apparatus for extinction diameter measurement.

Fig. 3.4.1.9 shows the measured d^* for R-32, R-717, and HFC-254fb as a function of h. The plots at h = 0 indicate d_q in Table 3.4.1.1. In the small h region, d^* decreased rapidly with increasing h. As h increased further, d^* decreased gradually and finally reached almost a constant value. d^* at $h = \infty$ is less than half of d_q. This tendency may reflect the formation process of stable flames.

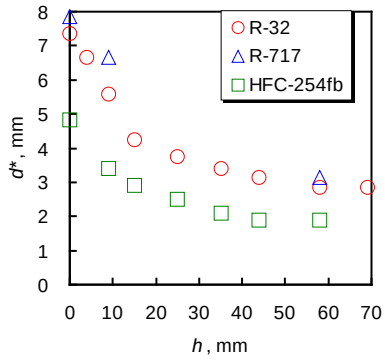

Fig. 3.4.1.9 d^* vs. h for R-32, R-717, and HFC-254fb.

For R-1234yf, 14 mm < d^* < 14.5 mm at h = 73 mm in 1-g, and $d^* \approx$ 10 mm at h = 58 mm. Fig. 3.4.1.10 shows direct images of R-1234yf/air flame from the μ-g experiment (bird's-eye view of Fig. 3.4.1.8).

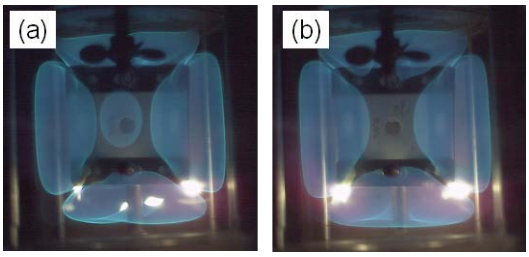

Fig. 3.4.1.10 Flame propagation of R-1234yf/air mixture from d^* measurement in μ-g. Both images are at 10 vol%, d = 10 mm, and h = 58 mm. (a) Flame could go through the opening. (b) Flame could not go through the opening.

Considering the application of d^* to practical risk assessment, the effect of the shape of openings on d^* is also of interest. We measured the extinction size of rectangular openings with length-to-width (l/w) ratios of 3 and 5.

Fig. 3.4.1.11 shows the results of 21 vol% R-32/air using rectangular openings and circular openings. Fig. 3.4.1.11(a) shows the width (w) vs. h. The value of extinction w decreased with increasing l/w ratio. However, further quantitative discussion is difficult using just this graph. We then introduced the effective diameter (d_{eff}), which may be taken as the hydraulic diameter: i.e.,

$$d_{eff} = 4A/P\,, \qquad (3.4.6)$$

where A is the cross-sectional area of the opening and P is the perimeter of the opening. For a circle, $d_{eff} = d$.

Fig. 3.4.1.11(b) shows d_{eff} vs. h. The results of the rectangular openings sufficiently agreed with those of the circular openings, which validated the introduction of the hydraulic diameter. Thus, we can generalize the extinction diameter of openings.

Consider the application of d^*. Assuming that the value of d^* is dominated by $1/S_u$, d^* of a 2/2L

boundary refrigerant is almost the same as d^* of HFC-254fb, as shown in Fig. 3.4.1.9. If we measure the distance between the ignition point and opening (h) and d_{eff} of electric equipment and the combination of h and d_{eff} lies below the d^* curve of HFC-254fb in Fig. 3.4.1.9, the flame of the 2L refrigerant does not pass through the opening. Otherwise, it may be necessary to change h and/or d_{eff} of the equipment until the combination falls below the d^* curve in Fig. 3.4.1.9.

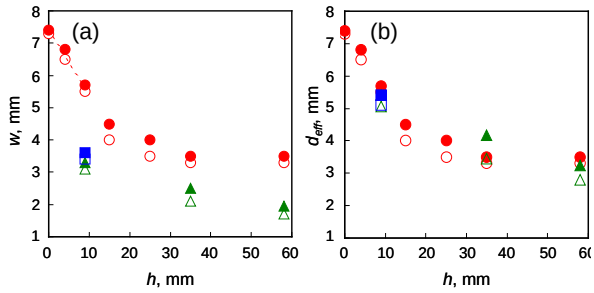

Fig. 3.4.1.11 Extinction size of the opening vs. h for R-32. (a) w vs. h. (b) d_{eff} vs. h. Circle: circular opening. Square: rectangular opening with l/w = 3. Triangle: rectangular opening with l/w = 5. Filled symbols represent "go," and open symbols represent "no go."

There may be a question as to whether an increase in pressure inside the enclosure enables the flame to go through the small openings. To answer this question, we measured d^* using small acrylic combustion vessels.

Fig. 3.4.1.12 shows a schematic drawing of the experimental apparatus. An acrylic vessel with dimensions of 30 mm × 30 mm × 50 mm was set in a 155 mm diameter cylindrical vessel. The top and bottom plates were made of PTFE with a thickness of 1 mm and were interchangeable.

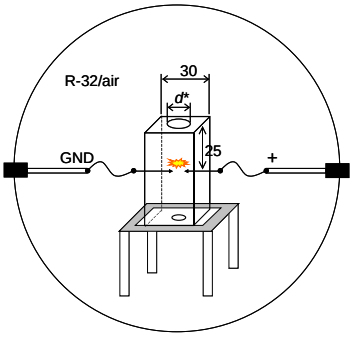

Fig. 3.4.1.12 Apparatus of extinction diameter measurement using a small acrylic vessel in a 3.8 L cylindrical vessel.

The experimental conditions and results are summarized in Table 3.4.1.3. First, we used the vessel with the bottom closed (Test No. 1). The extinction diameter of R-32 flame was found to be 10 mm < d^* < 11 mm for the top opening. Second, we used the vessel with the top closed and obtained 11.1 mm < d^* < 12 mm for the bottom opening. Thus, we decided to focus on the top opening because it provided more conservative values than the bottom opening. Hereafter, go/no go judgment was only performed for the top opening; the bottom opening was used only for varying the increase in pressure inside the acrylic vessel.

Table 3.4.1.3 Extinction diameter of R-32/air using a small acrylic vessel in millimeters.

Test No.	1	2	3	4	5
Top opening	Variable				
Bottom opening	close	open	d = 12	d = 3.2	Same size as top opening
d_NoGo	10	3.9	5.0	11	6.0
d_Go	11	4.0	5.5	12	6.5

Fig. 3.4.1.13 shows d against the increase in pressure inside the acrylic vessel (p_{red}). p_{red} was obtained by the NFPA 68 method under the assumption of K_{G} = 1.9 MPa·m/s for R-32/air. An

anomalous tendency was found between d^* and p_{red}. Two different phenomena appeared to occur: a laminar flame passing through the opening when p_{red} < 100 kPa, and turbulent flow igniting gas far outside the opening when p_{red} > 100 kPa. Typical flame behaviors for R-32/air flames are shown in Fig. 3.4.1.14. In any case, d^* was at its minimum value when $p_{red} \approx 0$; this indicates that the gas flow increases the probability of extinction of R-32 flame owing to the increasing rate of heat loss from the flame to the surrounding fresh gas. Thus, if we consider the worst case for ignition due to electric equipment, we should employ d^* at p_{red} around 0, such as the extinction diameter in the quiescent condition as shown in Figs. 3.4.1.9 and 3.4.1.11. Currently, data on d^* using a small vessel are limited to a few cases of R-32/air. Accumulating more data is necessary to clarify the effects of an enclosure's structure on d^*.

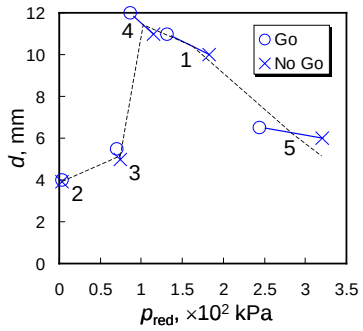

Fig. 3.4.1.13 Extinction diameter of R-32/air using a small acrylic vessel as a function of p_{red}. The number in the figure corresponds to the test number in Table 4-4-1-3.

Fig. 3.4.1.14 R-32/air flame going through the opening(s) of a small acrylic vessel. The number in the figure corresponds to the test number in Table 3.4.1.3.

3.4.2 Flammability limits

3.4.2.1 Temperature and humidity effects on the flammability limits of several 2L refrigerants

To study the effects of temperature and humidity on the flammability limits of 2L refrigerants, typical 2L compounds were measured. The measurements were made in a 12 L spherical glass flask following the ASHRAE method. The temperature dependency was examined over the range of 5°C–100°C. The observed temperature coefficients of the flammability limits are shown in the following table.

Table 3.4.2.1 Temperature coefficients of flammability limits

Refrigerant	LFL		UFL	
	Obs.	Pred.	Obs.	Pred.
Ammonia	-0.0086	-0.0095	0.0208	0.0189
R32	-0.0070	-0.0064	0.0091	0.0133
R143a	-0.0051	-0.0038	0.0080	0.0093
R1234yf(d)	-0.0133	-0.0029	0.0102	0.0052
R1234yf(w)	-0.0045	-0.0028	0.0098	0.0071
R1234ze(w)	-0.0104	-0.0029	0.0174	0.0061

In general, the temperature dependence of the lower flammability limits can be explained by White's rule. According to this rule, the lower flammability limit L at temperature t is expressed as follows:

$$L = L_{25}\left\{1-\frac{100C_{p,L}}{L_{25}\cdot Q}(t-25)\right\} \quad , \qquad (3.4.7)$$

where L_{25} is the lower flammability limit (vol%) at 25°C, $C_{p,L}$ is the heat capacity of unburned gas at the lower flammability limit, and Q is the molar heat of combustion of the fuel gas. Similarly, the upper flammability limit can be written as follows:

$$U = U_{25}\left\{1+\frac{100C_{p,L}}{L_{25}\cdot Q}(t-25)\right\} \quad . \qquad (3.4.8)$$

As shown in the above table, the temperature dependences of the flammability limits for

ammonia, R-32, and R-143a basically agree with the values predicted by the above equations. However, the temperature dependences of the flammability limits for R-1234yf and R-1234ze(E) were considerably larger than those predicted by these equations.

With regard to the humidity effect on the flammability limits, measurements were taken over a humidity range of 0%–90% corrected for 23°C. The flammability limits of ammonia, R-32, and R-143a were found to not be greatly affected by the humidity of air. On the other hand, the flammable ranges of R-1234yf and R-1234ze(E), whose molecules contain more F-atoms than H-atoms, were found to be markedly dependent on the humidity. Fig. 3.4.2.1 shows the humidity effect on the flammability limits of R-1234yf and R-1234ze(E).

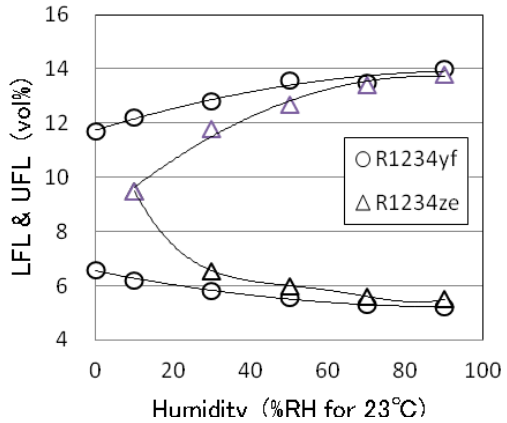

Fig. 3.4.2.1 Humidity effects on flammability limits of R-1234yf and R-1234ze(E)

3.4.2.2 Flammability property of nonflammable refrigerants under high humidity condition

The effect of relatively high humidity on the flammability property was measured in air for R-410A, R-410B, R-134a, and R-125. Relatively high humidity means humidity of up to 50% at 60°C. The measurements were done in a 12 L spherical glass flask following the ASHRAE method. Under this humidity condition, samples of R-410A, R-410B, and R-134a became flammable, whereas R-125 did not. For the first three samples, the limiting humidity condition to make the gas flammable was determined. In addition, the effect of temperature up to 100°C was examined for these materials at a relative humidity of 50% corrected for 23°C. The results showed that all four samples remained nonflammable under this condition. Table 3.4.2.1 shows the observed flammability limits of R-410A, R-410B, and R-134a at 50% relative humidity for 60°C.

Table 3.4.2.1 Flammability limits of R-410A, R-410B, and R-134a

Refrigerant	LFL		UFL	
	vol%	±	vol%	±
R134a	11.5	0.3	15.9	0.4
R410A	15.6	0.2	21.8	0.4
R410B	16.3	0.3	20.9	0.4

3.4.2.3 Flammability limits for binary mixtures of ammonia with multifluorinated compounds

Flammability limits for binary mixtures of ammonia with R-1234yf, R-1234ze(E), R-134a, and R-125 were measured in dry air. The measurements were taken in a 12 L spherical glass flask using the ASHRAE method. The flammability limits of ammonia and R-1234yf mixtures were found to be very different from the values predicted by Le Chatelier's equation. Le Chatelier's equation was modified by the introduction of an ellipse function to analytically express the flammability limits of the mixtures of arbitrary concentrations. The following is the modified ellipse equation:

$$1/L = \left(c_{am}/L_{am}\right)\left(1 + p_1 c_{yf} + p_2\sqrt{c_{yf} - c_{yf}^2}\right) + \left(c_{yf}/L_{yf}\right)\left(1 + p_3 c_{am} + p_4\sqrt{c_{am} - c_{am}^2}\right)$$

, (3.4.9)

where L, L_{am}, and L_{yf} are the flammability limits of the mixture, ammonia, and R-1234yf, respectively. c_{am} and c_{yf} are fractions of ammonia and R-1234yf, respectively, in the binary mixture, and $c_{am} + c_{yf} = 1$. p_1–p_4 are parameters that are adjusted to appropriately explain the observed values. Fig. 3.4.2.2 compares the observed flammability limits with the calculated

values for ammonia/R-1234yf mixtures: open circles represent the observed values, solid lines show the calculated values, and dotted lines show the values predicted by Le Chatelier's equation.

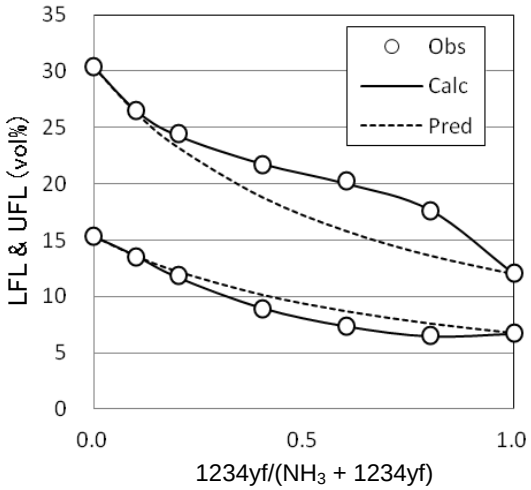

Fig. 3.4.2.2 Flammability limits for R-717/1234yf mixtures.

R-1234ze(E) was found to be nonflammable in dry air but flammable if more than 4% ammonia was added. If the content of ammonia exceeded 20%, the flammability limits became very close to the corresponding ones for R-1234yf and ammonia. In contrast, the flammable regions of ammonia mixed with those of R-134a and R-125 were much narrower than the mixtures of R-1234ze(E). The ellipse-modified Le Chatelier's equation was extended to successfully explain the flammability limits of these mixtures. The ellipse-extended equation is as follows:

$$1/L = (x_{am}/L_{am})\left(1 + q_1 x_{ze} + q_2\sqrt{x_{ze} - x_{ze}^2}\right) + (x_{ze}/L_{FIP})\left(1 + q_3 x_{am} + q_4\sqrt{x_{am} - x_{am}^2}\right) \quad (3.4.10)$$

where L and L_{am} are the flammability limits of the mixture and ammonia, respectively, and L_{FIP} is the limiting mixture concentration at FIP. $x_{ze} = c_{ze}f$ and $x_{am} = 1 - x_{ze}$, where f is the extension factor and c_{ze} is the fraction of R-1234ze(E) in the mixture. q_1–q_4 are parameters to be adjusted by fitting the procedure to the observed values. Note that Eq. (3.4.10) coincides with Eq. (3.4.9) when the factor f is equal to unity. Fig. 3.4.2.3 compares the observed and calculated flammability limits of the ammonia/R-1234ze(E) mixtures. In this case, FIP was located at $c_{ze} = 0.96$; therefore, the extension factor became 1.04. The flammability limits of ammonia/R-134a and ammonia/R-125 mixtures can also be explained by using the above equation.

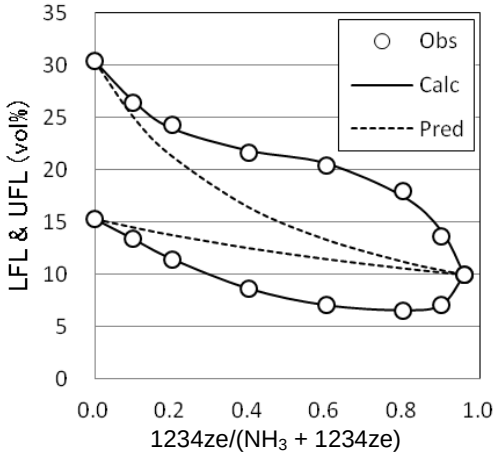

Fig. 3.4.2.3 Flammability limits for R-717/1234ze(E) mixtures.

3.4.2.4 Tentative proposal for limiting methane concentration

Various fluoro-compounds are currently being developed to establish suitable replacements for CFCs. Most of these compounds contain hydrogen atoms, and some are flammable. There is a wide range of flammable and nonflammable fluoro-compounds. The nonflammable compounds also have different degrees of nonflammability. Newly developed refrigerants are commonly mixtures of a few different compounds. To adequately estimate the flammability of such mixtures, accurate knowledge on the flammability property of each component compound is necessary. In the present study, the concept of limiting methane concentration (LMC) was tentatively proposed for assessing the degree of nonflammability of nonflammable gases and vapors. LMC is the minimum methane concentration to be added to a nonflammable gas or vapor to make the resulting gas

mixture flammable. Conversion of LMC to a new index—i.e., F_x-number—can make predicting the flammability and/or nonflammability of refrigerant blends possible. F_x-number is defined by the following equation:

$$F_x = \left(\frac{U-L}{L}\right)^2 = \left[\frac{F(2-F)}{(1-F)^2}\right]^2 . \qquad (3.4.11)$$

Fig. 3.4.2.4 plots F_x-number and F-number against the nitrogen concentration of methane–nitrogen mixtures, where white circles represent F_x-number and black circles represent F-number. Here, the value of F_x-number is normalized to be 0.44 when no nitrogen is added. The linearity of F_x-number is clearly much better than F-number. From now on, we are going to explore the viability of LMC for a wide variety of compounds.

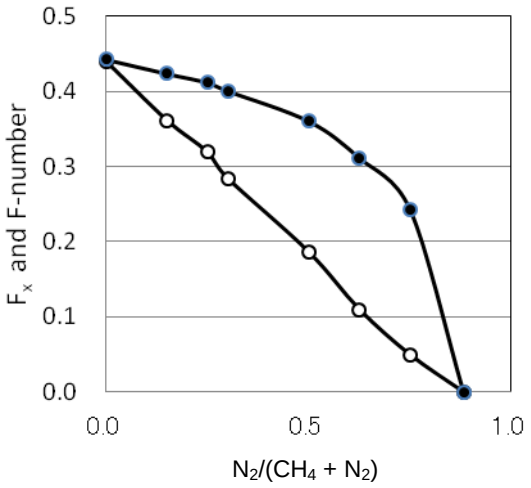

Fig. 3.4.2.4 F_x-number for CH_4–N_2 system.

3.4.3 Thermal decomposition of refrigerant

The thermal decomposition of refrigerants was investigated using flow reactor. A schematic diagram of the experimental apparatus is shown in Fig. 3.4.3.1. Flow rates of refrigerant and air were measured and controlled by calibrated mass flow controllers, and the refrigerant/air mixture was continuously supplied to a heated tube reactor (Inconel, 12.7 mm outer diameter, 10.2 mm inner diameter, 44 cm length). The reaction temperature was measured by thermocouples (1 mm outer diameter, Type K) that were inserted in the tube (Inconel, 3.175 mm in outer diameter, 1.4 mm inner diameter, 62 cm length) at a center of the reactor tube. The concentrations of the refrigerant and decomposition products such as HF were measured using FT-IR (cell length was 10 cm, ZnSe windows). The O_2 concentration was measured by GC (TCD detector, Ar carrier, 3 mm diameter × 3 m length SUS column packed with Molecular Sieve 13X-S, column temperature of 30°C). To adjust the IR intensity, N_2 was added to the reaction gas immediately behind the reactor. Before introduction to GC, the gas was treated with soda lime. The exhaust gas was also treated with soda lime. The experiment was started at room temperature, and the temperature was increased in a stepwise fashion. The refrigerant, O_2 and products were measured under a steady state.

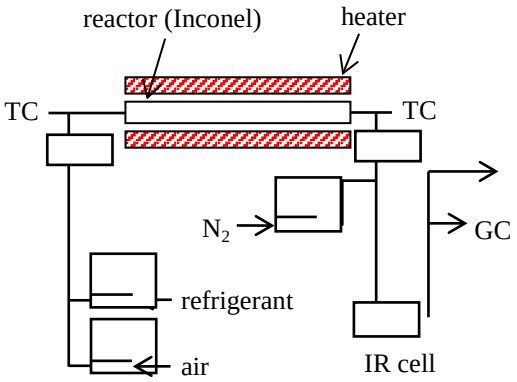

Fig. 3.4.3.1 Schematic diagram of experimental apparatus.

Figure 3.4.3.2 shows the thermal decomposition results for R-1234yf (CH_2=$CFCF_3$). Here, O_2 consumption and productions such as HF were based on the supplied mole of R-1234yf. Figure 3.4.3.2 shows the three experiment runs; the results were consistent with each other. Consumption of R-1234yf and O_2 was observed at a temperature of around 600°C or more; consumption considerably increased at this temperature. The major products

were HF, COF_2, CO_2, and CO; these were observed at a temperature of around 600°C or more. No detectable differences were observed between the clean reactor and reactors that had been used for previous experiments.

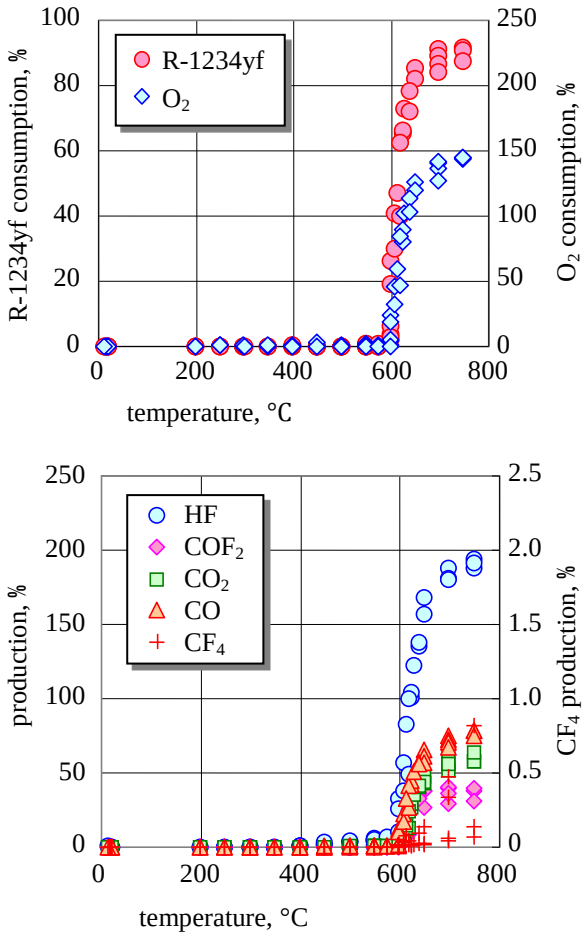

Fig. 3.4.3.2 Results of thermal decomposition of R-1234yf. R-1234yf = 7.8 vol% (φ = 1), total flow rate = 100 cm^3/min.

Figure 3.4.3.3 shows the thermal decomposition results of R-1234ze(E) ((E)–CHF=$CHCF_3$). Consumption of R-1234ze(E) was observed at around 550°C or more, and consumption of O_2 and the products such as HF were observed at around 600°C or more when the clean reactor was used in the experiment. When a contaminated reactor was used in the experiment, however, consumption of R-1234ze(E) was observed at about 350°C or more, whereas consumption of O_2 and products such as HF was not observed up to around 550°C. The reproducibility of the consumption rate for R-1234ze(E) at 350°C–550°C was good; however, the open small symbols in Fig. 3.4.3.3 represent the results of three experiment runs, and the amount of decomposition products in the reactor may have differed. Note that, at around 550°C–600°C, R-1234ze(E) consumption was observed; in contrast, O_2 consumption and products were not observed in this temperature range if a clean reactor was used. Therefore, in this temperature range, the consumption of R-1234ze(E) may be affected by trace amounts of decomposition products. When the reactor tube was contaminated by more than the threshold value of decomposition products, the temperature for consumption initiation of R-1234ze(E) decreased by approximately 200°C; the consumption of R-1234ze(E) did not depend on the amount of decomposition products that was attached to the reactor tube.

Figure 3.4.3.4 shows the thermal decomposition results of R-22 (CHF_2Cl). The consumption of R-22 and O_2 and products such as HF were observed at around 450°C or more when a clean reactor was used for the experiment. At around 450°C–650°C, the consumption and products gradually increased with increasing temperature. When a contaminated reactor was used for the experiments, R-22 consumption was observed at about 350°C or more, whereas O_2 consumption and products such as HF were not observed up to around 450°C. At around 450°C or more, no differences between clean and contaminated reactors were observed for O_2 consumption and products such as HF. When a contaminated reactor was used, a large scatter was observed for R-22 consumption at around 350°C–600°C. Thus, R-22 consumption may depend on the amount of decomposition products.

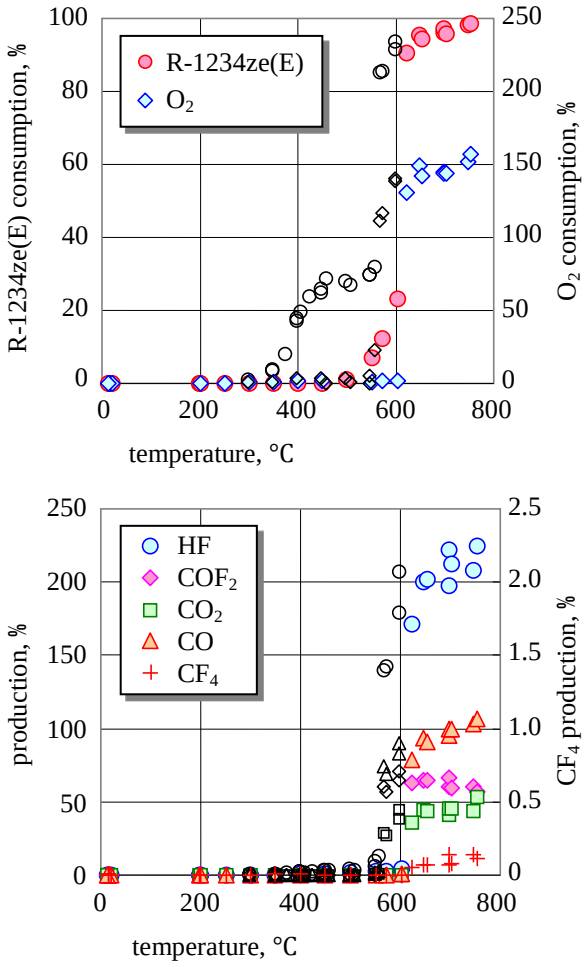

Fig. 3.4.3.3 Thermal decomposition results of R-1234ze(E). R-1234ze(E) = 7.8 vol% (φ = 1), total flow rate = 100 cm^3/min. Open small symbols represent measurements taken when decomposition products contaminated the reactor.

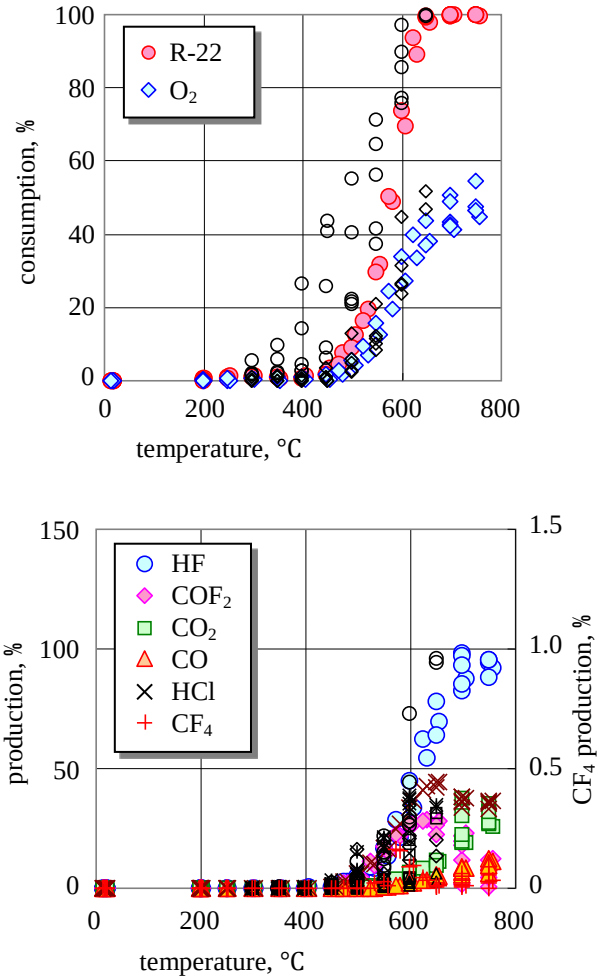

Fig. 3.4.3.4 Results of thermal decomposition of R-22. R-22 = 21.9 vol% (φ = 1.0), total flow rate = 100 cm^3/min. Open small symbols represent measurements taken when decomposition products contaminated the reactor.

3-5. Physical Hazard Evaluation on Explosion and Combustion of A2L Class Refrigerants

Tei SABURI, Akira MATSUGI, Akifumi TAKAHASHI, Hiroumi SHIINA, Masayuki SAGISAKA and Yuji WADA

Research Institute of Science for Safety and Sustainability,
National Institute of Advanced Industrial Science and Technology

Summary

Promoting the conversion of air-conditioning equipment from conventional refrigerants to the lower-flammability refrigerants of A2L[3.5.1)], which have a low global warming potential (GWP), is important to addressing the issue of global warming. The experimental flammability of gases such as R32 and R1234yf was analyzed using a large spherical combustion vessel to assess the safety. Flammability properties such as the flame velocity, burning velocity, and deflagration index were evaluated. The effects of flame lifting due to buoyancy and humidity on the flammability characteristics were considered. The developed numerical combustion model, estimated potential risk of combustion and explosion, and autoignition temperature of A2L/2L refrigerants are described.

3.5.1 Introduction

Difluoromethane (R32, CH2F2) and 2,3,3,3-tetrafluoropropene (R1234yf, CH2=CFCF3) are expected to be next-generation refrigerants with zero ODP and low global-warming potential (GWP). R1234yf is an especially promising candidate that performs better than existing refrigerants; it has a low GWP of less than 150[3.5.2)]. Although these refrigerants perform better than other existing refrigerants in terms of lower ODP and GWP, they exhibit a mild flammability. Thus, evaluating the combustion safety of A2L refrigerants in the event of leakage into the atmosphere owing to an accident is necessary.

3.5.2 Combustion and explosion assessment for A2L/2L

3.5.2.1 Combustion and explosion assessment for A2L/2L

To utilize these mildly flammable gases safely, ASHRAE added an optional 2L subclass to the existing Class 2 – Lower Flammability Classification for the safety classification of refrigerants[3.5.1)]. R32 and R1234yf are classified as A2L, which is defined as low toxicity and low flammability with a maximum burning velocity of ≤10 cm/s. A2L refrigerants have such low burning velocity that a lifted flame front due to buoyancy significantly affects their combustion behavior. In terms of safety, investigating the fundamental flammable properties of these alternative refrigerants is important. To observe and evaluate the effect of buoyancy on the flammable properties of R32 and R1234yf, a large-volume spherical vessel was prepared in this study, and the flame propagation behaviors of R32 and R1234yf were observed using a high-speed video camera; the flame propagation velocity was estimated by image analysis of the high-speed video images. The burning velocity was estimated from the flame speed and pressure profile measurement using the spherical vessel method under the assumption of a spherical flame front expansion[3.5.3)]. The maximum peak pressure (i.e., maximum overpressure relative to the pressure in the vessel during combustion) and deflagration index (i.e., constant that defines the maximum rate of pressure increase with time of combustion)[3.5.4),3.5.5)] were evaluated according to the pressure profile. Ignition tests using mixture gases with an electric discharge were conducted for a varying equivalent ratio φ, which is the ratio of the fuel–oxygen ratio to the stoichiometric fuel–oxygen ratio: φ0.8−φ1.2 for R32 and φ1.2−φ1.4 for R1234yf.

Experiment

Fig. 3.5.1 shows the experimental apparatus with the spherical vessel. The spherical vessel had a diameter of 1 m and volume of 0.524 m^3. A pressure transducer was placed on top of the vessel. The pressure profile formed during combustion was recorded by a data logger. The burning behavior was observed with a high-speed video camera through a PMMA viewing port. The R32 burning behavior was investigated at equivalent ratios of ϕ0.8–ϕ1.2. The R1234yf burning behavior was evaluated at equivalent ratios of ϕ1.2–ϕ1.4 against a reference ratio of ϕ1.325 (mixing ratio of 10 vol%, which gives the maximum burning velocity for R1234yf as reported by Takizawa et al.[3.5.3)] using the spherical vessel method[3.5.6),3.5.7)]). Pressure transducers were used to introduce fuel gas into the vessel up to a certain partial pressure (BGs in Fig. 3.5.1). Air was then introduced into the vessel until the total pressure in the vessel was conditioned at a atmospheric pressure of 101,325 Pa. For the gas introduction and mixing procedure, gas circulation was maintained by a diaphragm pump (DP in Fig. 3.5.1) during the R1234yf test. The electrode for the electric spark was a set of horizontally opposed tungsten wires that were 1 mm in diameter; the gap length between wires was 7 mm. The electrode provided a spark upon the application of a high-voltage power supply to ignite the mixture gas. The discharge voltage and current were recorded by an oscilloscope, and the discharge energy was estimated. The flame front expansion behavior was recorded by the high-speed camera, and the recorded video image sequences were visually analyzed; the flame velocities in the side and upper directions were evaluated.

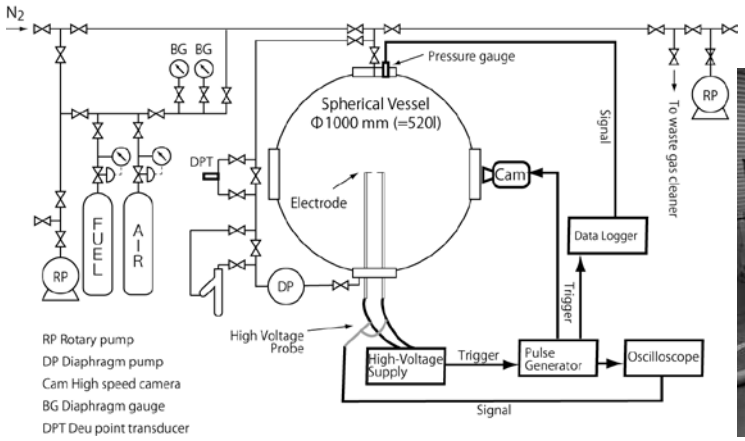

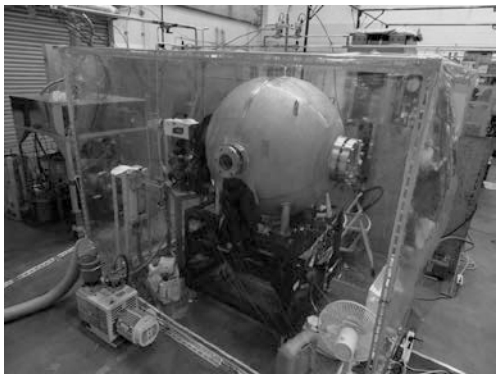

Figure 3.5.1. Schematic drawing of experimental apparatus.

Flame velocity and burning velocity

The burning velocity S_u was evaluated from the flame speed S_f as follows:[3.5.8)]

$$S_u = \left(\frac{\rho_b}{\rho_u}\right) \cdot S_f, \quad (1)$$

where ρ is the density (m^{-3}) and subscripts u and b of ρ denote unburned and burned gas, respectively. ρ_u is the density at the initial condition, and the unknown ρ_u density was estimated using a chemical equilibrium calculation[3.5.9)] under the assumption of a constant pressure during combustion. S_f is the flame speed ($cm \cdot s^{-1}$). In this study, the upward flame speed S_f was estimated from the rate of change in the flame top position (cm) with time along with the sideward flame speed S_f, which was estimated from the rate of broadening of the half-flame width r_f (cm)[3.5.8)]. The sideward S_f minimizes the influence of buoyancy, whereas the upward S_f involves the apparent speed due to buoyancy.

The burning velocity S_u was also calculated by the spherical vessel method[3.5.6),3.5.7)] under the assumption of a spherical flame front expansion as follows:

$$S_u = \frac{R}{3}\left[1-(1-x)\left(\frac{P_0}{P}\right)^{\frac{1}{\gamma_u}}\right]^{-2/3} \cdot \left(\frac{P_0}{P}\right)^{\frac{1}{\gamma_u}} \frac{\mathrm{d}x}{\mathrm{d}t},$$

where R is the inner radius of the chamber (m), x is the mass fraction of burned gas, P_0 is the initial pressure in the chamber (Pa), P is the instantaneous pressure during burning in the chamber (Pa), and γ_u is the specific heat ratio. The values of x and γ_u for each instantaneous pressure were estimated using the equilibrium code[3.5.9)]. Fig. 3.5.2 shows example high-speed video images for the flame front propagation behaviors of R32 ϕ0.9 and ϕ1.2. The flame expanded while slowly climbing upward. The shape of the flame front, which is the interface between the unburned and burned gas, was distorted under the influence of buoyancy and viscosity. The expansion behaviors between ϕ0.9 and ϕ1.2 were almost the same other than their temporal response. Fig. 3.5.3 shows high-speed video images for the flame front propagation behavior of R1234yf ϕ1.35. No clear and smooth flame front was observed; the flame front was convoluted without symmetry and floated upward. Furthermore, the ignition characteristics of R1234yf were unstable and depended on experimental conditions such as the discharge energy, duration of discharge, and electrode geometry.

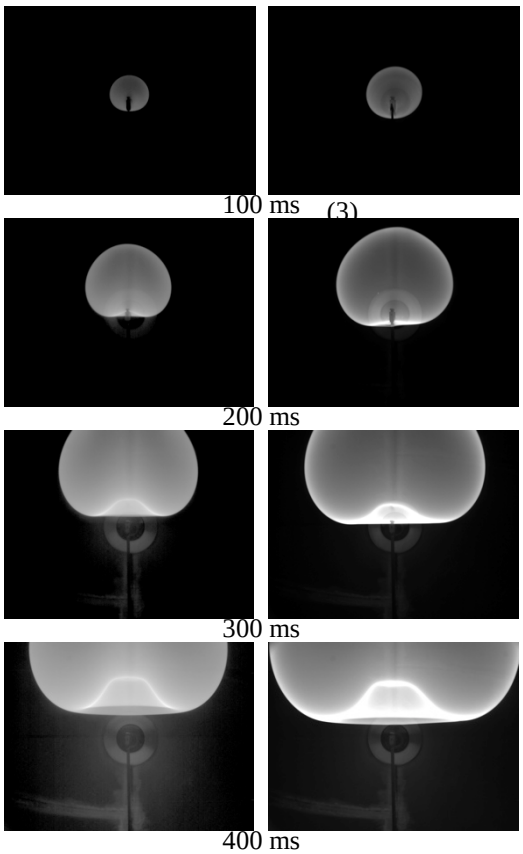

Figure 3.5.2. Images of flame front propagation for R32 (ϕ0.9 for left, ϕ1.2 for right).

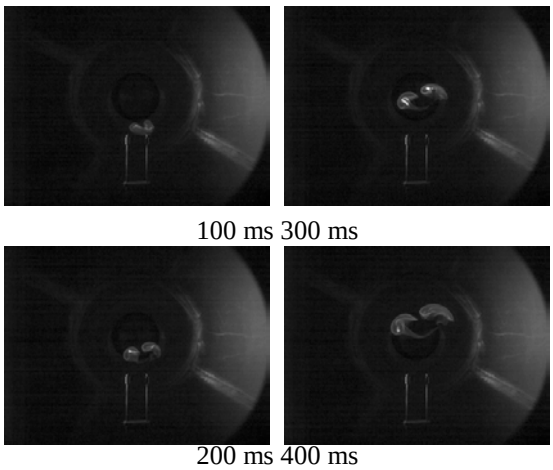

Figure 3.5.3. Images of flame propagation for R1234yf (ϕ1.35).

Fig. 3.5.4 shows pressure profiles for R32 ϕ0.8–1.2 as measured by a pressure transducer. The profiles all seemed to show that the pressure increased in stages. A possible cause may be the influence of the

reflected flame front from the top wall. The arrival time of the upper direction flame front to the top of the vessel could be predicted from image analysis: about 0.5 s for φ0.9 and 0.46–0.47 s for φ 1.0–1.2. Thus, the pressure reached a peak maximum far behind the arrival time of the flame front. The flame front rose in the upper direction owing to buoyancy, whereas the unburned gas remained in the lower half of the vessel. The underside of the flame front was accompanied by a complicated flow of unburned gas.

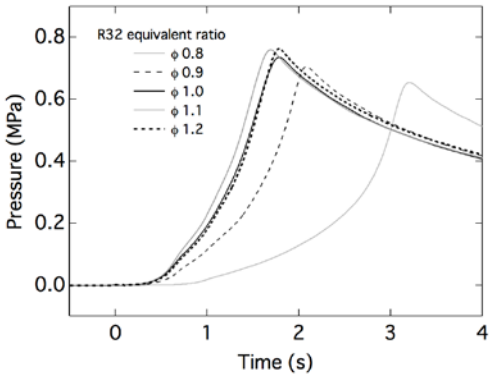

Figure 3.5.4. Measured pressure profile for R32 (ϕ0.8–1.2).

Pressure profiles for R1234yf were also measured; these are shown in Fig. 3.5.5. The profile trends associated with the equivalent ratio were not simple. This seems to be due to the influence of the unstable ignition characteristics. The pressure increased to the peak maximum very gradually compared with R32 and took more than 6 s. The profile for the pressure increase at ϕ1.35 was small, and no increase in pressure was observed at ϕ1.4; therefore, most fuels seemed to remain without burning.

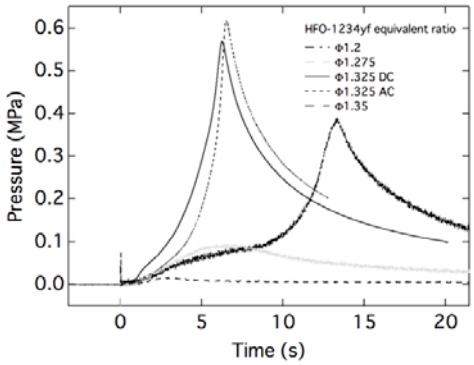

Figure 3.5.5. Measured pressure profile for R1234yf (ϕ1.2–1.35).

The maximum flame width and flame top position from the ignition point were visualized for R32, and the flame speed S_f was estimated based on the temporal differentiation of the flame width and height of the flame top profile, as shown in Fig. 3.5.6. The flame speeds in the upper direction increased 1.2–2.0 times more than those in the side direction as time progressed owing to buoyancy associated with the increase in volume of the burned side. For R1234yf, proper evaluation of the maximum flame width and flame top position was difficult because a clear and smooth flame front was not observed.

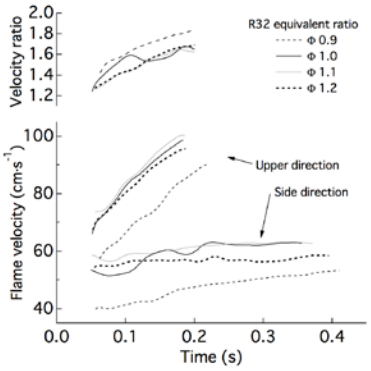

Figure 3.5.6. Evaluated flame speed (upper and side directions) and velocity ratio between upper and side directions for R32 (ϕ0.9–1.2).

As shown in Fig. 3.5.7, the burning velocity S_u was estimated using the sideward flame speed S_f [3.5.8)] for R32. The burning velocity according to the spherical-vessel (SV) method[3.5.6),3.5.7)] was also

estimated from the obtained pressure profiles and numerical computation under the assumption of spherical flame propagation for R32, as shown in Fig. 3.5.7. Although the flame did not propagate with a spherical shape, as shown by the high-speed video images presented in Fig. 3.5.2, S_{u0} was estimated and used to investigate the deviation due to distortion from buoyancy. During analysis, the pressure increase profile did not depart from the scope of the spherical flame front expansion in the early stages. S_{u0} was compared with the reference S_{u0} values for R32[3.5.10]. The burning velocities based on the flame speed and SV method showed similar equivalent ratio dependencies, but the SV method slightly underestimated S_{u0}.

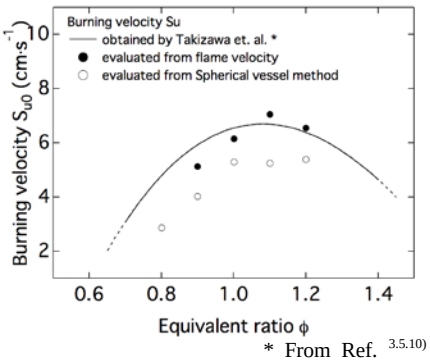

* From Ref. [3.5.10]

Figure 3.5.7. Estimated burning velocity for R32.

As shown in Figs. 3.5.3 and 3.5.5, the flame front expansion was convoluted except for ϕ1.325, and applying the SV method was difficult. Therefore, the burning velocity S_{u0} was estimated for R1234yf ϕ1.325 only; this is shown in Fig. 3.5.8. For R1234yf, the buoyancy had a particular influence on the flame expansion behavior. $S_{u0\text{-}ug}$, which was estimated in a microgravity environment[3.5.11], is shown as a reference in Fig. 3.5.8.

Effect of moisture

The effects of temperature and humidity on the flammability limits of some A2L/2L refrigerants have been reported[3.5.12]; this is an important issue, especially with the hot and humid climate of Japan. Temperatures of over 30°C and 80% humidity are often recorded in the summer.

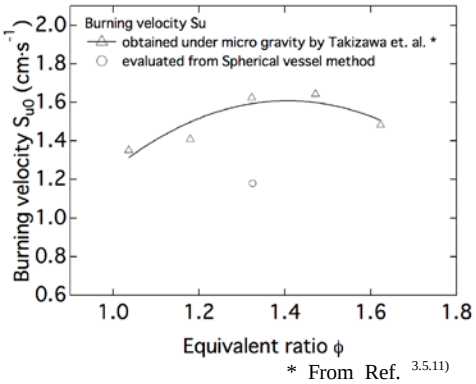

* From Ref. [3.5.11]

Figure 3.5.8. Estimated burning velocity for R1234yf.

To control the humidity in the mixture gas, the dew-point transmitter MICHELL SF72 was used to measure dew point in the chamber and set in the circulation loop, as shown in Fig. 3.5.1. The moisture was added to the mixture gas on the circulation loop by a bubbler, as shown in Fig. 3.5.10. The humidity of the mixture gas was evaluated according to the dew point (dp) and temperature. In the experiment, about 56% RH was attained at the given temperature of 30°C.

Fig. 3.5.11 shows example pressure profiles for R1234yf ϕ1.325 under dry (10°C and 30°C) and wet (56% RH at 30°C) conditions. Research on the effect of buoyancy on the flammability behavior while considering humidity will continue to be conducted.

Figure 3.5.9. Picture of bubbler on circulation loop.

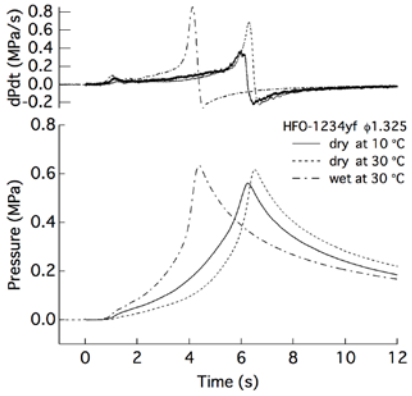

Figure 3.5.10. Pressure profile difference between dry and wet conditions (R1234yf, ϕ1.35).

K_G value

The deflagration index K_G was estimated to analyze the recorded pressure profiles. K_G is commonly used for estimating and designing the explosion venting area of enclosures; it is described according to the equation[3.5.4), 3.5.5)]

$$K_G = \left(\frac{dP}{dt}\right)_{max} \cdot V_{vessel}^{\frac{1}{3}},$$

where P is the pressure (100 kPa), t is the time (s), and V_{vessel} is the volume of the vessel (m^3). A larger K_G requires a larger venting area to prevent the enclosure from bursting. The deflagration indices for gases K_G [3.5.6)] of each refrigerant are summarized, along with other properties such as P_{max}, S_f, and S_u, in Table 3.5.1. It is necessary to pay attention to the physical interpretation that K_G is determined after the reflection of the flame front at the top wall, but the evaluated values may be useful for designing the venting area.

Table 3.5.2 lists P_{max} and K_G with other major gases in descending order of K_G. The table shows that K_G values for R32 and R1234yf were considerably small and the same as or less than that 10 for ammonia[3.5.5)].

Table 3.5.1. Summary of evaluated properties for refrigerants.

Refrigerant	Equivalent Ratio φ	P_{max} (100 kPa)	K_G (100 kPa · m · s^{-1})	Flame speed S_f		Burning velocity S_u		
				$S_{f,t=0.1s.}$ (cm · s^{-1})	S_f (cm · s^{-1})	S_u (cm · s^{-1})	S_{u0} (cm · s^{-1})	S_{u0} (cm · s^{-1})
R32	0.8	6.5	9.4	–	–	–	2.87	4.80 [a]
	0.9	7	9.2	41.4	39.8–53.3	5.13	4.03	5.93 [a]
	1	7.4	8.1	52.4	51.6–63.1	6.15	5.29	6.55 [a]
	1.1	7.6	8.7	58.6	56.4–63.3	6.76	5.24	6.69 [a]
	1.2	7.6	8.9	56.0-	54.4–58.6	6.5	5.38	6.39 [a]
R1234yf	1.2	3.9	1.5	–	–	–	–	–
	1.275	1	0.6	–	–	–	–	–
	1.325	6.2	5.6	–	–	–	1.18	1.625 [b]
	1.35	0.2	0.2	–	–	–	–	–

[a]From Ref. [3.5.10)]

[b]From Ref. [3.5.11)]: Obtained data under micro gravity ($S_{u0\text{-}ug}$).

3.5.2.2 Numerical simulation for combustion of A2L/2L

To apply refrigerants safely to air-conditioning equipment in actual situations, using numerical simulation to assess safety and establish countermeasures is effective at addressing a variety of evaluation endpoints, such as installation configuration of air-conditioners, accident conditions, and the scale of leakage. A numerical combustion model for A2L/2L−air premixed gases should be constructed, and the development of a computational fluid dynamics (CFD) code incorporated with the combustion model will enable the simulation of combustion behavior for refrigerants under various conditions and help estimate the flame propagation distance and blast pressure. The combustion model can be validated by simulating and reproducing the combustion behavior in experiments. The basic concept of the combustion model is based on ref.

3.5.13); it is the solution to a transport equation for variable c with regard to the degree of reaction progress using a function for the burning velocity S_u. The burning velocity is obtained as a time-dependent variable by analysis of experimental data obtained during the project and is believed to be a laminar flame based on the current results. The mean reaction rate used in the transport equation is modeled as follows using the reaction progress source term S:

$$\rho S = \rho_u S_u \nabla c,$$

where ρ is the density and ρ_u is that of the unburned gas. On a practical scale, there is concern over some deviations from the experimental results owing to various instabilities, especially those resulting from the effect of buoyancy. Development of a model that considers these factors is in progress.

3.5.3 Combustion and explosion of A2L/2L by excess energy

3.5.3.1 Estimation of potential risk of explosion

To achieve practical application of A2L/2L refrigerants and enhance safety, the potential risk of explosion, including detonation, should be considered. At present, there have been few reports on this matter. As an implicit but useful reference, a comparison of explosion characteristics, such as the minimum ignition energy (MIE), detonation limit, and K_G, with other flammable gases should be very informative. Table 3.5.2 summarizes some data on P_{max}, K_G, burning velocity, and flammability and detonation limits for mixtures with air from ref. 3.5.14). Further comparison for the combustion and explosion risks of A2L/2L refrigerants with other flammable gases should be considered.

3.5.3.2 Autoignition temperature

The autoignition temperature is the lowest temperature at which a flammable substance will ignite in air at normal atmospheric pressure without an external energy supply such as a spark and flame. To estimate the autoignition characteristics of A2L/2L refrigerants, a test will be conducted according to the ASTM E 659 standard test method[3.5.15)]. This method determines the autoignition temperature of liquid chemicals in air or solid chemicals that readily melt and vaporize at temperatures below the test temperature, in a uniformly heated vessel at atmospheric pressure. We will employ this method for flammable gases in the presence of moisture; some metals will used as catalysts.

The test equipment, which has an operating temperature range of up to 1000°C, is shown in Fig. 3.5.11; it will be introduced and operated in the next quarter. The autoignition characteristics of A2L/2L refrigerants and other flammable gases such as propane and ammonia will be compared.

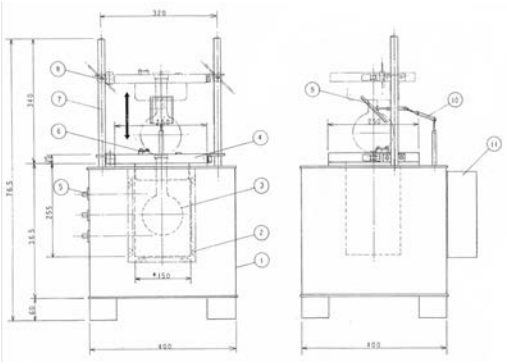

Figure 3.5.11. Illustration of ASTM E 659 autoignition test equipment.

3.5.4 Conclusion

The physical hazards with regard to the explosion and combustion of A2L class refrigerants were evaluated. Flammability characteristics, such as the flame speed, burn velocity, K_G value, and peak pressure, were evaluated using a premixed gas combustion test; the effects of buoyancy and moisture were considered through numerical simulation. To assess the explosion risk of A2L/2L refrigerants, the burning velocity and detonation limits were compared with those of other flammable gases.

Table 3.5.2. Comparison of P_{max}, K_G, and other parameters with other gases.

Flammable Material	P_{max} (100 kPa)	K_G (100 kPa·m·s^{-1})	Burning velocity (cm·s^{-1})	Flammability limits(%)	Detonation limits(%) *3	
					Cofined tube	Unconfined
Acetylene	10.6 *1	1415 *1	166 *2	2.5—80.0 *3	4.2—50.0	
Hydrogen	6.8 *1	550 *1	312 *2	4.2—75.0 *3	18.3—58.9	
Ethylene			80 *2	2.70—36.0 *3	3.32—14.70	
Diethyl ether	8.1 *1	115 *1	47 *2			
Benzene			48 *2	1.3—7.9 *3	1.6-5.55	
Ethane	7.8 *1	106 *1	47 *2	3.0—12.4 *3	2.87—12.20	4.0–9.2
Propane	7.9 *1	100 *1	46 *2	2.1—9.5 *3	2.57—7.37	3.0–7.0
Butane	8.0 *1	92 *1	45 *2	1.8—8.4 *3	1.98—6.18	2.5–5.2
Ethyl alcohol	7.0 *1	78 *1		3.3—19.0 *3	5.1—9.8	
Methanol	7.5 *1	75 *1	56 *2			
Methane	7.1 *1	55 *1	40 *2			
Ammonia	5.4 *1	10 *1	7.2 *4	15—28 *5		
R32	7.6 †	9 †	5 †	13.3—29.3 *6		
R1234yf	6.2 †	6 †	1 †	6.2—12.3 *6		

*1 From Ref. 3.5.5), Table E.1 (0.005ft3 sphere; E=10J, normal condition). *2 From Ref. 3.5.5), Table D.1.
*3 From Ref. 3.5.14), Detonation limits obtained for confined tube. *4 From Ref. 3.5.16)
*5 From Ref. 3.5.17) *6 From Ref. 3.5.18)
† This work.

References

3.5.1) ASHRAE, Designation and Safety Classification of Refrigerants, ANSI/ASHRAE Standard 34-2007 Addendum ak (2010).

3.5.2) European Commission, "Proposal for a Regulation of the European Parliament and of the Council on Certain Fluorinated Greenhouse Gases," COM(2012) 643 final, (2012).

3.5.3) K. Takizawa et al., "Flammability Assessment of CH_2=$CFCF_3$: Comparison with fluoroalkenes and fluoroalkanes," Journal of Hazardous Materials, 172 1329–1338 (2009).

3.5.4) ISO 6184-2, Explosion Protection Systems – Part 2: Determination of Explosion Indices of Combustible Gases in Air, (1985).

3.5.5) NFPA, NFPA 68 Guide for Venting of Deflagrations 2007 Edition, NFPA (2007).

3.5.6) M. Metghalchi, J. C. Keck, Combustion and Flame, 38 143–154 (1980).

3.5.7) P. G. Hill, J. Hung, Combustion and Flame, 123 7–30 (2000).

3.5.8) U. J. Pfahl et al., Combustion and Flame, 123 140–158 (2000).

3.5.9) S. Gordon, B. J. McBride, Computer Program for Calculation of Complex Chemical Equilibrium Compositions and Applications I. Analysis, NASA RP-1311 (1994).

3.5.10) K. Takizawa et al., "Burning Velocity Measurement of Fluorinated Compounds by the Spherical-Vessel Method," Combustion and Flame, 141 298–307(2005).

3.5.11) K. Takizawa et al., "Flammability Assessment of CH_2=$CFCF_3$(R-1234yf) and Its Mixtures with CH2F2 (R-32)," 2010 International Symposium on Next-Generation Air Conditioning and Refrigeration Technology, Tokyo (2010).

3.5.12) S. Kondo, K. Takizawa and K. Tokuhashi, "Effects of temperature and humidity on the flammability limits of several 2L refrigerants," J. Fluorine Chem., 144 130–136 (2012).

3.5.13) V. Zimont, "Gas premixed combustion at high turbulence. Turbulent flame closure combustion model," Experimental Thermal and Fluid Science, 21 179–186 (2000).

3.5.14) Sam Mannan, ed., Lee's Loss Prevention in the Process Industries, 3rd ed., Elsevier, 2–17 12 (2005).

3.5.15) American Society for Testing and Materials, Standard Test Method for Autoignition Temperature of Liquid Chemicals, ASTM E 659–78 (2005).

3.5.16) ISO/DIS 817:2010: Refrigerants - Designation and safety classification, International Organization for Standarization, Geneva, Switzerland, (current DRAFT DFS/ISO/FDIS 817:2012).

3.5.17) NFPA, NFPA 325 Guide to Fire Hazard Properties of Flammable Liquids Gases, and Volatile Solids, NFPA (1994).

3.5.18) Japan Fluorocarbon Manufacturers Association: Environmental and safety data list of specified fluorocarbons (CFC / HCFC) and other fluorocarbons (in Japanese), http://www.jfma.org/database/table.pdf (2013).

4. Progress of the Japan Refrigeration and Air Conditioning Industry Association (JRAIA)

4-1. Mini-split Air-conditioner Risk Assessment SWG: The risk assessment result of the residential air-conditioner, and the study of the mini-split air-conditioner for small business use

Kenji TAKAICHI

JRAIA, Mini-split Air-conditioner Risk Assessment Sub-working Group

4.1.1 Introduction

As a substitute refrigerant for mini-split air conditioners aimed at preventing global warming, R32 used alone and a mixture of refrigerants containing R1234yf and R134a with added R32 have been proposed. The mini-split air-conditioner risk assessment SWG of the Japan Refrigeration and Air Conditioning Industry Association (JRAIA) studied the safety of these flammable refrigerants. SWG uses the FTA approach to compare the A2L refrigerants of R32, R1234yf, and a natural refrigerant, R290.

To assess the probability of risk, the existence of ignition sources and of a flammable region were considered simultaneously in the FTA studied, “Risk assessment for room air conditioner with propane,” in 2000[4.1.1)].

Refer to “Risk assessment handbook business editing,” published by the Ministry of Economy, Trade and Industry[4.1.2)].

Fig. 4.1.1 shows the matrix based on R-Map applied to the consumer product. This map expresses rationally and effectively an evaluation, an estimate, and the reduction of a risk.

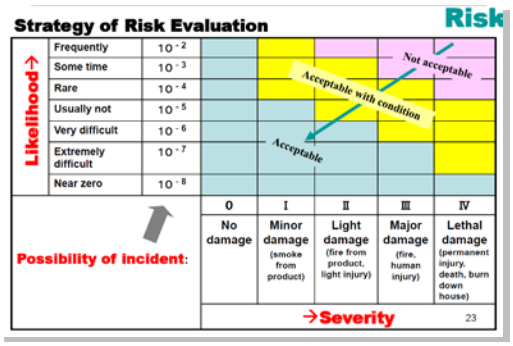

Fig. 4.1.1 R-Map

4.1.2 Assumption of Source of Ignition and Its Evaluation

4.1.2.1 Electronic parts as a source of ignition

For ignition test results for R32 refrigerant released to the environment when a mini-split air conditioner is used and a flammable atmosphere is created, DOE/CE/23810-92 reports were submitted to AHRI in 1998 by ADL, and are available on the website[4.1.3)].

In this literature, many ignition sources for R32 flammable vapor were examined.

For example, the vapor was ignited by the arc of a high-voltage power supply, a high-temperature electric wire, the 120-V or 240-V power supply current of the excessive compressor electric motor of a high-voltage power supply, and naked flame.

However, it was not ignited by the spark from a surface-wall switch, an electric motor, an electric drill, a tungsten-halogen lamp, a low-voltage arc, and the usual load current of 120 V.

Although the ADL evaluated the ignition ability of the sparks that occur with the magnetic contactor in the main circuits that are assumed to generate the largest energy without ignition, using 20 opening-and-closing examinations, it differs from the IEC standard.

The point of contact of the magnetic contactor used for the Japanese product is enclosed with a cover that has only small crevices. The latest research of the National Institute of Advanced Industrial Science and Technology (AIST) shows that there is no flame propagation from a magnetic contactor with a 12-kVA rating capacity and a cover with a crevice with a 3-mm circumference point of contact[4.1.4)].

Parts with a larger contact capacity are not lit because the minimum ignition energy of R1234yf and R1234ze is larger than that of R32[4.1.5)4.1.6)].

4.1.2.2 Interior of a Room and the Source of Ignition of an Exterior Unit Circumference (Mainly Residential)

The existence of ignition sources changes with the use of the room. This examines small-scale ignition sources used mainly for housing use and in the kitchen instruments described below.

(1) Naked flame

In a kerosene apparatus, gas apparatus, a candle, firewood, charcoal, tobacco, and a lighter, flame occurs with ignition sources using A2L refrigerant.

However, with an ascending flow, such as in a gas range, the refrigerant concentration is diluted. As a result, it becomes difficult to light the refrigerant. Furthermore, when the speed of the ascending flow increases faster than the burning velocity of the refrigerant, flame propagation becomes impossible[4.1.8)].

Moreover, the ignition of R32 does not occur with burning tobacco that does not emit a flame[4.1.7)].

(2) Ignition equipment

A piezoelectric element, a magneto, the arc of a high-voltage transformer assembly, a flint system, and a nickel–chrome alloy wire were used for the ignition equipment of kerosene and gas apparatus. These types of ignition equipment cannot ignite R324.13[4.1.3)].

(3) Electrical appliance

The arc-discharge sparks that occur between contacts when an apparatus with large inductance is turned on and short-circuit sparks are considered to be ignition sources in an electrical appliance.

Moreover, the generation of heat that occurs because of energy concentration in the high-current region of a circuit connected to a huge capacitor, the power activation past a contact part, the sparks caused by melting, and the spatter-contact ring also serve as ignition sources in an electrical appliance. Although the sparks from a worn brush also are considered to be ignition sources, they do not light in the case of a motor in which the crevice of the casing is smaller than the quenching distance or when the motor is fully closed.

(4) Static electricity

Static electricity generally occurs from the friction of a synthetic material. Its charge is correlated with the electric capacity, the relative humidity of the material, and the dielectric breakdown voltage.

When it is charged to about 12 kV when the relative humidity (RH) is low and the electric capacity is set to 100 PF, the electric discharge energy is 7.2 mJ [4.1.9)] .When conditions are dry such as with an RH of 7%, according to 4-2 of IEC61000-4-2, the voltage may be raised to about 15 kV. The electric discharge energy at this voltage amounts to about 11.3 mJ.

Usually, the electric discharge between a doorknob and the human body is about 1 mJ in winter, or the same as the electric discharge that occurs when you remove clothing.

In general, the conditions lighting a flammable gas using the minimum ignition energy of an electric discharge are as follows. The ignition conditions are cases in which the point discharge of an electrode is very thin and where distances, such as the quenching distance, cause a separation with a discharge part that is greater than the influence of cooling.

Because the insulation performance of air is 3,000 v/mm, it will influence cooling and a flame will not spread if the distance between electrodes is small; thus, the possibility that A2L refrigerant will be lit because of static electricity is very small.

In this risk assessment, the ignition source was mainly considered to be a naked flame because of the above consideration.

4.1.3 Examination Result of Flammable Region

4.1.3.1 About the flammable space

The flammable space assumed by this risk assessment is same as the space described in “Risk

assessment for room air conditioner with propane”[4.1.1)]. As an indoor space using an air conditioner is the most important for risk assessment, 7 m^2 of floor area of a 2.4-m high small room was used for the leakage space and the installation position of the indoor unit was set at a height of 1.8 m from the floor.

The outline of the indoor space is shown in Fig. 4.1.2.

The warehouse of the semi-fireproof construction provided in the Building Standard Law was set up. To be considered narrow and high-risk, the capacity was 1000 m^2 and was assumed to store 10000 air conditioners..

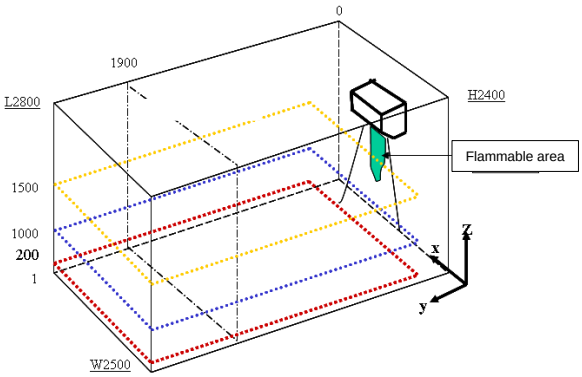

Fig. 4.1.2 Indoor space

4.1.3.2 Generation of a flammable region

To generate the flammable region, which becomes important when performing a risk assessment of A2L refrigerant, a value of R32 was obtained using the same technique used for the data calculated by “Risk assessment for room air conditioner with propane,” but the simple method was improved. The simulation was performed under the same conditions at the University of Tokyo, the result was in agreement with the value calculated in the simple method[4.1.10)].

For this first-step risk assessment, the simple value and the value obtained at the University of Tokyo are shown in Table 4.1.1

Refri-gerant	No	Leal Hight (m)	Leak Weight (kg)	Leak Flow Rate (g/min)	Flow	Flammable Volume and Time Integration (min·m³)
R32	1	0.5	0.5	250	no	3.12
	2	0.5	1	250	no	99.65
	5	1.8	1	250	no	0.024
	27	1.8	1	250	Circulator(1 m³/min)	4.7153E-05
	22	1.8	1	250	yes: Ventilation Fan (1.0m³/min)	3.68907E-06
	28	0.1	1	250	yes: Window(1 m/sec)	0.00907395
R290	3	0.5	0.125	60	no	116.21
	4	0.5	0.25	60	no	984.11
	9	0.5	0.5	60	no	8511.04
	6	1.8	0.25	60	no	213.48
	11	1.8	0.5	60	no	7156.26
	7	1.8	0.5	60	Circulator(1 m³/min)	14.06
	12	1.8	0.5	60	yes: Ventilation Fan (1.0m³/min)	1.1
	8	0.1	0.5	60	yes: Window(0.5m/sec)	0.775

Table 4.1.1 Flammable time volume

4.1.4 Questionnaire of Installation and Servicing

A questionnaire about refrigerant leakage or use of fire during installation and servicing by construction vendors and service shops was sent by JRAIA and nearly about 600 replies were obtained. The incidence of refrigerant leakage or fire use is as follows.

The incidence of refrigerant leakage at installation was 0.74%, which is compatible with the value of 0.77% at servicing. However, refrigerant leakage during charging and recovery increased. There may have been a small amount of leakage when detaching and attaching a charge hose and a connection joint. It is thought that value called about 1/100 as the actual value of refrigerant leakage is appropriate.

With respect to fire use, the amount of smoking at servicing was 1.3% and the use of other types of fire use was 4.2%. At servicing, there are situations when a pipe must be welded, so the use of fire sources such as burners or ignition lighters for a burner is assumed, and it is expected that the rate of fire usage will increase.

Smoking is mentioned later.

4.1.5 Result of Risk Assessment

4.1.5.1 Outline of Risk-Assessment Result

The first risk-assessment results for each life step—logistic, installation, using, servicing, and disposal—for R32 and R290 are shown in Table

4.1.2. Values shown in this table represent the additional probability rate for a flammable hazard when applying an air conditioner to flammable refrigerant.

According to the literature of the National Institute of Technology and Evaluation (NITE), the major accident probability in a home appliance is described for 10^{-8} sets/year (1 million set base).

Table 4.1.2 Result of risk assessment

Stage	Risk : Ignition Probability	
	R32 Current	R290 Current
Logistic	1.3×10^{-16}~2.0×10^{-14}	1.9×10^{-8}~5.0×10^{-6}
Installation	6.1×10^{-7}~1.3×10^{-6}	1.5×10^{-6}~1.7×10^{-5}
Using	1.3×10^{-13}~2.5×10^{-9}	6.1×10^{-9}~1.1×10^{-4}
Servicing	1.8×10^{-6}~9.0×10^{-6}	9.3×10^{-6}~1.7×10^{-5}
Disposal	4.5×10^{-9}	1.8×10^{-5}~1.3×10^{-4}

The total number of mini-split air conditioners and home air conditioners in Japan is about 100 million sets, so the target in the calculation becomes 10^{-10} or fewer sets/year. The ignition probability when using R32 is 1.34×10^{-13}–2.52×10^{-9}, whereas for R290 it is 6.1×10^{-9}–1.1×10^{-4}. The value is larger than the target, but it is safe. However, the values are 6.1×10^{-7}–1.3×10^{-6} or 1.8×10^{-8}–9.0×10^{-8}, respectively, for logistic and servicing using R32. It seems that the values are smaller than the target, so we thought that certain countermeasures were required. The target value is the value that users have demanded when all of the hazards in the risk map of Fig. 4.1.1 assume a fatal fire accident. For the production step, we decided that each company has an individual value because differences in the plants and equipment of each company cause the outflow of manufacturing know-how.

The following chapter explains the risk-assessment calculation in detail for the servicing step.

4.1.5.2 Risk Assessment Reexamination at Servicing.

Risk assessment at the servicing of R32 was performed on an FTA basis. First, the FTA of R290 was replaced by R32, and the ignition probability was examined. According to the replacement refrigerant, the numerical value of 2 refrigerant properties was changed. The first value is the flammable volume and time integration in Table 4.1.2; the value for R32 is will be calculated as 1/10 of R290. The second value is the "spreading probability." According to the ADL report, because the R32 value uses 1/1000 of R290, we used the value of ADL. As a result of changing the aforementioned 2 values, the ignition probability was set to 1.8×10^{-6}–9.0×10^{-6} and was equivalent to that of R290 (1.7×10^{-6}–9.3×10^{-6}) (See Table 4.1.3.) This is because the ignition probability caused by a serviceman's smoking is large and it is the dominant factor in the whole value of the risk assessment at servicing.

Table 4.1.3 Servicing Ignition

	R32		R290	
	current	measure	current	measure
Servicing Ignition	1.8×10^{-6} ~9.0×10^{-6}	1.7×10^{-10} ~4.0×10^{-10}	1.7×10^{-6} ~9.3×10^{-6}	2.3×10^{-7} ~5.5×10^{-7}
R290 rate	100/103	1/1400	–	–

In the latest study at the Tokyo University of Science, Suwa, A2L refrigerants such as R32 do not light from the fire of a cigarette or from the fire of a piezoelectric-type lighter[4.1.11)]. These examination results are reflected in the FTA. A lighter flame lasts for a short duration compared to the smoking time. Adding "the rate of smoking time to a service period," "the rate of time which has stuck the lighter during smoking," and "the ignition source existence probability of the area within flammable" to the probability of ignition from smoking adds the concept of time to the improved FTA limited to the ignition in an oil lighter and a match. As a result, the ignition probability and the improved FTA are set to 1.7×10^{-10}–4.0×10^{-10} and to 1 over 1400. This is shown in Table 4.1.3 and Fig. 4.1.3.

4.1.5.3 Reexamination of the Risk-Assessment Result

The FTA was reexamined at each life step, i.e., logistic, installation, using, servicing, and disposal,

in the preceding chapter. The FTA value of the risk assessment result is shown in Table 5.2.4.

The value of the ignition probability at servicing, 4.0×10^{-10}, is the largest, and is close to the values at installation and disposal.

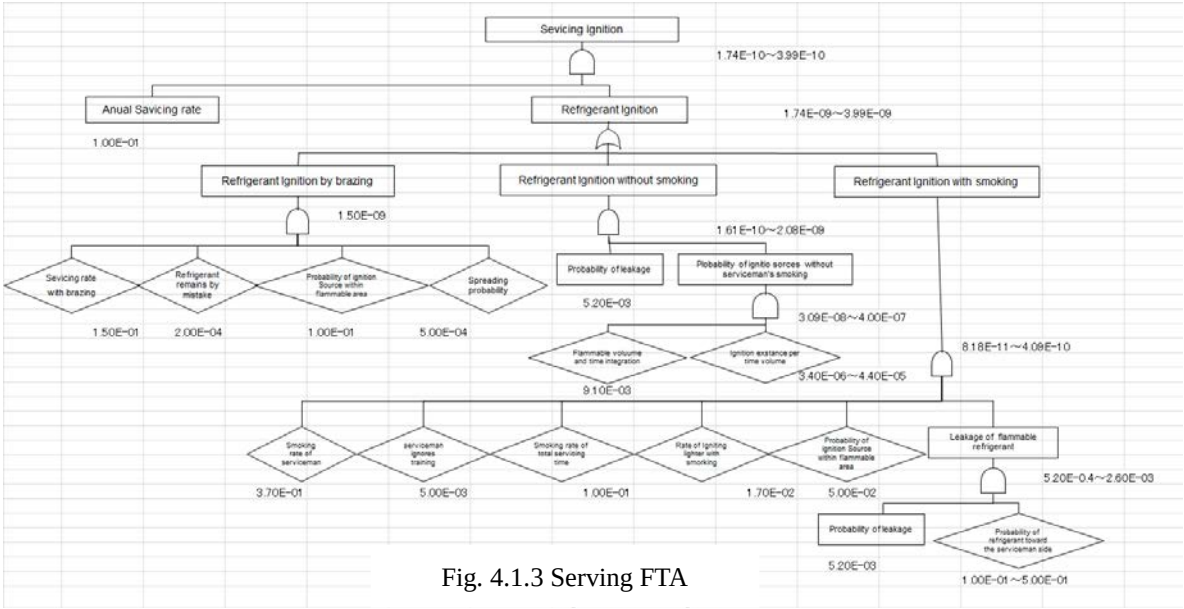

Fig. 4.1.3 Serving FTA

Table 4.2.4 Result of risk assessment

Stage	Risk : Ignition Probability	
	R32 Current	R32 Measure
Logistic	1.3×10^{-16}~2.0×10^{-14}	3.3×10^{-19}~4.6×10^{-16}
Installation	6.1×10^{-7}~1.3×10^{-6}	4.3×10^{-11}~3.2×10^{-10}
Using	1.3×10^{-13}~2.5×10^{-9}	5.7×10^{-15}~1.1×10^{-10}
Servicing	1.8×10^{-6}~9.0×10^{-6}	1.7×10^{-10}~4.0×10^{-10}
Disposal	4.5×10^{-9}	3.3×10^{-10}

This value is bigger than the 10^{-10} or fewer sets/year that represents the number of air conditioners in Japan. Even if the value demanded by workers increases to a range from 1/10 to 1/100, it should still be safe.

As will be mentioned later, manuals should be corrected to reflect the lower ignition probability.

4.1.6 Examination of Unexpected Risk

The FTA described so far has considered the risk based on common conditions expected at each life step (logistic, installation, using, servicing, and disposal).

However, re-extraction of the phenomenon was performed for unexpected conditions.

(1) Conditions outside the expected range that not happen easily, and require too little space, a lot of leakage, and a strong ignition source.

- Example: Installation of an air conditioner for a 16 m^2 by 3 m^2 kitchen. At installation, a worker mistakenly fills the refrigerant twice, and leakage occurs before the use of the air conditioner.

(2) Conditions in which expansion damage is produced using A2L refrigerant, beyond the damage from a natural disaster such as an earthquake, a large fire, and a tsunami.

- Example: Many air conditioners fall in a warehouse during an earthquake. There is a lot of refrigerant leakage from a piping crease and when it ignites, a warehouse fire breaks out.

(3) Conditions in which damage is not prevented and human error makes the situation worse.

- Example: There is decreased oxygen because of a large leakage of a refrigerant. An ignition explosion occurs when a worker accidentally trips a big current breaker.

From the SWG members, the unexpected risks of 34 events were extracted at each of the life steps (logistic, installation, using, servicing, and disposal),

and we evaluated each one.

Only 1 of the 34 events influenced the FTA.

This was described as follows: “When a home appliance retail store transfers air conditioners for installation by a minivan, leakage occurs, driver lights the cigarette, and the refrigerant is ignited and causes an explosion.” It was used as the unexpected risk. We studied this risk to improve the FTA.

The value of the FTA used as an outline in Chapter 4 was the correct value for a stationary state in general, and for the logistic, installation, using, servicing, and disposal stages. For the unsteady risk assumption, the calculated value of the FTA was suitable as the commonsense range. There are no conditions that change this significantly at each life step.

4.1.7 Physical hazard evaluation of generated chemical substance

Above, we have described the fire hazard from the ignition combustion of A2L.

However, even nonflammable refrigerants, such as conventional R410A and R22, can come in contact with burning appliances or high-temperature surfaces and will generate harmful chemical substances.

According to Imamura’s newest result, the exposure of refrigerant from a wall-mounted air conditioner to the heating apparatus of a reflective-type oil stove or a kerosene fan heater by contact with a heating apparatus causes an HF concentration exceeding the 3-ppm concentration permitted for workers.

There was no difference among R1234yf, R32, or R410A (the present refrigerant).

However, the following conditions are required to create a situation that is harmful to people, regardless of the kind of refrigerant that reacts to generate HF.

(1) HF should be generated.

(2) HF should reach inhabited areas.

(3) Evasive action is not taken despite the presence of HF.

Moreover, HF can appear at concentrations tens of times greater than the 3-ppm concentration allowed for workers.

The interviews for the mini-split risk assessment SWG indicate that an old air conditioner can have a nasty smell.

However, although the use of R410A and R22 in contact with burning appliances or high-temperature surfaces can generate harmful HF and produce a nasty smell, this has not led to major damage (III) in Fig4.1.1; the combustion products have not caused serious illness or hospital treatment for the past 20 years or more. Generally speaking, small children and bedridden elderly people cannot take evasive action to avoid exposure to HF, but because there are very few situations in which the individuals in these groups live independently in areas with the concurrent use of R410A and R22 air conditioner and a heating appliance with burning or high-temperature surfaces, it don’t lead to major damage (Ⅲ).

Even if the rapid burning of R1234yf and R32 due to heating appliances does not occur, the use of A2L refrigerants including R410A may produce this phenomenon and create a physical hazard by generating HF and other chemical substances.

4.1.8 Future Subject

The adaptation of A2L refrigerant based on FTA was analyzed. At each stage of the life cycle, installation and servicing have high risk, when fire and cigarette lighters were assumed to be the ignition sources. With regard to these ignition sources, a risk assessment conducted at Tokyo University of Science, Suwa, was re-evaluated.

We succeeded in examining the risks of re-extraction and in manually lowering the risk. We will publish a new manual based on the JRAIA manual describing the conversion of R22 at R410A. We have proposed measures that can be implemented during installation. This manual is distributed to each company belonging to JRAIA, and each company is reflected in the contents of

their manual.

During the disposal stage, the mini-split air conditioner is transported to a home-appliance recycling plant in Japan. Even if the probability of risk is high, it is difficult to create problems in a managed recycling plant. Recycling plants have a large floor area and airflow by ventilation, so the refrigerant does not stagnate, and the risk is comparatively low. However, refrigerant will leak inside the refrigerant-recovery machine, and if a flammable concentration is reached and the electric part of the recovery machine ignites by failure, ignition combustion may occur. Thus, we propose installing a ventilator in the refrigerant recovery machine itself or changing the inverter so that a large current will not flow during failure of the electric circuit to drive the compressor.

4.1.9 Conclusion

In the mini-split air-conditioner risk assessment SWG, a risk assessment was performed to evaluate the safety of R32-type of A2L refrigerant, and to provide the first examination of a strongly flammable refrigerant.

Regarding the high-risk step, we produced a service and installation manual proposing the measures that can be implemented. The accuracy of the FTA was evaluated using the examination result from the University of Tokyo; Tokyo University of Science, Suwa; and AIST, which will take part in the A2L refrigerant risk-assessment study group from now on. Moreover, this clarifies the hazard grade.

In this way, the risk assessment of the mini-split air conditioner has been promoted.

Acknowledgments

In this report, the author summarizes the surveillance study for the JRAIA mini-split air-conditioner risk assessment SWG. I am thankful to 9 committee members: Mr. Ryuta Onishi of Sharp Co.; Mr. Haruo Onishi, Shigeharu Taira, and Tsuyoshi Yamada of Daikin Co.; Mr. Koichi Yamaguchi of Toshiba Carrier Co.; Mr. Ryoichi Takafuji of Hitachi Appliance Co.; Mr. Toshiyuki Fuji of Fujitsu General Co.; and Mr. Takao Hirahara and Mr. Hiroaki Makino of Mitsubishi Electric Co.

I am also thankful to Manager Matsuda and Section Chief Hasegawa of JRAIA for their secretarial work.

References

4.1.1) Risk assessment of propane room air-conditioner, The International Symposium on New Refrigerants and Environmental Technology, Yao et al. (2000.9)

4.1.2) Practical Business Method for Risk Assessment Handbook, MITI, (2011.6)

4.1.3) Risk Assessment of HFC-32 and HFC-32/134a (30/7 wt%) in Split System Residential Heat Pumps: DOE/CE/23810-92

4.1.4) Study on Minimum Ignition Energy of Mildly Flammable Refrigerant, Kenji Takizawa, AIST (2011)

4.1.5) Flammability Characteristics of HFO-1234yf, Minor, AIChE Process Safety Progress (Vol. 29, No. 2)

4.1.6) Determining Minimum Ignition Energies and Quenching Distances of Difficult to Ignite Components, Dean Smith, Journal of Testing and Evaluation, Vol. 31, No. 3

4.1.7) Research on the ascending current of the pan installed in the residential gas range, The Society of Heating, Air-Conditioning and Sanitary Engineers of Japan, Honda, Osaka University(2011)

4.1.8) Evaluation of Fire Hazards of A2L Class Refrigerant, The International Symposium on New Refrigerants and Environmental Technology, Imamura et al. (2012.11)

4.1.9) Compact Handbook of Static Electricity, Static Electricity Society

4.1.10) Evaluation of Refrigerant Leakage, The International Symposium on New Refrigerants and Environmental Technology, Hattori et al.

(2012.11)

4.1.11) Physical Hazard Evaluation for using Air-Conditioning Systems Having Low-Flammable Refrigerants with the Fossil-fuel Heating System at the Same Time, Academic Journal Reito of JSRAE, Vol. 29 No. 4, pp. 401-411, Imamura et al. (2012)

4-2. VRF Risk Assessment SWG: The 1st Risk Assessment of VRF System with A2L Refrigerant and Future Tasks

Ryuzaburo YAJIMA

JRAIA, Variable Refrigerant Flow Air-conditioner Risk Assessment Sub-working Group

4.2.1 Introduction

To reduce the warming effect caused by air-conditioner refrigerants in Japan, academia, government, and industry are working together to conduct risk assessments in the case of the use of mildly flammable, low-GWP (Global Warming Potential) refrigerants such as R32, R1234yf, and R1234ze. Furthermore, based on the results of risk assessments, new rule making will be done to mitigate the risk sufficiently.

Because VRF (Variable Refrigerant Flow) has a variety of system configurations, it is necessary to examine the risks in many installation cases. This SWG (sub-working group) then divided the risk assessment of the VRF system into a 1st and 2nd assessment so that its activities could be conducted in phases. An outline of the schedule is shown in Fig. 4.2.1. The risk assessment was conducted for each life stage as shown in Fig. 4.2.2.

In the 1st risk assessment, we estimated the probability of fire accidents for the installation case thought to be most prevalent in the market. The basic data and methodology are necessary to clarify the risk by fault tree analysis (FTA), including an estimate of the probability of a refrigerant leak occurring in the market, evaluation of the various ignition sources, and examination of the calculation method to determine the probability of fire. Based on these basic data and this methodology, we prepared fire accident scenarios and an FTA for the prevalent installation case in the market. This paper reports the results.

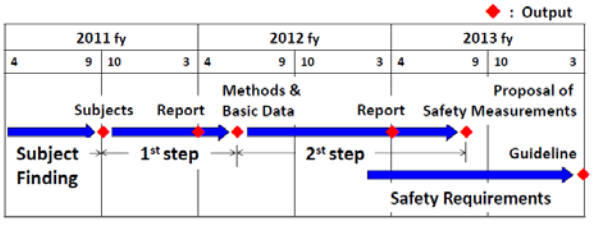

Fig.4.2.1 Schedule of Risk Assessment for VRF with A2L

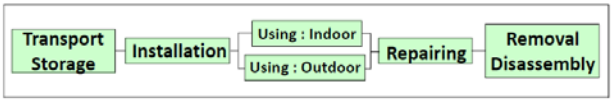

Fig.4.2.2 Life Stage of Risk Assessment

In the future 2nd risk assessment, we will conduct a risk assessment of installation cases that are rare in the market but are thought to pose large risk and will propose safety measures to reduce risk if it is unacceptable.

At the end of fiscal 2013 (end March 2014), we plan to propose safety guidelines for the safe use of mildly flammable refrigerants in VRF systems.

4.2.2 Features of VRF Systems

Fig. 4.2.3 shows the features of VRF systems. The most distinctive feature is the large amount of refrigerant charge in the refrigerant circuit that, in the case of an indoor refrigerant leak, could be completely discharged from one indoor unit. As there are many connections in the refrigerant piping, rigorous refrigerant leak checks are conducted in a double-check system after the piping is installed; one check comes in the form of a tightness leak test at positive pressure and the other is intended to check for vacuum leaks at negative pressure. Additionally, specialist technicians and highly skilled service providers normally conduct mounting installation, repairs, and maintenance, which lower the occurrence of operational error.

4.2.3 Characteristics of A2L Refrigerants

Figs. 4.2.4 and 4.2.5 show the relationship between burning velocity (BV) and other indicators based on the burning

- Large amount of refrigerant charge and all of that can leak into just one room.
- A lot of joints connecting refrigerant circuit or parts of valves, vessels and sensors.
- Sealing and leak of refrigerant are strictly checked.
- Highly skilled personnel for installation, repair and maintenance.
- A variety of system configuration, mode free type, water cooled or ice storage type, etc.
- Wide range of capacity of outdoor and indoor units.

Fig.4.2.3 Features of VRF system

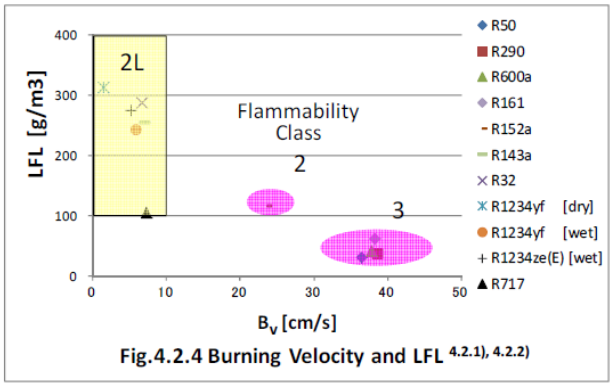

Fig.4.2.4 Burning Velocity and LFL [4.2.1), 4.2.2)]

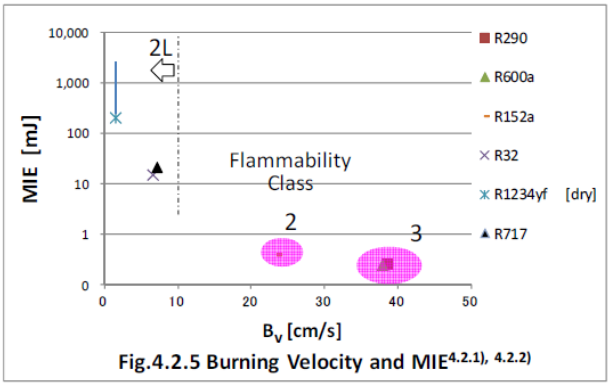

Fig.4.2.5 Burning Velocity and MIE[4.2.1), 4.2.2)]

characteristics of each refrigerant. Many of the data points were presented in reference materials from Kenji Takizawa [4.2.1), 4.2.2)].

As shown in Fig. 4.2.4, when BV is small, the lower flammable limit (LFL) is higher, and consequently, the probability of a flammable space occurring during a leak is reduced markedly. In addition, as shown in Fig. 4.2.5, when BV is small, the minimum ignition energy (MIE) increases, and consequently, the range of ignition sources having the potential to ignite the gas is limited compared to propane (R290) gas. It is important to specify the ignition sources during the risk assessment.

4.2.4 Results of the 1st Risk Assessment

(1) Establishing the representative models

In VRF systems, there is a wide range of system capacity, from 5 to more than 50 hp, and the size of the corresponding

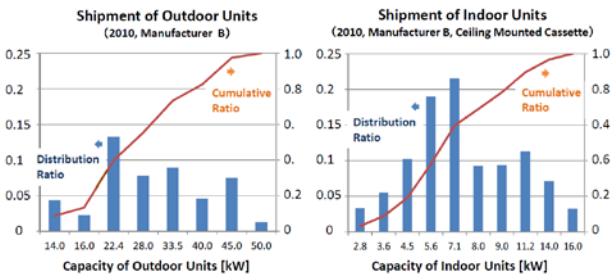

Fig.4.2.6 Shipment distribution of VRF for office

Table 4.2.1 Refrigerant charge amount of models

			Charge Amount [kg]		
			R32	R1234yf	R410A
Outdoor Unit	56[kW]		16.1	18.1	19
Indoor Unit	7.1[kW]×4[unit]×2 rooms		-	-	-
Pipe	ϕ15.9	40 [m]	6.5	7.2	7.6
	ϕ9.5	72 [m]	3.7	4.1	4.3
Total of Charge Amount			26.3	29.4	30.9

Table 4.2.2 Required safety measures for models

		Office 1		Office 2	
Refrigerants		R32	R1234yf	R32	R1234yf
Floor Area A	[m2]	40.6		164.7	
Room Volume V	[m3]	109.6		444.8	
Charge Amount M	[kg]	26.3	29.4	26.3	29.4
M/V	[kg/m3]	0.240	0.268	0.059	0.066
		> QLAV		< RCL	> QLMV, < QLAV
Safety Measures required		2 measures		none	Natural ventilation

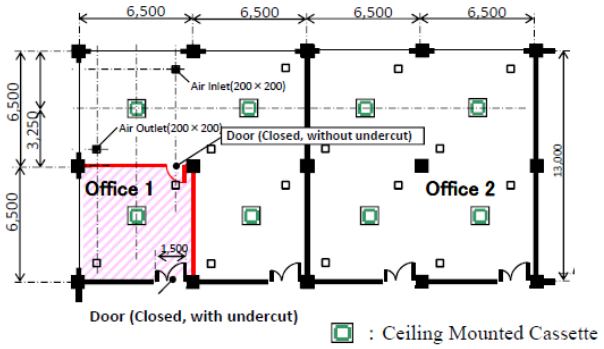

Fig. 4.2.7 Model of Offices

refrigerant charge varies between several kilograms to several tens of kilograms. Indoor units also range from 1 to 10 hp, with a corresponding diversity of room sizes, room zoning, and indoor-unit configurations, which range from ceiling-mounted to floor-standing models.

VRF systems are installed in office buildings, hospitals, stores, schools, and houses, among other buildings. As most systems are used for office buildings, we selected some office models as representative indoor installations.

The indoor unit type with the highest shipped volume is a 4-way ceiling-cassette-type. The capacity distribution of outdoor units and 4-way ceiling-cassette-type indoor units shipped for office installations can be seen in Fig. 4.2.6. For outdoor units, a connected 22.4 kW and 33.5 kW unit represents the median capacity, and for indoor units, a 7.1 kW unit is the median. Therefore, we assumed the case of a 56-kW outdoor unit connected to eight indoor units consisting of 7.1-kW ceiling cassettes as the typical office model. This model is shown in Fig. 4.2.7. Two room-sized variants were assumed, Office 1 and Office 2. Table 4.2.1 shows the amount of refrigerant charge for the model units. In selecting models, we selected typical cases in the market in which the effects of implementing safety measures could be evaluated.

Table 4.2.3 Indexes of Refrigerant Charge in ISO5149/FDIS

M/V		R32	R1234yf	Remarks
RCL	[kg/m3]	0.061	0.060	Refrigerant Critical Limit, =LFL/5
QLMV	[kg/m3]	0.063	0.062	Quantity Limit with Minimum Ventilation
QLAV	[kg/m3]	0.160	0.150	Quantity Limit with Additional Ventilation, =LFL/2
LFL	[kg/m3]	0.307	0.289	Lower Flammable Limit

Table 4.2.4 Safety Measures required in ISO5149/FDIS

M/V	Floor othe than the lowermost underground	The lowest floor of the basement
< RCL	none	none
RCL<, <QLMV	Natural ventilation	1 measure
QLMV<, <QLAV	1 measure	2 measures
QLAV <	2 measures	Reduce of M

【Safety measures】 ①Gas leak sensor + Safety alarm
②Natural ventilation or Gas sensor + Mech. Ventilation
③Gas sensor + Shut off valve
If occupants restricted, safety alarm alone is not allowed.

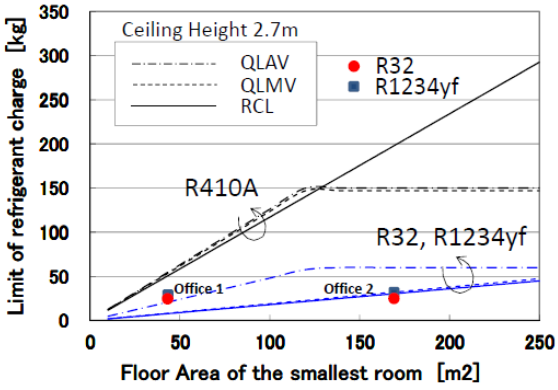

Fig. 4.2.8 The limits of charge amount in ISO5149/FDIS

In the work to revise ISO 5149 [4.2.3)], the international safety standard for air conditioners, the requirements to safely use A2L refrigerant in VRF systems are examined, and many proposals also have been made by the Japan Refrigeration and Air Conditioning Association (JRAIA) [4.2.4)]. The requirements listed in the revision draft are shown in Tables 4.2.3 and 4.2.4. If the concentration of total refrigerant, M, divided by volume, V, of the room in which the indoor unit is installed exceeds 1/5 of the LFL (RCL), some type of safety measure will need to be implemented in the room. Table 4.2.2 shows the safety measures required for the office model in Fig. 4.2.7.

Fig. 4.2.8 shows the upper refrigerant charge limits for R32 and R1234yf as well as the points of Office 1 and Office 2. The upper charge limit for R410A to prevent a lack of oxygen is also shown.

In Office 1, both R32 and R1234yf require implementation of two safety measures. In Office 2, safety measures are not required for R32, whereas one safety measure is required for R1234yf.

A model also was assumed for the outdoor units, as shown in Fig. 4.2.9. This model does not represent a serious case, because leaked refrigerant can spread far from the outdoor unit. In addition to this case, the use (outdoor) and disposal stages and cases with installation in narrow spaces such as semi-basements were also assumed.

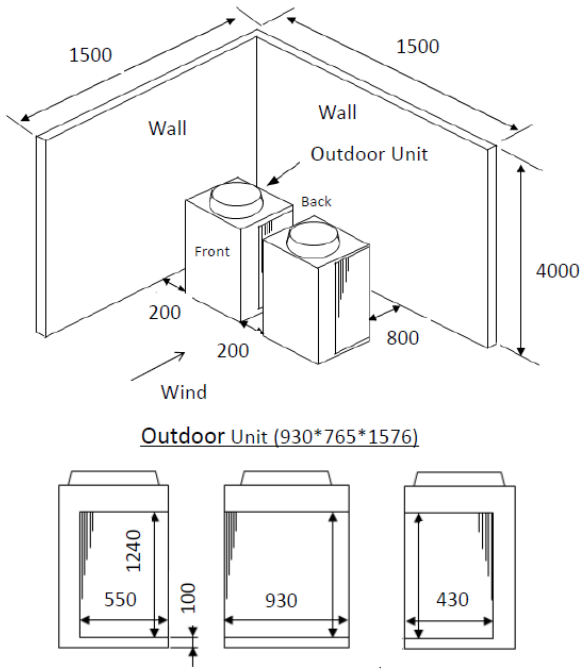

Fig. 4.2.9 Model of Outdoor Units

(2) Probability of the number of leaks classified to different refrigerant leak velocities

The international standard determining refrigerant-charge amount standards for flammable refrigerants is currently IEC 60335-2-40; for VRF systems, standards are specified in Chapter A5 of ISO 5149/FDIS. In the former standard, which pertains to the refrigerant leak velocity indoors, a leak velocity in the case of all of the refrigerant leaking in 4 min is adopted, whereas in the latter standard, a leak velocity of 10 kg/h is adopted with conditions including no source of vibration from the compressor.

To understand the actual conditions, we recovered parts that had caused refrigerant leaks in the real market and found the hole diameters using a leak velocity test conducted with nitrogen. We then determined the refrigerant leak velocity in case of R32 from these hole diameters and the refrigerant pressure.

Fig. 4.2.10 shows the results of measuring 22 indoor unit parts with leaks that were recovered from the real market. Here, the bars with red arrows above them indicate emergency calls based on customer reports of white smoke coming out of the indoor units. Of the four instances, the leak velocity of the liquid leak was relatively large in three cases, ranging from slightly less than 1 to 10 kg/h or less. In only one case, the leak velocity was

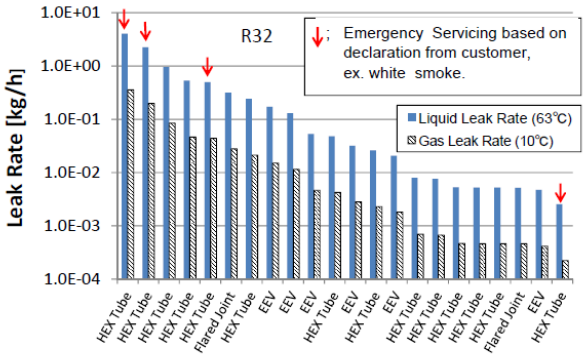

Fig. 4.2.10 Leak Rate of Indoor Field Samples

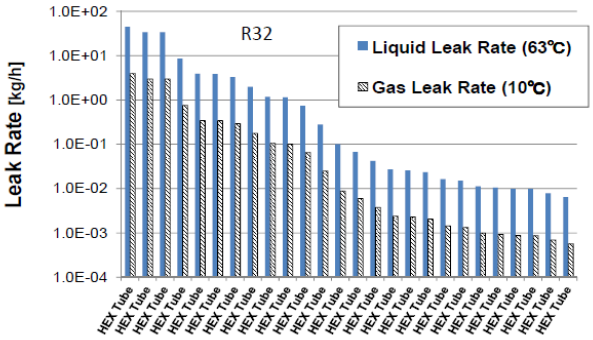

Fig. 4.2.11 Leak Rate of Outdoor Field Samples

0.01 kg or less. In this one case, it is assumed that there was no high-speed refrigerant leak and the customer reported the incident after seeing steam produced from the operation of the equipment after it had run out of gas.

Except for this instance, the cases with white smoke indicate a refrigerant leak velocity close to 10 kg/h, and it can be inferred that, in the event of a high-speed leak, the customer often would see white smoke and realize that there was an abnormality.

Using a similar method, we also measured 26 leak samples from outdoor units. The results are shown in Fig. 4.2.11. Compared with the indoor units, outdoor units have relatively higher leak velocities, and in three cases, the leak velocity exceeded 10 kg/h.

Table 4.2.5 Probability of Leak classified in Leak Rate

Numbers of leak with declaration showing rapid leak, 2010, Manufacturer B

	White Smoke	Smelling Burnt	Hole of Pipe	Nrp
Indoor Unit	0	1	0	1
Outdoor Unit	1	3	3	7

Probability of Leak classified in Leak Rate

		Total	Slow leak ~1[kg/h]	Rapid leak ~10[kg/h]	Burst leak ~75[kg/h]
Indoor Unit	Distribution Ratio [-]	1	0.986	0.014	0
	Probability of leak [ppm]	350	345	5	0
Outdoor Unit	Distribution Ratio [-]	1	0.806	0.176	0.018
	Probability of leak [ppm]	7600	6126	1338	137

【Method】
Probability of leak : Weighted Mean Value of probability of each manufactures of JRAIA
Number of rapid leak = Nrp × 10 (indoor) or 100 (outdoor)
Number of burst leak = Number of rapid leak × 0.10.1 (outdoor) , 0 (indoor)
Number of slow leak = Total − (rapid+burst)

Nrp : Number of leak with declaration from customer or service person that shows it is rapid leak, white smoke, smell from customers, breakage or hole of pipe from service person.

Based on the aforementioned results from the samples, we conclude that it is difficult to find the probability of the number of leaks at different velocities on the order of ppm. Therefore, for all cases of leaks handled by service technicians over a year, we extracted the number of cases of customers reporting white smoke or an abnormal smell as well as the number of cases that were diagnosed by service technicians as a broken pipe or a hole in the heat exchanger or pipe. For indoor units, we multiplied this number by 10, and for outdoor units we multiplied the number by 100 to calculate the number of high-speed leaks. Because there are no so-called "burst" leaks with the indoor units of VRF systems, we calculated the number of burst leaks as zero. We judged that the remaining leaks were slow leaks of 1 kg/h or less. For outdoor units, as there were samples of leaks exceeding 10 kg/h, we calculated that 1/10 of rapid leak cases were burst leaks. The results are shown in Table 4.2.5.

(3) Estimate of flammable space occurrence

Table 4.2.6 shows the flammable space (m^3) multiplied by continuous duration time (min) and the average volume (m^3) of the flammable space during an indoor unit leak in Office 1. These analyses were conducted by the University of Tokyo. Compared with Condition No. 1, no ventilation, we confirmed that natural ventilation from a gap at the bottom of a door (10 mm*1800 mm) had the effect of substantially reducing concentration. In comparison of the effects of safety measures provided in ISO 5149/FDIS, the effect was the largest in order of shutoff valve (No. 8), mechanical ventilation (No. 6), and natural ventilation (No. 2). Even under Condition No. 1, the flammable space was formed only in proximity to the leak opening, and the flammable area did not reach the vicinity of the floor. This is because the leaked refrigerant, which is heavier than air, mixes with the surrounding air and becomes diluted as it falls from ceiling height. Because the concentration of R32 was more than 11%, we estimate that a flammable area would occur near the floor if the refrigerant charge amount were further

Table 4.2.6 R32 leak simulation results for office 1

No	Condition			Flammable Region			
	Mech. Ventila-tion	Natural Ventila-tion	Shut-off Valve	Space-Time Product [min*m^3]	Time [min]	Ave. Volume [m3]	Concentration*) [%]
1	None	None	None	1.70	158	1.1E-02	11.7/11.6/11.0
2	None	Yes	None	0.83	158	5.3E-03	6.5/6.5/5.5
5	Yes	Yes	None	0.70	158	4.4E-03	4.0/4.0/2.8
6	None →Yes	Yes	None	0.73	158	4.6E-03	4.1/4.0/2.8
8	None	Yes	None →Yes	0.03	8	3.8E-03	1.5/1.3/0.8

*1) 0.01/0.6/1.5m above on floor

Table 4.2.7 Estimation for Flammable Region of VRF with R32

Stage	Space-Time Product of Flammable	
	Office1	House
Transport, Storage	8.38E-03	8.68E-04
Installing : Indoor	8.30E-02	1.30E-04
Installing : Outdoor	1.22E+00	1.23E-01
Refrigerant Charging	1.22E+05	1.26E+03
Operating : Indoor	7.00E-05	8.98E-07
Stopping : Indoor	7.00E-01	8.98E-03
Operating : Outdoor	1.22E-03	1.23E-04
Stopping : Outdoor	1.22E+01	1.23E+00
Connecting Pipe	1.22E+05	1.26E+03
Repairing	1.22E+00	1.23E-01

increased.

Table 4.2.7 shows the flammable space (m^3) multiplied by continuous duration time (min) used in the ignition probability calculation for each life stage. We considered the difference in the charge amount and floor space from past concentration analysis results of room air conditioners and supposed the flammable space multiplied by duration time for the transport and storage stages for the outdoor unit, connecting piping, refrigerant charging, and repairs by multiplying the results of the simplified estimate by the safety coefficient of 10, because the CFD analysis has not be done for the outdoor unit.

(4) Assessment of ignition sources

Ignition sources, including light switches, electrical outlets, indoor magnetic contacts, and electronic lighter ignition devices, that were determined in experiments by AIST and Tokyo University of Science, Suwa, to be clearly unable to ignite mildly flammable refrigerants such as R32, R1234yf, and R1234ze were excluded. The ignition sources in the 1st risk assessment include a water heater, boiler, combustion devices using gas and kerosene, and brazing burners. In addition, the assessment results of the mini-split SWG were used in the assessment of ignition sources related to electric sparks, ignition devices, high-temperature surfaces, and internal-combustion engines.

As a result, the probability of the existence of unit space–time ignition sources was set at 1/5 of R290.

(5) Prediction of probability of human error

Refrigerant leaks at life stages accompanied by human work including mounting installation, repair, and disposal occur as a result of human error, such as the incorrect use of a valve. Table 4.2.8 shows the error rate corresponding to worker conditions.

The range between 1E-2 and 1E-5 represents normal, relaxed conditions. As workers handling VRF systems have completed

Table 4.2.8 Probability of Human Error [4.2.5)]

Phase	Mode of conciuosness	Physiological state	Probability
0	Unconsious, Syncope	Sleeping	1
I	Blurring	Weary, Snoozing	> 1E-1
II	Normal, Relaxed	at rest, Usual working	1E-2 to 1E-4
III	Normal, Clear	Active state	< 1E-5
IV	Excited	in a hurry, panic	> 1E-1

a relatively large amount of education and training, we chose 1E-4 for the probability of human error occurring within the FTA.

(6) How probability of fire is calculated

Fire occurs when a refrigerant leak causes the formation of a flammable space and when an ignition source that can ignite the A2L refrigerant encounters the flammable space in both space and time. Table 4.2.9 shows this probability calculation.

The fire trigger—for example, an electric spark—is the activation of the ignition source. In the case of a flammable gas coming into contact with a burning open flame and igniting, the fire trigger is the formation of a flammable space. If the formation of a flammable space happens first in time, the trigger is the activation of the ignition source, whereas if the ignition sources are first operating in a continuous state, the trigger is the flammable gas. Theoretically, the probability of fire occurring

Table 4.2.9 Calculation of Probability of Fire

Trigger of Fire	PF	PT	PS
Ignition of Device	$PF_i = N/V_r * M * PL$ $= N/V_r * V_f * T_f * PL$	$PT_i = N*T_f$	PS= V_f/V_r
Generation of Flammable Space	$PF_g = N* T_b * V_f/V_r*PL$	$PT_g = N*T_b$	
Total	$PF = PF_i + PF_g$ $= N*V_f/V_r * (T_f + T_b) * PL$ $= PT * PS * PL$	PT $= PT_i+PT_g$ $= N*(T_f + T_b)$	PS= V_f/V_r

PF	: Probability of Fire	[time/(year*unit)]
PL	: Probability of Leak	[time/(year·unit)]
PT	: Probability of Encounter in time between Ignition Source and Flammable Gas	[-]
PS	: Probability of Encounter in space between Ignition Source and Flammable Gas	[-]
N	: Number of Operation of Ignition Source	[time/min]
V	: Volume	[m^3]
T	: Duration	[min/time]
M	: Time multiplied Volume of Flammable Region	[min*m^3/time]

$$M = \int (V_f * T_f) dt$$

suffix

i : Trigger is Operation of Ignition Source
g : Trigger is Generation of Flammable Space
r : Room
f : Flammable Region Being
b : Ignition Source Working

from one ignition source is the sum of these two triggers. For the risk calculation for each life stage, one of the two triggers is calculated after determining which trigger is dominant.

(7) Results of probability of fire

In the 1st risk assessment, we made an FTA for Office 1 with more rigorous conditions than Office 2 and determined the probability of fire. R32 was used as the refrigerant.

Table 4.2.10 shows the results. As reference, the values when using an R290 room air conditioner are also shown [4.2.6)]. Table 4.2.11 shows the ignition sources having the most influence on the probability of fire at each stage. Table 4.2.12 shows the main factors causing the formation of flammable space.

(8) Risk assessment

The acceptable probability of a fire accident is typically different depending on the degree of danger, but as the assessment of the degree of danger is not finished at present, we considered the acceptable probability of fire after assuming that all accidents were serious, fatal accidents. As there are approximately 10 million indoor units in use in the VRF market in Japan, if the permissible probability of the occurrence a serious accident were once every 100 years, the permissible level would be 10^{-9} or less during use. At stages other than during use, the workers who normally handle equipment, not consumers, are involved and are responsible for controlling risk [4.2.7)] ; it is possible that the degree of danger would be reduced through self-protection even if an accident occurred. Therefore, the acceptable probability of an accident is increased by a factor of 10 to 10^{-8} or less.

Compared with the aforementioned acceptable level, the probabilities of accidents during transport/storage and during use (indoor and outdoor) reach the permissible level. During use, the assessment is of a situation in which mechanical ventilation is in operation. Use (outdoor) exceeds the permissible level, and, therefore, when installing equipment in a narrow space, it is necessary to take safety measures. Regarding mounting installation, repair, and disposal, education and training for workers and the use of safety tools are necessary.

For the outdoor unit during use, the probability of fire is relatively higher from the estimate on the risk side due to a simplified calculation of the size of the flammable space and its continuous duration. At the disposal stage, during the removal of an outdoor unit from a narrow space such as a semi-basement, the probability of fire was higher because of the assumption of a 2% probability of a leak in which the piping was dismantled with incomplete refrigerant recovery and the refrigerant blew out. In the future, it will be necessary to conduct analyses including 3-dimensional concentration analysis and refrigerant recovery process analysis for outdoor use as well as a fact-finding survey on dismantling fieldwork to determine values more reflective of actual conditions.

Table 4.2.10 Probability of fire accident without safety measures [unit/(unit*year)]

Life stage	VRF with R32 Office1 : 40.6m^2 Leak : 26.3kg, 10kg/h	[Ref.] RAC with R290 House : 7m^2 Leak : 0.5kg, 15kg/h
Transport, Storage	**5.1E-15～5.8E-15**	1.9E-12～5.0E-10
Installation	**2.3E-07**	1.5E-06～1.7E-05
Using (Indoor)	**2.5E-10**	5.9E-09～1.1E-04
Using (Outdoor)	**8.5E-09**	9.7E-13～1.9E-08
Repairing	**7.9E-10～1.5E-08**	9.3E-06～1.7E-05
Disposal	**1.5E-05～6.7E-05**	1.8E-05～1.3E-04

Table 4.2.11 Main Risks of Ignition Source without safety measures

Life stage	VRF with R32	[Ref.] RAC with R290
Transport, Storage	・Spark from forklift claw	・Spark from forklift claw
Installation	・Electric parts within walls (Other than outlet and switch)	・Smoking, Spark, Open flame
Using (Indoor)	・Oil lighter, Gas range, Gas hot water heater	・Smoking, Spark, Open flame
Using (Outdoor)	・Boiler, Gas/Oil equipment	・Smoking, Spark, Open flame
Repairing	・Boiler, Gas/Oil equipment	・Smoking, Brazing burner
Disposal	・Brazing burner	・Brazing burner

Table 4.2.12 Main Risks of Flammable Region without safety measures

Life stage	VRF with R32	[Ref.] RAC with R290
Transport, Storage	・Leak in packing	・Leak in packing
Installation	・Leak within wall	・Leak indoor
Using (Indoor)	・Leak in stopping	・Leak in stopping
Using (Outdoor)	・Leak in stopping	・Leak in stopping
Repairing	・Error in recovery	・Error in recovery, Emittion
Disposal	・Failure in recovery	・Error in recovery, Emittion

4.2.5 How to Proceed with 2nd Risk Assessment

In the 2nd risk assessment, installation cases that are rare in the market but thought to carry large risk will be assessed.

For all VRF models, the risk of a flammable space formation encountering an ignition source will be extracted at each life stage and the installation cases that should be subject to the 2nd risk assessment will be decided.

The risk of flammable space formation in rooms is the highest in the case of floor-standing equipment installations in

Table 4.2.13 Sales mix ratio of indoor units classfied with risks (Man. B)

		Risk of occurrence of flammable space ← Small Large →				Total
		Ⅳ	Ⅲ	Ⅱ	Ⅰ	
Risk of ignition source ↑ Large ↓ small		Wall, Ceiling Mounted,	Slim concealed ceiling	Floor concealed standing	Floor standing	
A	Restaurent	1.35%	0.02%	0.004%	0.01%	1.4%
B	Factory	6.29%	0.004%	0.07%	0.10%	6.5%
C	Hotel, Appartment, house	16.36%	0.21%	0.34%	0.14%	17.0%
D	Office, Shop, Hospital, Scool	72.84%	0.40%	1.26%	0.61%	75.1%
Total		96.8%	0.6%	1.7%	0.9%	100.0%

which the height of the leak is low. In addition, risk in Japanese restaurants in which there are ignition sources such as an open flame is assumed to be high. Table 4.2.13 shows a rough classification of risk based on the type of business where indoor units are installed and their installation mode as well as on the sales mix.

The offices and ceiling cassettes used in the 1st risk assessment are considered to be the installation case with the lowest risk. Although a conclusive determination is difficult, the 2nd risk assessment will proceed assuming that Japanese restaurant and floor-standing cases carry the highest risk.

In cases of outdoor installations, the assessment will be proceed assuming high risk in semi-basements, installation on each floor, and installation in machine rooms. In addition, considering leaks from piping, risks under the roof will be examined.

4.2.6 Formulation of Safety Guidelines

ISO/FDIS 5149 has already set refrigerant charge-amount standards for R32 and R1234yf. In addition, the refrigeration equipment installation standards [facilities edition (KHK S 0302-3) for flammable gases (including mildly flammable)] from The High Pressure Gas Safety Institute of Japan defines detailed requirements for refrigerant charge-amount standards as well as for indoor units, outdoor units, and refrigerant piping installation. Based on the results of this risk assessment, these requirements will be readjusted, the safety measures determined to set an acceptable risk level, and safety guidelines for VRF systems formulated.

Requirements when handling flammable refrigerant during mounting installation, repair, and disposal are listed in IEC 60335-2-40 as the requirements that should be listed in each handling manual, but these requirements are for all flammable refrigerants including highly flammable refrigerants, and therefore the requirements are not necessarily appropriate for mildly flammable refrigerants. While using these as reference and elaborating on this risk assessment in more detail, we will decide the requirements using these as a base.

The refrigerants under assessment will be R32, R1234yf, R1234ze, and refrigerant blends using these refrigerants.

Acknowledgments

This report has been created through the joint cooperation of Toshihiro Yamamoto (Toshiba Carrier), Kenji Takaichi (Panasonic), Hiroaki Tsuboe (Hitachi Appliances), Shuntaro Ito (Fujitsu General), Koji Yamashita (Mitsubishi Electric), Tatsumi Kannon (Mitsubishi Heavy Industries), and Chief Investigator Ryuzaburo Yajima (Daikin Industries). In addition, Satoru Fujimoto (Daikin Industries), Hiroichi Yamaguchi (Toshiba Carrier), Kenji Tojo (Hitachi Appliances), Takuho Hirahara (Mitsubishi Electric), and Katsuyuki Tsuno (Panasonic) lent their cooperation as observers. We would like to express our deep appreciation to Osami Kataoka and Kazuhiro Hasegawa (JRAIA Secretariat) for their valuable advice and the time and support received from the Secretariat office.

References

4.2.1) Takizawa, Flammability Assessment of CH2CFCF3: Comparison with Fluoroalkenes and Fluoroalkanes, Journal of Hazardous Materials, Vol. 172, pp. 1329-1338, 2009

4.2.2) Takizawa, Progress Report on Risk Assessment of A2L Refrigerants, pp. 26-31, Apr. 2011

4.2.3) ISO5149-1, 2, 3, 4/FDIS, ISO Website

4.2.4) JRAIA, Guideline of Design Construction for Ensuring Safety against Refrigerant Leakage from Multi-split System Air Conditioners, JRA GL-13

4.2.5) Hashimoto, Japan Ergonomics

4.2.6) Yao et al., Risk Assessment of Room Air Conditioner using R290, 2000, International Symposium on Environment and Alternative Refrigerants 2000, Kobe, http://www.jraia.or.jp/product/com_aircon/pac_gl13.html

4.2.7) Mukaidono, Concept of Safety, Trends in Academic, Sep., 2009, p. 14

4.2.8) Kataoka et al., Experimental and Numerical Analyses of Refrigerant Leaks in a Closed Room, ASHRAE Transact., Vol. 105, Pt. 2, 1999

4-3. Chiller Risk Assessment SWG: Risk assessments policy of the chiller and guideline planning taking IEC60079 into consideration

Kenji UEDA

JRAIA, Chiller Risk Assessment Sub-working Group

4.3.1 Introduction

The heat-source system supplying hot or cold water to air-conditioning systems uses hydrofluorocarbon (HFC) refrigerants, R410A or R134a. Both refrigerants have a significant impact on global warming because their GWP exceeds 1000. Therefore, it is important to substitute them with low GWP refrigerants. Some low GWP refrigerants such as R1234yf, R1234ze (E), and mixed refrigerants have been evaluated in retrofit and performance tests. All of these low GWP refrigerants are mildly flammable. Risk assessments (RAs) of chillers in which the aforementioned two refrigerants and R32 are added, with focus on the ignition and burning characteristics of the refrigerants, have been performed to evaluate security against fire accidents and burns.

The WG (chiller SWG), which consists of professional chiller engineers, was set up in the Japan Refrigeration and Air Conditioning Industry Association (JRAIA) and RAs are being performed. Requirements for the design and facilities that incorporate the measures and the actions defined by the RAs will be established as JRAIA guidelines (GLs) in 2013. Progress toward this end is summarized in this report.

Table 4.3.1 Risk assessment process chart of chiller SWG

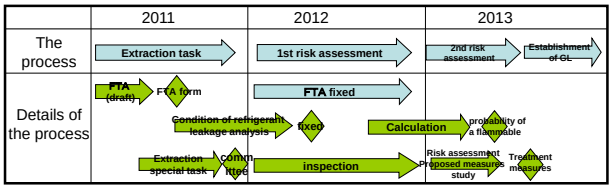

4.3.2 Scope

Within the scope of these requirements are air-cooled heat pumps installed outdoors and water-cooled chillers installed in a machine room as a central air-conditioning heat source and with a cooling capacity ranging from 7.5 to 17500 kW.

4.3.3 Prerequisite for performing risk Assessments

Because the equipment has the same structure and application as conventional equipment, the RAs[4.3.1),4.3.2)] that have been performed are generally effective. The RAs have been performed in a manner that improves their consistency and focus on the differences in the flammability characteristics of refrigerants. In addition, we reference studies of the mini-split air conditioner and the multiple packaged air-conditioning unit system for which RAs have been performed.

4.3.3.1 Risk map

Risks are clarified using the FTA method and a numerical evaluation is performed by plotting a risk map (R-map) (Fig. 4.3.1) based on the probability of occurrence and severity of harm of each probable ignition source and refrigerant leak case. If a risk level is in the A or B region, measures and actions to reduce the probability of occurrence and the severity of harm are studied to shift the risk level to the C region.

(1) Probability of occurrence

The stock of water-cooled chillers and air-cooled heat pumps in the Japanese market is estimated to be 134,000 units according to JRAIA shipment statistics. This represents less than one-thousandth of the stock of mini-split air conditioners. The

probability of occurrence of harm, based on the handbook[4.3.3)] (HB), is described in Table 4.3.2.

(2) Severity of harm

The severity of harm is based on the definition of fire in the HB[4.3.3)] (Table 4.3.3).

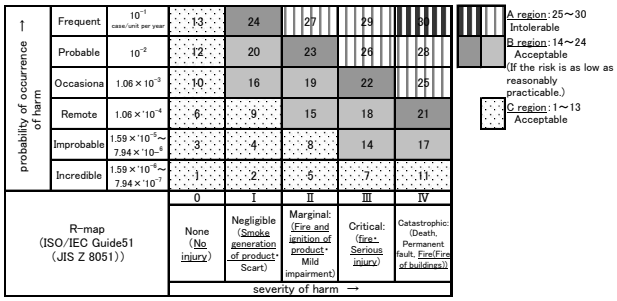

Fig. 4.3.1 Risk-assessment map

Table 4.3.2 Probability of occurrence of harm

Probability of occurrence of harm		Industrial-level product (adoption)
5	Frequent consumer goods:10^{-3} industrial-level product:10^{-1} (case/unit per year)	Number of accidents : once a year (per 10 units)
4	Probable consumer goods:10^{-4} industrial-level product:10^{-2} (case/unit per year)	Number of accidents : once a year (per 100 units)
3	Occasional consumer goods:10^{-5} industrial-level product:10^{-3} (case/unit per year)	Number of accidents : 134 times a year
2	Remote consumer goods:10^{-6} industrial-level product:10^{-4} (case/unit per year)	Number of accidents : 14 times a year
1	Improbable consumer goods:10^{-7} industrial-level product:10^{-5} (case/unit per year)	Number of accidents : once or twice a year
0	Incredible consumer goods:10^{-8} industrial-level product:10^{-6} (case/unit per year)	Number of accidents : once or twice ten years

Table 4.3.3 Severity of harm

	Qualitative representation	Severity of harm
Ⅳ	Catastrophic	Fire of buildings
Ⅲ	Critical	Fire
Ⅱ	Marginal	Fire and ignition of product
Ⅰ	Negligible	Smoke generation of product
0	None	No injury

4.3.3.2 Definition of life stages

"Overhaul" is added to the life stages in the existing reports[4.3.1),4.3.2)], and six life stages were defined: "Logistics," "Installation," "Usage," "Repair," "Overhaul," and "Disposal." Each life stage is distinguished as a water-cooled chiller or air-cooled heat pump, based on the installation condition.

4.3.3.3 Evaluation by the risk-assessment list

In the study, risks are quantified using the risk-assessment list. Combinations of extracted ignition sources and causes of leak are listed for each life stage. The risk evaluation using the R-map in accordance with the probability of occurrence and severity of harm and the evaluation of hazardous area levels using JISC60079-10[4.3.4)] are conducted simultaneously. Then, combinations with sufficiently low risk of ignition sources and leak cases are eliminated, and combinations with a risk to be evaluated are extracted.

The intrinsically safe design and requirements to be fulfilled for cases involving a risk, as well as the facility requirements in KHK0302-2[4.3.5)], JISC60079s[4.3.4)], and ISO5149-3[4.3.6)], are specified to explicate the actions to be taken in the GL.

Examples of the issues under consideration are as follows.

- The condition of equipment in the Logistics stage (transportation and storage) covers a broad range. There needs to be a large sticker alerting to the charging of a mildly flammable gas and indicating the handling method of the equipment.
- In the outdoor situation, wind velocity as ventilation needs to be specified in the analysis.
- Magnetic contractors, with capacity less than 20 kVA, are in the scope of IEC60335-2-40[4.3.7)] and as a result of study in the mini-split air conditioner SWG, the contractors are not considered an ignition source.
- There is no technical standard defining chiller units that avoid accumulated refrigerant gas due to a structural characteristic such as having outer panels. Therefore, requirements such as the opening space not being a sealed structure will be described in the GL as an intrinsically safe design.
- For the Disposal stage, the refrigerant recovery operation is focused and the risk is evaluated.

4.3.4 Setting of the flammable space analysis model in the event of a refrigerant leak

The existing time and volume of the flammable space are calculated when a refrigerant is leaked.

4.3.4.1 Analysis model of a machine room

(1) Definition of machine room

A water-cooled chiller is normally installed in a machine room. Even if inert gas is charged in the units, the ventilation system is installed in accordance with the technical standards[4.3.5~8] to avoid the danger of suffocation. The restriction of ventilation volume and the installation of ignition sources in the standards are applied to the analysis model.

(2) Area of machine room

The mean value, minimum value, and the maximum value of the machine room area to the chiller volume are summarized in the List of Completion Facilities Research of the Journal of Heating and Air-Conditioning Sanitary Engineering (2007–2010). In the analysis, the mean value is used to calculate the formation of flammable space from the maximum value to the minimum value.

(3) Installation position of equipment

The shape of the machine room floor is a 1:2 rectangle. The chiller is assumed to be installed on one half of the floor and auxiliaries on the other half. The maintenance space has 1.2 [m] or more on the front of the control panel and the other sides have 1.0 [m] or more (Fig. 4.3.2).

(4) Assumption of ventilation volume and air supply and exhaust louver area

The air is ventilated by mechanical forced ventilation five times or more per hour[4.3.9]. The air supply and exhaust louver area are determined by reference to “Mechanical Equipment Construction Edition” of the Kagoshima Prefecture Building Standards. An air-supply port is installed immediately above the equipment body and an exhaust port on the wall of the equipment side (Fig. 4.3.2). The analysis is performed because the flammable space to be formed varies depending on the leak position/direction and the installation positions of the air supply and exhaust ports.

4.3.4.2 Analysis model of equipment installed outdoors

Compared to a water-cooled chiller installed inside the machine room, an air-cooled heat pump installed outdoors has a smaller chance of forming a flammable space. Therefore, based on the soundproof installation procedure described by the manufacturer, the analysis model had two walls(Wall A and B) and two walls(Wall C and D) with a 25% aperture ratio, thus creating an environment in which a flammable space is most readily formed (because there is no wind) (Fig. 4.3.3).

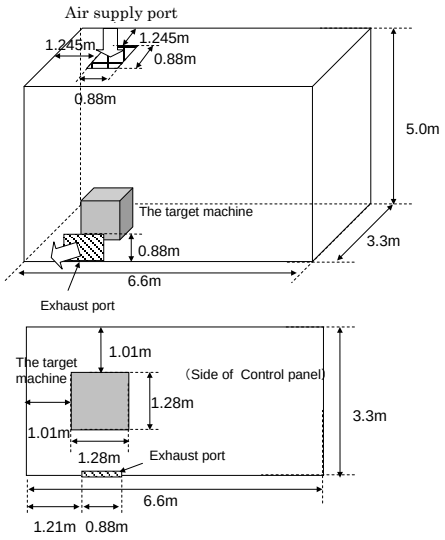

Fig. 4.3.2 Machine room outline

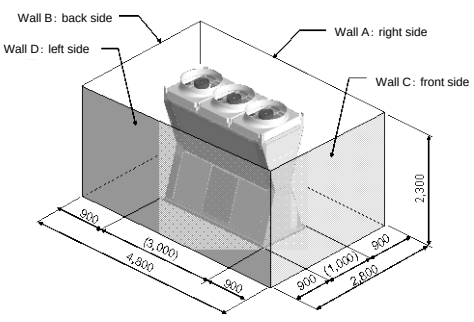

Fig. 4.3.3 Air-cooled chiller model for analysis

The following are the refrigerant leak areas:

(1) Air–heat exchanger

(2) Inside the decorative panel of the unit

In regard to (2), after a refrigerant is filled inside the panels, it is leaked to the area outside the unit. The parts inside the heat pump are also evaluated as an ignition source.

4.3.4.3 Definition of flammable region and amount of leaked refrigerant

The representative physical properties of the three target types of refrigerants are shown in Table 4.3.4. The leak areas of a chiller have the same sized structure as in a multiple packaged air-conditioning unit system. Therefore, the leak rate is determined in accordance with JRA GL-13 [4.3.8] (Table 4.3.5).

Table 4.3.4 Flammability of refrigerants[4.3.10), 4.3.11)]

Refrigerant	Limit of flammability 4.3.10)		Burning velocity 4.3.11)	Minimum ignition energy 4.3.11)	Diffusion coefficient
	LFL vol%	UFL vol%	cm/s	mJ	cm^2/s
R32	13.3	29.3	6.7	15	0.135
R1234yf	6.2	12.3	1.5	500	0.075
R1234ze(E)	7.0	9.5	–	–	0.074

Table 4.3.5 Weight flow of leak

		Case of refrigerant leak		
		Slow leak	Rapid leak	Burst leak
Leak Rate	R32	1kg/h or less	10kg/h	75 or 200kg/h
	R1234yf	0.9kg/h or less	8.9kg/h	67 or 178kg/h
	R1234ze(E)	0.7kg/h or less	7.3kg/h	54 or 145kg/h
Probability of occurrence		It is unknown whether it is capable of detecting	Occasional	Remote
Position of occurrence		Pinhole, Welded part, Brazing part, cauterization part	Cracking flare , Flare welding part , Cauterization part	slipping-out accident from flare fitting joint , Pipe fitting

4.3.4.4 Analysis procedure for a refrigerant leak

The existing time and volume of a flammable space are calculated during the time period from the start of a refrigerant leak to its cessation. The seven cases for three refrigerants shown in Table 4.3.6 are analyzed and evaluated.

Table 4.3.6 List of analyses

Case	chiller type (kg)	Case of refrigerant leak [kg/h]		Machine room area[m^2]	(Airflow[m/s]) or Ventilation airflow[m^3/h]	Refrigerant type
8	water -cooled (23.4kg)	Burst leak	75	22	3,267	R32
9					545	
10					0	
11			54		3,267	R1234ze(E)
4					545	
12					0	
13		Rapid leak	7	22	3,267	R1234ze(E)
1			10	22	545	R32
2			7		545	R1234ze(E)
3			9		545	R1234yf
5			7	22	0	R1234ze(E)
14			10(R32) 7(ze) 9(yf)	6	972	R32, R1234ze, R1234yf
15					162	
16					0	
17		Slow leak	1(R32), 0.7(ze), 0.9(yf)	22	3,267	R32, R1234ze, R1234yf
18					545	
19					0	
20	air -cooled (11.7kg)	Burst leak	75	–	(0)	R32
6		Rapid leak	10	–	(0)	
21		Slow leak	1	–	(0)	
22		Burst leak	75	–	(0)	
7		Rapid leak	10	–	(0.5)	
23		Slow leak	1	–	(0)	

4.3.5 Basic configuration of FTA

Conditions particular to the machine room include the small number of operators and servicemen who can access it, the existence of electrical equipment with a relatively large capacity, and the installation of equipment in addition to combustion equipment, such as a boiler. However, unlike the situation with a mini-split air conditioner or a multiple packaged air-conditioning unit system, the periphery of a machine room can be sufficiently controlled.

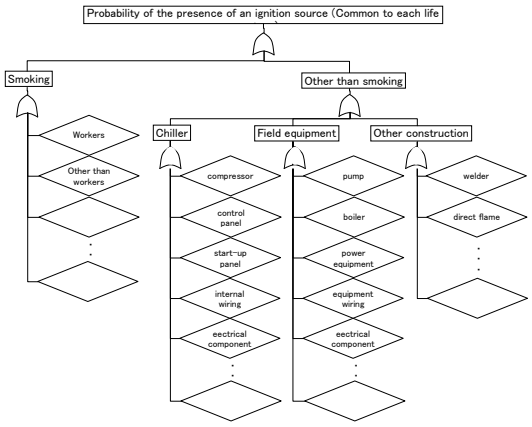

Fig. 4.3.4-a Basic FTA for every life stage

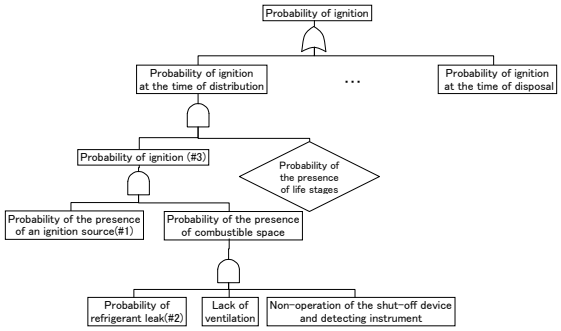

Fig. 4.3.4-b Probability of ignition

The basic FTA is configured to ensure consistency among the aforementioned six life stages in the encounter probabilities of refrigerant leaks and the ignition source (Fig. 4.3.4-a).

In addition, the common FTA is configured for the existing probability of an ignition source so that it would not be overlooked in each life stage (Fig. 4.3.4-b). The probability of leak also is studied (not shown in a figure).

4.3.6 Machine-room requirements in KHKS0302-3 and ISO5149

KHKS0302-3[4.3.5)] is written in accordance with related standards such as the Refrigeration Safety Regulations based on the High Pressure Gas Safety Act. To maintain the safety of the machine room, it is composed of standards concerning the (1) ventilation through an opening or the installation of mechanical ventilation, (2) additional installation of safety valves and gas-release tubes, (3) explosion-proof lighting for ensuring the performance, and (4) fire prevention/extinguishing systems.

The most important difference between KHKS and ISO5149-3 (FDIS version) is the necessary ventilation volume. Whereas KHKS calculates the volume using the legal refrigerant ton, ISO uses the refrigerant filling volume. The beginning of 3.2.3., "Prevention of Stagnant Refrigerants," of KHKS states that "The machine room must be maintained such that the concentration of refrigerant does not exceed its limit concentration even in the event of a leak of its entire amount." If a subsequent calculating formula is based on the legal refrigerant ton, it will not derive the correct value. Therefore, the refrigerant filling volume will be used in the GL.

The next biggest difference is related to the standards for installation of ignition sources in a machine room. ISO specifically prohibits open flames but has no surface-temperature standard for equipment inside a machine room. For the GL, a surface-temperature standard based on the RAs will be necessary.

Regarding the refrigerant discharge function in the event that it is necessary to take emergency measures against a refrigerant leak, whereas the descriptions by ISO are generally qualitative and do not use a ventilation-volume calculation formula, those by KHKS are specific. The GL will aim to set a new standard regarding mildly flammable refrigerants (using KHK facility criteria, if possible) based on basic property data and the leak simulation.

4.3.7 Estimation of refrigerant leak accident probability

To estimate the probability of a refrigerant leak accident, the following were investigated:

(a) Accidents, occurring in 2010, listed in the High Pressure Gas Safety Act

Types of target equipment and cases of refrigerant leak (burst/rapid/slow) are extracted and gathered.

(b) Number of refrigerant leak accidents investigated by each company participating in the chiller SWG

The number of refrigerant leak accidents that occurred at each company participating in the SWG is investigated. In addition, taking into consideration the contribution ratio to the number of chillers in stock in the market from the volume of shipments made by each company, the number of chillers with an accident to the number of in-stock chillers in the market is calculated.

The composition ratios of the two investigation results generally match. Therefore, the accident probability was calculated based on the result of (b). The calculation result is as follows:

Burst leak: 1.0×10^{-5}/chiller per year [Improbable]

Rapid leak: 1.6×10^{-4}/chiller per year [Remote]

4.3.8 Legal handling of ammonia

Ammonia is a typical gas in mildly flammable refrigerants. Its upper explosive limit is 28 vol% and lower explosive limit is 15 vol%. Similarly to the refrigerants subject to the RAs, it has mild flammability. This chapter summarizes the handling of ammonia according to the Refrigeration Safety Regulations.

5.4.8.1 Refrigeration Safety Regulations

Ammonia is listed as a flammable gas and as a toxic gas in Article 2. Based on these characteristics, a technical standard of its handling is specified. The overview of the handling of flammable gases is as follows:

(1) The structure of the machine room shall be such that it is free of any stagnant gas in the event of a refrigerant-gas leak. (Article 7, item 3)

(2) The location of the opening of the release tube for safety valves and similar equipment shall be appropriate to the properties of the refrigerant gas. (Article 7, item 9)

(3) The level instrument of a liquid receiver shall be something other than a round glass level instrument. For a glass tube level instrument, breakage prevention measures and leak prevention measures in the event of breakage shall be taken. (Article 7, items 10 and 11)

(4) In accordance with its scale, appropriate fire extinguishing equipment shall be installed in appropriate locations. (Article 7, item 12)

(5) The electric equipment (flammable gases excluding ammonia) of electric and refrigerant equipment shall be structured such that it has an explosion-proof capacity appropriate to the installation location and type of refrigerant gas. (Article 7, item 14)

(6) Leak-detection equipment shall be installed in any place where a gas may be stagnant. (Article 7, item 15)

(7) Measures shall be taken to remove refrigerant gases in a safe and quick manner. (Article 7, item 16)

(8) Measures shall be taken to prevent any dangers at the time of maintenance. [Article 9, item 3 (b)]

4.3.8.2 Exclusion from the application of Article 7, item 14

Ammonia is excluded from the application of item (5) (Article 7, item 14). This exclusion is in accordance with the technical reference[4.3.12)]. An experiment was conducted to determine: 1) the concentration within the range of explosion limit in which a gas easily ignites, 2) amount of ignition energy if it ignites, 3) spatiality and the concentration distribution condition, and 4) connection of ignition frequency and time. The reference states that the validity of the Refrigeration Safety Regulations was reconfirmed based on factors 1) through 4).

Accordingly, in this SWG, the validity of the explosion-proof capacity also is evaluated by focusing on 1) through 4) as a guideline.

4.3.9 Derivation of ignition probability

The probability of ignition is derived by the procedure that follows.

4.3.9.1 Surface temperature of equipment in the machine room

Among the machines and instruments installed in the same area as the target equipment, those listed below, which have relatively high surface temperatures, are investigated.

1) Heat source unit (e.g., boiler)
2) Electric motor drive (e.g., pump motor)
3) Ventilation (e.g., ventilation fan)
4) Lighting apparatus (e.g., fluorescent light,

incandescent lamp)

5) Heating appliance (e.g., electric heater)

The result of ignition tests of mildly flammable refrigerants[4.3.13–15] performed at places such as Tokyo University of Science, Suwa, and the National Institute of Advanced Industrial Science and Technology will be compared to the surface temperatures of equipment inside the machine room to specify the surface-temperature limits inside a machine room.

4.3.9.2 Smoking rate

Burning cigarette ends and lighter/match flames can be considered ignition sources. The smoking rate of servicemen and their smoking behaviors were investigated.

- Fifty-three percent of the servicemen smoke and 28% have smoked on-site. During the past year, the smoking rates on site represent 7% of the entire sample.
- A lighter is used as the ignition equipment by 99.6% and 0.4% use a match.

Assuming that the smoking rate of the servicemen is 7%, the number of cigarettes smoked per person per day is 19.1[4.3.16], the working hours per day is 8, and the time when an open flame exists per smoking event is 2 s, the existence probability (ignition frequency) of an ignition source because of smoking is estimated to be on the order of 10^{-7} through 10^{-8}.

4.3.9.3 Electric components

Among electric components (e.g., electric motor drive, electromagnetic switch, electromagnetic contactor, printed-wiring board, and transformer) to be mounted on a chiller unit, an electromagnetic contactor in which an arc is generated has the possibility of ignition. The rating capacity of the electromagnetic contactor for each type and the capacity (horsepower) of the chiller are summarized.

For a chiller, the capacity range of the target equipment is wide and electromagnetic contactors with a wide range of capacities are used. For a product with 20 or fewer horsepower, the capacity is generally less than 20 kVA. Electric components with capacities less than 20 kVA are not considered ignition sources in accordance with the evaluation of other SWGs. This report's evaluation focuses on those with capacities of 20 kVA or more.

To estimate the maximum risk, an electric component with a capacity of 20 kVA or more is assumed to be always an ignition source following its first startup/shutdown. Assuming that the maximum number of startup/shutdown cycles per day is 6 per h (screw chiller)/2 per h (centrifugal chiller) and that the presence time of the electromagnetic contactor is 1 s, the existence probability of the ignition source, as with the case of a lighter, is estimated to be the on order of 10^{-4}. Compared to a lighter, this probability is large; a further detailed study will be conducted.

4.3.10 Guideline planning taking IEC60079-10-1 into consideration

Table 4.3.7 Influence of independent ventilation on type of zone

Grade of release	Ventilation Degree: High / Availability: Good	Ventilation Degree: High / Availability: Fair	Ventilation Degree: High / Availability: Poor	Ventilation Degree: Medium / Availability: Good	Ventilation Degree: Medium / Availability: Fair	Ventilation Degree: Medium / Availability: Poor	Ventilation Degree: Low / Availability: Good, fair or poor
Continuous	Non-hazardous	Zone2	Zone1	Zone0	Zone0 + Zone2	Zone0 + Zone2	Zone 0
Primary	Non-hazardous	Zone2	Zone2	Zone1	Zone1 + Zone2	Zone1 + Zone2	Zone1 or Zone0
Secondary	Non-hazardous	Non-hazardous	Zone2	Zone1	Zone2	Zone1	Zone1 and even Zone0

4.3.10.1 Principle of IEC60079-10-1

The following principle is crucial: "Installations in which flammable materials are handled or stored should be designed, operated and maintained so that any releases of flammable material, and consequently the extent of hazardous areas, are kept to a minimum, whether in normal operation or otherwise, with regard to frequency, duration and quantity."

The classification of hazardous areas in which a danger may arise due to a flammable gas is

defined in IEC60079-10-1[4.3.17)]. The areas are graded into three hazardous and non-hazardous areas based on their grade of release and two indexes of the ventilation condition: “degree of ventilation” and “availability of ventilation” (Table 4.3.7). In Japan, the classification of hazardous areas is established in JISC60079-10[4.3.4)], which is not different from that of IEC60079-10-1[4.3.17)]. In the chiller SWG, a study is conducted using JIS.

4.3.10.2 Guideline planning taking IEC60079-10-1 into consideration

In Japan, when a flammable gas is used in a chiller, the technical standard, JISC60079s[4.3.4)], and the Refrigeration Safety Regulations (Article 7, item 14) must be complied with, and the application of explosion-proof electric equipment is necessary. However, the relationship between the equipment installation standard to be referenced, KHK0302-3[4.3.6)] or ISO5149[7)], and JISC60079s[4.3.4)], is not specified. Although JISC60079s[4.3.4)] specifies that explosion-proof equipment is not required in a non-hazardous area as judged by the aforementioned availability-of-ventilation condition, this seems to be inconsistent with the application of explosion-proof equipment in the Refrigeration Safety Regulations.

Therefore, the RA implementation conditions, techniques, and results studied will be reported in the SWG. In addition, these will be applied to the requirements for the intrinsically safe design of the equipment in the GL, which will establish the incorporation of equipment installation requirements that do not require setting hazardous areas to the extent possible, in accordance with the principle of JISC60079s[4.3.4)].

Acknowledgments

This report was written by the author and Mr. Yosuke Mukai by compiling the research results of nine Committee members, as well as Mr. Masayuki Aiyama, Mr. Mikio Ito, Mr. Isao Iba, Mr. Tetsuji Saikusa, Mr. Yoshihiro Sumida, Mr. Mamoru Senda, Mr. Takuho Hirahara, Mr. Syuji Fukano, and Mr. Koichi Yamaguchi. Sincere appreciation is extended to the members concerned.

References

4.3.1) Report on the Result of Risk Assessment Consideration of Room Air-Conditioner with R290 Refrigerant: The Japan Refrigeration and Air Conditioning Industry Association Environment Committee Refrigerant Global Warming Response Commission: Summary of the Non-FC Refrigerant Consideration Session Meeting (1999).

4.3.2) “Risk Assessment of HFC-32 and HFC-32/134a (30/70wt%),” Split System Residential Heat Pump, Arthur D Little Inc., United States (1998).

4.3.3) Ministry of Economy, Trade, and Industry: Risk Assessment Handbook Practice Edition (2011).

4.3.4) JISC60079-10(2008): Electric Machinery and Instruments Used in Explosive Atmospheres -
Chapter 10: Classification of Hazardous Areas.

4.3.5) KHKS0302-3: Standards of Refrigeration and Air-Conditioning Equipment Facilities [Facilities with Flammable Gases (including low-flammable Gases)], (2011).

4.3.6) ISO5149: Refrigerating Systems and Heat Pumps – Safety and Environmental Requirements, (1993)
Part 1) Definitions, classification and selection criteria
Part 2) Design, construction, testing, marking and documentation
Part 3) Installation site
Part 4) Operation, maintenance, repair

and recovery.

4.3.7) IEC60335-2-40: Household and Similar Electrical Appliances –Safety –, (2005)
Part 2-40) Particular requirements for electrical heat pumps, air conditioners and dehumidifiers.

4.3.8) JRA GL-13: Guidelines for Ensuring Safety in the Event of a Refrigerant Leak from a Multi-Unit Air Conditioning System, (2011).

4.3.9) ASHRAE15: Proposed Addendum to Standard 15-2010, Safety Standard for Refrigeration Systems, (2010).

4.3.10) Japan Fluorocarbon Manufacturers Association, “List of environmental and safety data of specified CFCs (CFC/HCFC) and fluorocarbons ”, http://www.jfma.org/database/table.html

4.3.11) Kenji TAKIZAWA et al, “Flammability properties of 2L refrigerants ” , The International Symposium on New Refrigerants and Environmental Technology 2012,（2012）

4.3.12) T. Toyonaka: “Refrigeration,” **70** (811), 5 (1995).

4.3.13) T. Imamura: Evaluation of Fire Hazards of A2L Class Refrigerants, The International Symposium on New Refrigerants and Environmental Technology 2012, pp. 65-68, Kobe (2012).

4.3.14) T. Saburi: Combustion Characteristics of Flammable Refrigerant Gases, International Symposium on New Refrigerants and Environmental Technology 2012, pp. 69-72, Kobe (2012).

4.3.15) K. Takizawa: Flammability Property of 2L Refrigerants, International Symposium on New Refrigerants and Environmental Technology 2012, pp. 73-79, Kobe (2012).

4.3.16) JT website: http://www.jti.co.jp/investors/press_releases/2012/0730_01_appendix_02.html, (2013).

4.3.17) IEC60079-10-1: Explosive Atmospheres –Part 10-1: Classification of Areas – Explosive Gas Atmospheres.

5. Deregulation Activities in Japan for the Introduction of Mobile Air Conditioning Refrigerant R1234yf

Japan Automobile Manufacturers Association, Inc.
(Vehicle Maintenance Subcommittee)

5.1 Background to the Introduction of R1234yf in Japan

Worldwide efforts to reduce greenhouse gases (GHGs) have resulted in a growing demand for mobile air conditioning refrigerants with a low global warming potential (GWP). Since 2011, the European Union has banned the use of refrigerants with a GWP greater than 150 in new-model (i.e., newly type-approved) vehicles (from 2017 onwards, the ban will apply to all new vehicles). Japanese automakers are taking the necessary steps for vehicles destined for the EU market.

Preparations for the introduction of low-GWP refrigerants are also underway in North America. The United States-based international Society of Automotive Engineers (SAE) has completed a risk assessment study on R1234yf, and the American Society of Heating, Refrigerating and Air-Conditioning Engineers (ASHRAE) has classified R1234yf as a mildly flammable gas. In addition, on April 1, 2010 the U.S. Environmental Protection Agency (EPA) issued GHG regulations allowing vehicles that use a low-GWP refrigerant to be provided with credits.

In Japan, the Global Warming Prevention Measures Subcommittee under the Industrial Structure Council's Chemicals and Bio-industry Committee approved, on February 17, 2011, the interim course outlined during its discussions on substitute refrigerants. Specifically, the Subcommittee acknowledged an urgent need to promote refrigerant replacement through collaboration among automakers, government agencies, research institutes, and equipment manufacturers and recommended the resolution of various existing obstacles by 2014.

In response, the Japan Automobile Manufacturers Association, Inc. (JAMA), in concert with research institutes and the manufacturers of refrigerant retrieval/recharging equipment, launched a risk assessment study aimed at ensuring the safe and easy handling of R1234yf by automotive maintenance shops throughout Japan by the target year of 2014.

5.2 Obstacles to R1234yf Introduction

Table 5.1 summarizes, from the perspective of a vehicle's life cycle, the existing obstacles to the introduction of R1234yf and indicates the need (or not) for measures to address them.

Table 5.1 Obstacles & measures required

1) Vehicle production	Current flammable-gas explosion prevention requirements (government ministry-approved)	Deregulatory measures required
2) Charging gas (after-sales servicing)	No obstacles if: -Compliant with Announcement No. 139 -Charging gas pressure does not exceed 0.8 MPa at 35 °C and satisfies terms of Art. 4-3 in Announcement No. 139	No deregulatory measures required
3) Storage of charging gas	[As per High-Pressure Gas Safety Law] Current requirements on mandatory safe distance from fire/flammables	Deregulatory measures required
4) Retrieval/ recharging (after-sales servicing)	[As per High-Pressure Gas Safety Law] Current requirements on: -Mandatory safe distances from gas cylinders (Hospitals, schools: At least 15 m; Homes: At least 10 m) -Removal of static electricity, etc. -Mandatory licensing by prefectural governments of auto maintenance shops	Deregulatory measures required

A special ministerial approval scheme is currently in place in Japan to facilitate the approval of factory lines producing R1234yf-equipped vehicles based on the explosion-prevention measures taken. Because the number of these production lines is projected to increase in step with the growing number of vehicle models incorporating R1234yf, further deregulation of

R1234yf is necessary.

With regard to after-sales servicing, operators of varying types and scale—including auto maintenance shop operators, auto body repair shop operators, and electrical equipment repair shop operators—are engaged in the retrieval/recharging of refrigerants for vehicles in need of repair or that were in accidents. For many of these operators, making the large investment necessitated by regulations governing R1234yf is difficult.

JAMA's Vehicle Maintenance Subcommittee has singled out the requirements concerning mandatory safe distances from gas cylinders as the top-priority deregulation target (see item 4) in Table 5.1 above). Regarding the handling of R1234yf that may be generated from the dismantling of end-of-life vehicles, the Subcommittee decided not to address this matter in the present project because regulations on the retrieval of R1234yf at the vehicle dismantling stage have yet to be established.

5.3 Activities of JAMA's Vehicle Maintenance Subcommittee

In collaboration with the manufacturers of refrigerant retrieval/recharging equipment, refrigerant suppliers, auto maintenance shop associations and other stakeholders, JAMA has been carrying out activities aimed at resolving, by 2014, existing obstacles to the widespread use of R1234yf. One such activity was a study that used the risk assessment mapping method to assess risk, combining the "probability of injury" and the "severity of injury" in a 6 × 5 matrix. Supported by the risk assessment mapping data, JAMA will petition the government to review its safety regulations in order to more accurately reflect the actual risks of R1234yf.

As a first step in its risk assessment study, JAMA conducted hearings with refrigerant retrieval/recharging equipment manufacturers and a survey of retrieval/recharging operators to more clearly identify the risks at maintenance work sites. In cooperation with the Japan Automobile Service Promotion Association, Japan Auto Body Repair Association, and Japan Automotive Electrical Equipment Service Association, the survey questionnaire was distributed to a representative selection of auto maintenance shops, in terms of business scale and services offered, across Japan.

Completed questionnaires were received from a total of 756 auto maintenance shops. The information provided in the questionnaires received from the 533 shops that performed their own retrieval/recharging operations was compiled into basic data on auto maintenance shops (number of workers, number of vehicles repaired, shop layout information, etc.) and workers' on-the-job observations (on refrigerant leakage occurrence, ventilation conditions, the presence of ignition sources, etc.).

On the basis of data obtained from the survey questionnaire on leakage-prone points, leakage amounts, and ignition source specifications, JAMA conducted an ignition test and a leak simulation test, in both instances assuming worst-case R1234yf leakage conditions. The data obtained in these tests was used to calculate the probability and severity of injury caused by R1234yf leakage and map them for risk assessment. Based on the results of its risk assessment study, JAMA is now preparing to propose to the regulatory authorities a package of measures that would allow R1234yf to be treated as an inert gas (Table 5.2).

Table 5.2 JAMA's R1234yf-related activities

Conduct of risk assessment study (NEDO* project including questionnaire-based survey; data compilation commissioned from JARI) *New Energy and Industrial Technology Development Organization	Apr. 2011-Mar. 2013
Discussion of measures for regulatory exemption of R1234yf (Participation in METI-sponsored KHK project)	Oct. 2012-Mar. 2013
Submission of proposal for review by METI* *Ministry of Economy, Trade and Industry	Apr. 2013-

5.4 Ignition Test

5.4.1 Test method

The ignition test was carried out by Tokyo University of Science, Suwa, in the Hy-SEF explosive fire resistance test facility at the Japan Automobile Research Institute's Shirosato Test Center (Fig. 5.1).

Fig. 5.1 Overview of the Hy-SEF test facility

Based on data obtained from the survey questionnaire as described above, the identified risks were classified into four categories, as shown in Table 5.3, and prioritized according to the probability and severity of injury caused by R1234yf leakage. The two leading risks—namely, hose rupture and leakage from inside retrieval/recharging equipment—were examined to determine the answers to the following questions:

- In the event of refrigerant leakage from a pinhole in the hose, to what extent does flammable gas escape and aggregate? Does it cause ignition?
- In the event of refrigerant leakage inside the retrieval/recharging equipment, is there a risk of ignition owing to sparks from the electrical relay or other similar parts of the equipment?

Table 5.3 Risk Classification by JAMA's Vehicle Maintenance Subcommittee

	Risk Description	Leak Speed (amount/time)	Remarks
1)	Slow leak from a junction	1 kg/24 h (gas)	Ignition potential: Low
2)	Hose rupture (including hose pinhole)	1 kg/60 sec (gas)	Inner diameter of hose: 4 mm Internal pressure of hose: 0.5 MPa (at normal temperature)
3)	Cylinder safety valve activation (fusible plug)	24 kg/1 h (gas)	Activation possibility: Low
4)	Leakage from (safety valve, etc.) inside retrieval/ recharging equip-ment	300 g/60 sec (liquid) (initially 100 g/0.5 sec)	Activation possibility: Low

A testing space of 8 m × 8 m was secured within the test facility, and a testing apparatus (specifically, a 1 m × 1 m × 1 m acryllic box) that simulated retrieval/recharging equipment was installed inside the testing space. The testing apparatus featured a 20 mm-wide slit on two opposing sides that could be closed or opened for ventilation (Fig. 5.3).

In the hose pinhole ignition test, which was conducted in the open testing space, the refrigerant was made to leak continuously from a pinhole in the hose, and refrigerant concentrations were measured at various locations from the pinhole. The potential for ignition was then examined by applying electric sparks (both a single spark and repeated sparks) or a naked flame near the pinhole. In the retrieval/recharging equipment ignition test, a single spark was discharged to examine the potential for ignition when the ventilation slits were open and when they were closed.

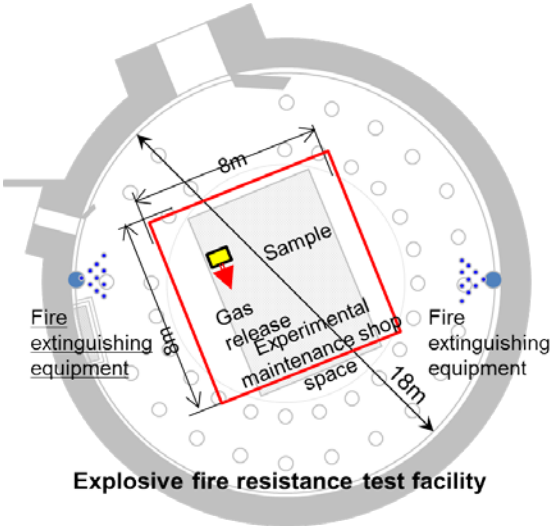

Fig. 5.2 Testing space simulating a work site

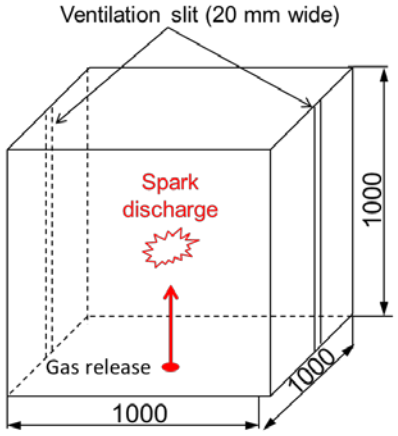

Fig. 5.3 Apparatus simulating retrieval/recharging equipment

5.4.2 Test results

As shown in Table 5.4, the results of the hose pinhole ignition test confirmed that the area within a 10-cm radius from the pinhole was flammable. Nevertheless, despite the application of an ignition energy of 10 J or more which far exceeded the maximum ignition energy existing inside the equipment (1.07 J at the relay contact), ignition could not be induced anywhere near or away from the pinhole. Similarly in the retrieval/recharging equipment ignition test and despite the application of a large ignition energy of 16 J, ignition did not occur, presumably because of the exchange of air between outside and inside the testing apparatus through the opened slits. As previously reported, combustion and flame propagation occurred when the slits were kept closed; however, no blast pressures were generated.

Table 5.4 Ignition test results

Priority Risk	Test Objective & Outline	Results
Hose rupture (including hose pinhole)	Leakage from Φ4 mm hose; observation of concentration distribution and potential ignition ▪ Leak speed: 470 g/min (cylinder heated to 50 °C) ▪ Ignition source: Repeated electric sparks	▪ Flammable area extending to a 10-cm radius from pinhole ▪ No ignition
Leakage inside retrieval/ recharging equipment	Leakage inside closed 1-m^3 space (acryllic box) with a vertical slit on 2 opposing sides ▪ Leak speed: 380 g/min ▪ Ignition source: Electric sparks (16 J, 6 Hz) ▪ Temp./humidity: 25 °C, 75%	▪ Generation of flammable area after leakage ▪ No ignition

5.5 R1234yf Leak Simulation Test

As stated in the preceding section in regard to retrieval/recharging equipment ignition testing, leaked R1234yf would not ignite when the slits on the testing apparatus were kept open for ventilation, even when electric sparks of a sufficiently large ignition energy were applied. An R1234yf leak simulation test was subsequently conducted to examine this phenomenon in greater detail through the analysis of refrigerant concentrations and flow velocity inside simulated retrieval/recharging equipment. The analytical conditions were established as follows:

- Analysis code: PHOENICS (thermal fluid analysis code)
- Analysis model: 1 m × 1 m × 1 m cube with slits (each 20 mm wide and 1 m high) on two opposing sides
- Gas discharge speed: 500 g/min (from bottom of equipment)
- Model size: 500,000 elements (100 × 100, 50 vertical partitions)
- Calculation method: 0.5 sec steps, 50 repetitions

Fig. 5.4 shows an analytical image of R1234yf concentrations during discharge. Given the known lower flammable limit (LFL) of 6.2 vol%,[5.1)] the distances of LFL and 1/4LFL from the leakage point proved to be 256 mm and 964 mm, respectively. Assuming that these distances hold true in the real world, the LFL distance of about 10 cm determined in the ignition test under review here signifies a 1/4LFL distance of approximately 38 cm.

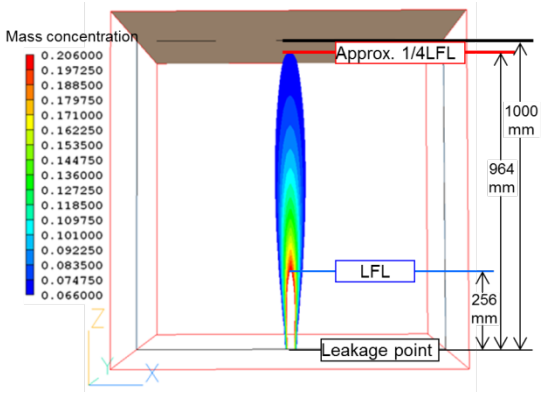

Note: The figures on the left denote mass concentration values.

Fig. 5.4 R1234yf concentrations during discharge

Figs. 5.5 and 5.6 show R1234yf's flow velocity 30 sec after the cessation of leakage. Areas of low flow velocity were found along the slits, where air flow velocity was moderated by the simultaneous entry and exit of air through the slits. In most of the other areas, the flow velocity was 2 cm/sec or faster, thus exceeding R1234yf's maximum

combustion speed of 1.5 cm/sec.[5.2)] This clearly demonstrates that R1234yf cannot ignite inside a ventilated container when air flow is present.

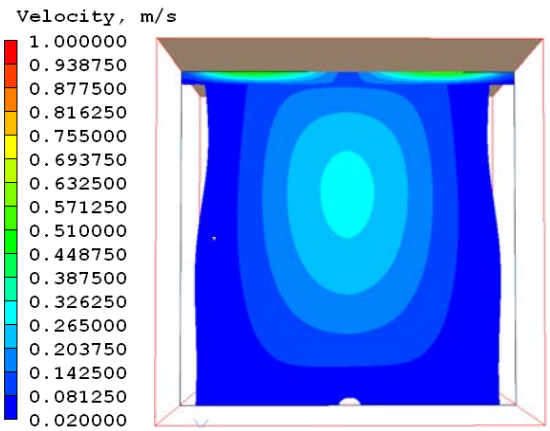

(Velocity display range: 0.02 m/sec-1 m/sec)

Fig. 5.5 R1234yf flow velocity 30 sec after leakage cessation

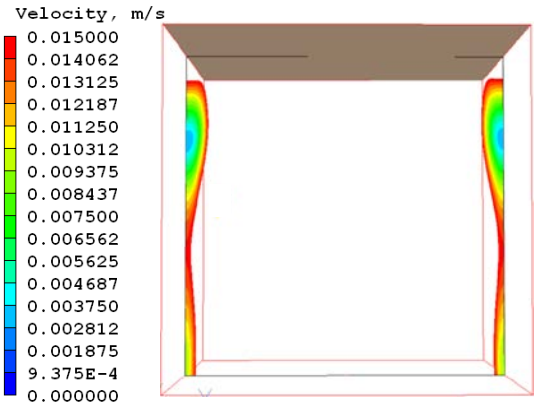

(Velocity display range: 0 m/sec-0.015 m/sec)

Fig. 5.6 R1234yf flow velocity 30 sec after leakage cessation

5.6 Risk Assessment and Mapping

5.6.1 Probability of injury

The probability of injury was calculated based on fault tree analysis (FTA) wherein unfavorable events (top events) are identified. The routes leading to a fault or accident, as well as probability values, are then established in a fault tree diagram to analyze the probability of top-event occurrence on the basis of lower-level events that cause the top events. A report on a fault tree analysis of ignition risks at automotive maintenance shops[5.3),5.4)] having already been published by the SAE, JAMA conducted its own fault tree analysis based on actual conditions in auto maintenance shops in Japan, taking into account the SAE's findings.

Fig. 5.7 shows the fault tree diagram used in the risk assessment. "Ignition" was identified as the top event. For ignition to take place, the following three events—i) the presence of refrigerant concentrations at flammable levels or between the lower and upper flammable limits; ii) the execution of maintenance work under unsatisfactory ventilation conditions; and iii) the presence of a flame source having an amount of energy exceeding the minimum ignition energy—would have to occur simultaneously. These three events were applied to each of three possible leakage locations—hose junction, hose rupture, and cylinder—and their leakage probabilities were determined on the basis of data obtained from the survey questionnaire and the ignition and leak simulation tests.

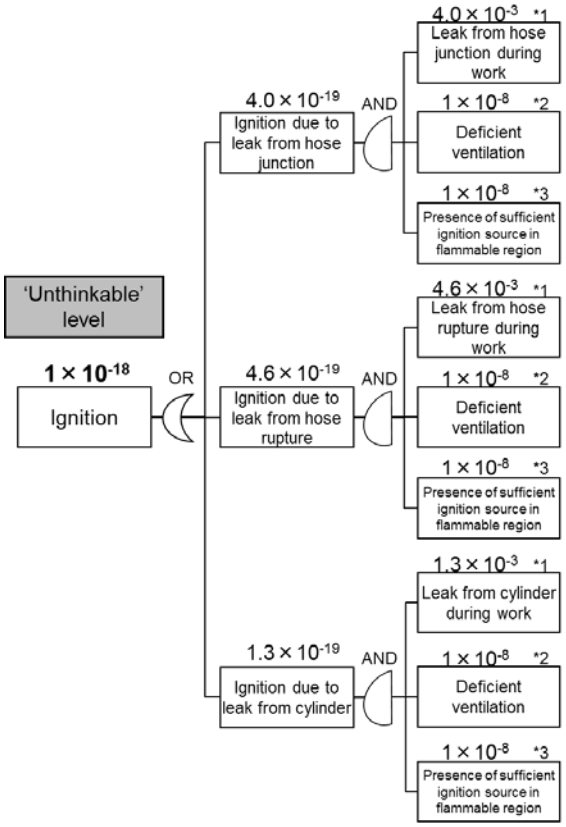

Fig. 5.7 Fault tree diagram

(a) Refrigerant leakage (*1 in Fig. 5.7)
Probabilities of refrigerant leakage were calculated from the leakage frequency data obtained from the survey questionnaire.

(b) Deficient ventilation (*2 in Fig. 5.7)
Fact 1: Presumably because ventilation is required by law, no survey questionnaire respondents answered that they had handled refrigerants in the absence of ventilation. Fact 2: The results of the ignition and leak simulation tests confirmed that because the flow velocity of leaked refrigerant exceeds its maximum combustion speed in the presence of ventilation, no stable flames are generated inside an indoor facility or a container with slits. In light of these facts and the impracticality of assuming there is no air flow at auto maintenance shop work sites in Japan, the probability of deficient ventilation was rated at 10^{-8}.

(c) Ignition source inside flammable area (*3 in Fig. 5.7)
In the ignition test, no stable flames were generated by 16-J sparks even in the flammable area within a 10-cm radius from the pinhole. This was presumably because air was stirred by convection in the indoor test facility. Moreover, it is hardly conceivable that trained maintenance technicians would handle a heater, welding machine, or other similar ignition source within 10 cm of a flammable refrigerant. In the case of retrieval/recharging equipment, the compressor-driven relay contact was the ignition source with the greatest ignition energy. Because most of the relay body was sealed from the atmosphere by a cover and in view of the fact that the quenching diameter (i.e., the maximum diameter of a hole through which flames do not pass) for R1234yf is 7-8 mm, it is unlikely that flames would propagate even if ignition occurred at the relay contact. Thus, the probability of the presence of a significant ignition source (to enable combustion) was rated at 10^{-8}.

(d) Ignition
Based on the observations and calculations described above, the probability of ignition was considered to be 1×10^{-18} for refrigerant retrieval/recharging equipment. This probability is unthinkably low compared to the standard probability of 10^{-8} assigned to relays in the guidelines introduced by the Union of Japanese Scientists and Engineers' R-Map study group.

Fig. 5.8 Retrieval/recharging equipment relay configuration (general-purpose model)

5.6.2 Severity of injury

The severity of injury was derived from the ignition test results relating to physical criteria (i.e., heat- and pressure-related factors including flame temperature, radiant heat, and sound pressure) and chemical criteria (i.e., hydrogen fluoride concentration, which is a toxic factor). Because ignition did not occur in the test setups simulating a maintenance work site and the inside of retrieval/recharging equipment, there was no generation of heat, pressure, or toxicity. Consequently, the severity of injury was rated at zero—i.e., no injury (Table 5.5).

Table 5.5 Injury at work site

Item Measured		Value Measured	Injury
Heat	Flame temperature	No temperature rise	None
	Radiant heat	None	None
Pressure	Sound (blast) pressure	None	None
Toxicity	HF concentration	None (0.0 ppm by densitometer)	None

A worst-case test was also conducted assuming the occurrence of combustion in a closed space. The test results are summarized in Table 5.6. According to video analysis, the flame spread to a vinyl

chloride side sheet 50 cm away 1.25 sec after ignition; this resulted in an estimated flame temperature of 400 °C or higher. Nevertheless, the combustion was moderate rather than explosive and was short-lived (lasting no more than several seconds); any injury incurred would therefore be only a slight burn, even if the flame were to come into contact with a human body. Because the hydrogen fluoride concentration exceeded the maximum permissible limit, a worker exposed to it would feel a skin irritation. The hydrogen fluoride, however, quickly dispersed, which would enable the worker to evacuate safely. For these reasons, the worst-case injury severity was rated at I (slight).

Table 5.6 Injury in worst-case (closed space) ignition testing

Item Measured		Value Measured	Injury
Heat	Flame temperature	Not measured (video analysis: ≥400 °C)	Slight
	Radiant heat	Not measured	
Pressure	Sound (blast) pressure	None (video analysis)	None
Toxicity	HF concentration	Exceeding maximum limit of 3 ppm	Slight

5.6.3 Risk mapping

On the basis of the probability and severity of injury derived in the tests described above, the ignition risk of R1234yf during retrieval/recharging was plotted in Region-C of the risk assessment map, even for the worst case (Fig. 5.9). The ignition risk of R1234yf can therefore be considered socially acceptable.

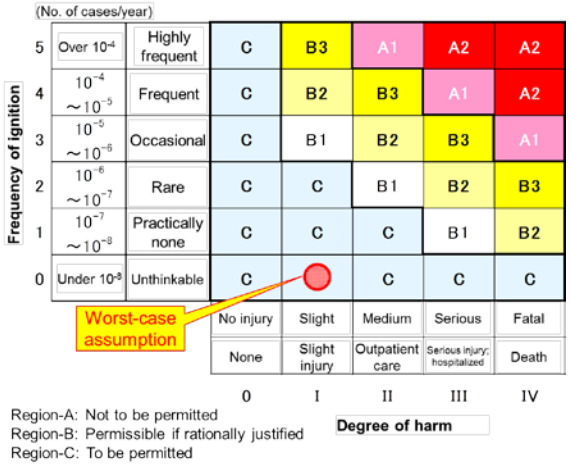

Fig. 5.9 Risk assessment map

5.7 Conclusions

Using the risk mapping method, the risk of R1234yf ignition during retrieval/recharging was assessed. Data obtained from a question-naire-based survey of automotive maintenance shops and from ignition and leak simulation tests was analyzed. As a result, the probability of ignition was rated at 10^{-18} (an extremely low level) and the severity of injury at I (slight), even for the worst case. The ignition risk of R1234yf was thus considered to be socially acceptable.

5.8 Future Actions

5.8.1 Measures for risk reduction

Because the ignition risk of R1234yf was found to be socially acceptable, measures targeted at the main body of retrieval/recharging equipment are unnecessary. Nevertheless, JAMA is studying measures to further reduce the risks of R1234yf, including structural modifications to retrieval/recharging equipment to enable constant ventilation and, in addition, the attachment of caution labels to indicate that R1234yf is a flammable gas.

5.8.2 Activities to promote deregulation

Given the risk assessment results and measures for risk reduction, JAMA, in concert with the High-Pressure Gas Safety Institute of Japan, is drafting a proposal for the exemption of R1234yf

from governmental regulations, in the hope that the proposal will be used as material for regulatory amendment discussion by the Ministry of Economy, Trade and Industry from April 2013 onwards.

Acknowledgments

JAMA expresses its gratitude to the Japan Automobile Service Promotion Association, Japan Auto Body Repair Association, and Japan Automotive Electrical Equipment Service Association for their assistance in the distribution of the survey questionnaire; to auto maintenance shop personnel for completing the questionnaire; to Dr. Tetsuya Suzuki of the Japan Automobile Research Institute and Mr. Yoshisuke Kusakari of Yamada Corporation for their advice on the risk assessment; and to Professor Osami Sugawa and Assistant Professor Tomohiko Imamura of Tokyo University of Science, Suwa, for their cooperation with the ignition test.

References

5.1) Japan Fluorocarbon Manufacturers Association, “List of Environmental and Safety Data on CFC/HCFC and Fluorocarbons”

5.2) Takizawa, Kenji et al., “Flammability Properties of 2L Refrigerants,” The International Symposium on New Refrigerants and Environmental Technology 2012 (2012)

5.3) Gradient Corporation, "Risk Assessment for Alternative Refrigerant HFO-1234yf" (2008)

5.4) Gradient Corporation, "Risk Assessment for Alternative Refrigerants HFO-1234yf and R-744 (CO_2)-Phase III" (2009)